Rimonabant: a CB_1 receptor antagonist as a direct interactional partner for μ- and δ-opioid receptor

Ph.D. thesis

Ferenc Zádor

Supervisor:

Dr. Sándor Benyhe

Institute of Biochemistry
Biological Research Center of the Hungarian Academy of Sciences

Szeged, Hungary

2014

TABLE OF CONTENTS

LIST OF PUBLICATIONS

This thesis is based on the following publications:

I. ***Zádor, F.***, Ötvös, F., Benyhe, S., Zimmer, A., Páldy, E. **Inhibition of forebrain μ-opioid receptor signaling by low concentrations of rimonabant does not require cannabinoid receptors and directly involves μ-opioid receptors.** *Neurochem Int* 61, 378-88 (2012).

(2.66 impact factor)

II. ***Zádor, F.***, Kocsis, D., Borsodi, A., Benyhe, S. **Micromolar concentrations of rimonabant directly inhibits delta opioid receptor specific ligand binding and agonist-induced G-protein activity.** *Neurochem Int* 67, 14-22 (2014).

(2.66 impact factor)

Other publications unrelated to this thesis:

Lackó, E., Váradi, A., Rapavi, R., ***Zádor, F.***, Riba, P., Benyhe, S., Borsodi, A., Hosztafi, S., Timár, J., Noszál, B., Fürst, S., Al-Khrasani, M. **A novel μ-opioid receptor ligand with high in vitro and in vivo agonist efficacy.** *Curr Med Chem* 19, 4699-707 (2012).

(4.07 impact factor)

Total impact factor: 9.39

LIST OF ABBREVIATIONS

AC: ..... adenylyl cyclase

ADP-ribosylation: ..... adenosine diphosphate ribosylation

AR.: ..... adrenergic receptor

BBB: ..... blood-brain-barrier

BMI: ..... body mass index

cAMP: ..... adenosine 3',5'-cyclic mono-phosphate

CB_1 K.O.: ..... CB_1 receptor knock-out

CB_1/ CB_2 K.O.: ..... CB_1/CB_2 receptor double knock-out

CB_1: ..... type 1 cannabinoid receptor

CB_2: ..... type 2 cannabinoid receptor

CHO: ..... Chinese hamster ovary cell line

CHO-mDOR: ..... Chinese hamster ovary cell line overexpressed with mouse δ-opioid receptor

CHO-rMOR: ..... Chinese hamster ovary cell line overexpressed with rat μ-opioid receptor

CNS: ..... central nervous system

cpm: ..... counts per minute, the index of ionizing radiation

DAMGO: ..... [D-Ala^2,N-MePhe^4,Gly^5-ol]-enkephalin, selective MOR agonist

DMSO: ..... dimethyl sulphoxide

DOR: ..... δ-opioid receptor

DPDPE: ..... [D-Pen^{2,5}]-enkephalin hydrate, selective DOR agonist

EC_{50}: ..... the agonist concentration that produces 50% of the maximal possible effect of ligand; it is the index for ligand potency

ECL: ..... extracellular loop

EGTA: ..... ethyleneglycol-tetraacetate

E_{max}: ..... the maximal effect of a G-protein after ligand modulated activation in a given tissue preparation; it is the index of G-protein efficacy

FDA: ..... Food and Drug Administration

GABA: ..... γ-aminobutyric acid

GDP: ..... guanosine 5'-diphosphate

GI: ..... gastrointestinal

GPCR: ..... G-protein coupled receptor

GRAFS: ..... Glutamate, Rhodopsin, Adhesion, Frizzled/Taste, Secretin; a GPCR classification system

GTP: ..... guanosine 5'-triphosphate

GTPγS: ..... Guanosine-5'-O-[γ-thio] triphosphate

IC_{50}: ..... the concentration of a drug that inhibits 50% of the specific binding of a competitor ligand; it is the index for a molecule's affinity

ICL: ..... intracellular loop

$Ile^{5,6}$deltorphin II: ..... Tyr-D-Ala-Phe-Glu-Ile-Ile-Gly-NH_2, a selective DOR agonist

JOM-6: ..... H-Tyr-c(S-Et-S)[D-Cys-Phe-D-Pen]NH_2, a selective MOR agonist

K_i: ..... equilibrium inhibition constant; it is the index for a molecule's affinity

KOR: ..... κ-opioid receptor

MMFF: ..... Merck Molecular Force Field family

MOR: ..... μ-opioid receptor

NAcc: ..... nucleus accumbens

nor-BNI: ..... norbinaltorphimine

PAG: ..... periaqueductal gray

pCHO: ..... parental CHO cell line

PLC: ..... phospholipase C

PMSF: ..... phenylmethanesulfonyl fluoride

rim.: ..... rimonabant

S.E.M.: ..... standard error of means

SGR: ..... substantia gelatinosa of Rolando

SN: ..... substantia nigra

TEM: ..... Tris-HCl, EGTA, $MgCl_2$

THC: ..... tetrahydrocannabinol

TM: ..... transmembrane domain

Tris-HCl: ..... tris-(hydroxymethyl)-aminomethane hydrochloride

w.t.: ..... wild type

1 REVIEW OF THE LITERATURE

1.1 G-protein coupled receptors (GPCR)

1.1.1 About GPCRs in general

Cell surface receptors are specialized integrated membrane (in most of the cases transmembrane) proteins, which take part in the communication between the cell's intra- and extracellular environments by sensing different types of extracellular signaling molecules. The molecule sensing initiates with the binding of the "first messenger" molecule (ligand) to the receptor, which triggers chemical alterations in the intracellular side of the cell. These chemical changes are called signal transduction and it is an essential biological process for the cell to maintain its own homeostasis, cellular activity or even the communication between other cells if possible. Among the cell surface transmembrane proteins the G-protein coupled receptors (GPCR) are one of the largest and diversified, encoded by more than 800 genes in the human genome [1]. GPCRs are only present in eukaryotic cells, mostly widespread within the Metazoa (animals) kingdom [1–3]. According to the GRAFS classification system [1] there are five main families within the GPCR superfamily: the glutamate (15 members), the rhodopsin-like (701 members), the adhesion (24 members), the frizzled/taste (24 members) and finally the secretin-like receptor family (15 members). One of the remarkable features of the GPCR superfamily is the large variety of extracellular signals that the receptors can detect, such as photons, odorants, ions, small organic molecules like lipids, catecholamines, as well as neuropeptides and the larger glycoproteins [4,5]. Because of the vast diversity of GPCRs they have a crucial role in numerous regulatory processes in physiological as well as in pathological conditions, which makes this receptor superfamily a very promising pharmacological target [6–9]. The importance of GPCRs is also emphasized by the fact that the 2012 Nobel Prize in Chemistry was awarded "for studies of G-protein-coupled receptors" by the work of Brian Kobilka and Robert Lefkowitz (**Fig. 1E**; see web reference [A]).

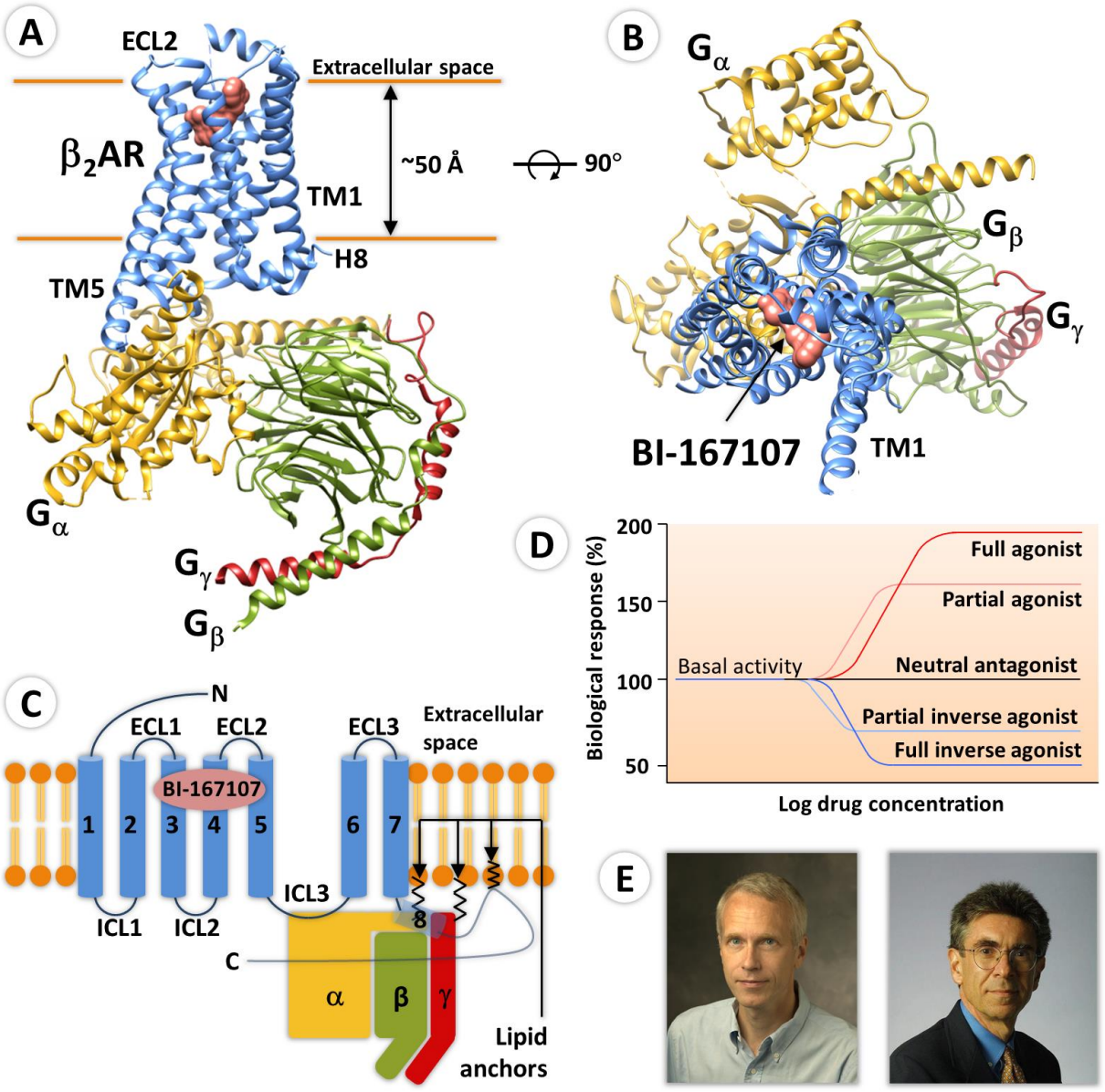

Figure 1 **A** and **B**: **The side and extracellular view of the 3D crystal structure of the β_2AR-G_s protein complex together with the β_2AR agonist BI-1617107**. The figures were constructed with Chimera [10], (a program for interactive visualization) based on the protein data bank ID of the receptor-ligand complex (PDBP ID: 3SN6). **C**: **The schematic 2D structural view of the β_2AR-G_s protein complex viewed along the lipid bilayer.** The blue cylinders indicate the transmembrane helixes numbered as 1-7, and the 8th helix (8) is also represented transparently. The 2D figure also highlights the lipid anchors of the receptor (palmitate [11]), the G_α (myristate/palmitate [11]) and the G_γ (isoprenylate [11]). 'α', 'β' and 'γ' indicates the G-protein subunits. The schematic structure of the heterotrimeric G-protein was constructed according to the review of Oldmann and Hamm [12], with modifications. **D**: **The spectrum of GPCR ligand efficacy.** The figure was constructed according to the review of Rosenbaum and co-workers [4] with modifications. **E**: **Brian Kobilka (left) and Robert Lefkowitz (right).** They received the 2012 Nobel Prize in Chemistry "for studies of G-protein-coupled receptors". **Abbreviations**: β_2AR: β_2-adrenergic receptor, ECL: extracellular loop, ICL: intracellular loop, TM: transmembrane domains.

1.1.2 The structure of GPCRs

In the past 12 years the number of solved GPCR crystal structures has grown exponentially, owing to innovative crystallography methods and protein engineering techniques [13,5]. Today more than 75 GPCR crystal structures of 18 different rhodopsin-like GPCRs have been determined [5], including notable GPCRs like rhodopsins, β-adrenoreceptors, dopamine and also opioid receptors.

The structure of all members of the GPCR superfamily can be divided into three parts [5,14] (**Fig 1A-C**): (1) the extracellular region, containing the N terminus and three extracellular loops (ECL1-ECL3); (2) the transmembrane (TM) region, consisting seven α-helices (TM1-TM7) and finally (3) the intracellular region, consisting of three intracellular loops (ICL1-ICL3), an intracellular amphipathic helix (H8), and the C terminus. Overall the extracellular region modulates ligand access; the TM region forms the structural core of the receptor, binds ligands which then induce conformational changes in the TM region [5]. This information is transmitted to the intracellular region which associates with cytosolic signaling proteins, most of all G-proteins (**Fig 1A-C**), but GPCR kinases, arrestins can also interact with GPCRs.

1.1.3 The spectrum of GPCR ligand efficacy and constitutive activity of GPCRs

There are several intermediate structure states of GPCRs, which are stabilized by distinct ligands [15–17]. The agonist type ligands stabilize the active conformational state of the GPCR [15], which then allows the receptor to alter the G-proteins conformation to the active (GTP-bound; see section **1.1.4**) state. In contrast, inverse agonists stabilize the inactive state of the receptor, in which the G-protein remains in the inactive state (GDP bound state; see section **1.1.4**; [18,19]). At the same time neutral antagonists are believed to bind equally to both receptor states, usually with a high affinity, thus possessing a physiological role by competitively inhibiting agonist and inverse agonist binding [18,19]. Accordingly there is a spectrum of efficacies of GPCR ligands initiating from the full and partial inverse agonists, through neutral antagonists to partial and full agonists [18] (**Fig 1D**). However there is increasing number of evidence showing that GPCRs still have low activity in the absence of an agonist ligand, thus they possess a constitutive or basal activity [18,19]. Agonists increase, inverse agonists decrease, while neutral antagonists do not alter GPCR basal activity. Interestingly in absence of basal receptor activity inverse agonists behave as competitive antagonist [20], which explains why many of the compounds originally described as neutral

antagonists, turned out to be inverse agonists [18]. Inverse agonism is a relatively new phenomenon, and according to increasing numbers of studies it has a potential therapeutic application against cancer [20] and other human diseases [21–24]. Rimonabant, one of the protagonist of this thesis is an inverse agonist too, and it will be discussed under section **1.3**.

1.1.4 GPCR signaling: the G-protein activation/deactivation cycle

Heterotrimeric G-proteins are often called molecular switches, since they can initiate and terminate intracellular signaling cascades generated by GPCRs during extracellular stimuli. G-proteins consist of three subunits: α, β and γ, where the G_α is the "main switch" and the only G-protein subunit making direct contact with the receptor, while G_β and G_γ form a functional unit, and can only be dissociated in denaturing conditions [25]. The key to the mediatory role of G_α is its GTP/GDP binding ability and GTPase (GTP hydrolyzing) activity.

After agonist-mediated conformational change of the receptor, the assumed pre-associated G-protein [26] also switches to the active conformational state, which allows the G_α subunit to exchange the already bound GDP to GTP (**Fig. 2**, step 2). The nucleotide exchange process then promotes the heterotrimeric complex to dissociate from the receptor and to divide to G_α and $G_{\beta\gamma}$ subunits, which afterwards interact with distinct effector molecules separately (**Fig. 2**, step 3). The effectors can be enzymes such as adenylyl cyclase, or phospholipases, and they can also be ion channels like G-protein-activated inwardly rectifying K^+ channels. Eventually the G_α subunit will hydrolyze the bound GTP back to GDP (**Fig. 2**, step 4), due to its intrinsic GTPase activity, restoring the initial state by re-associating with the $G_{\beta\gamma}$ subunit and starting a new cycle [12,27,28] (**Fig. 2**, step 4). The G-protein activation/deactivation cycle can be studied by the [^{35}S]GTPγS binding assay which will be discussed in detail under section **3.5.3**.

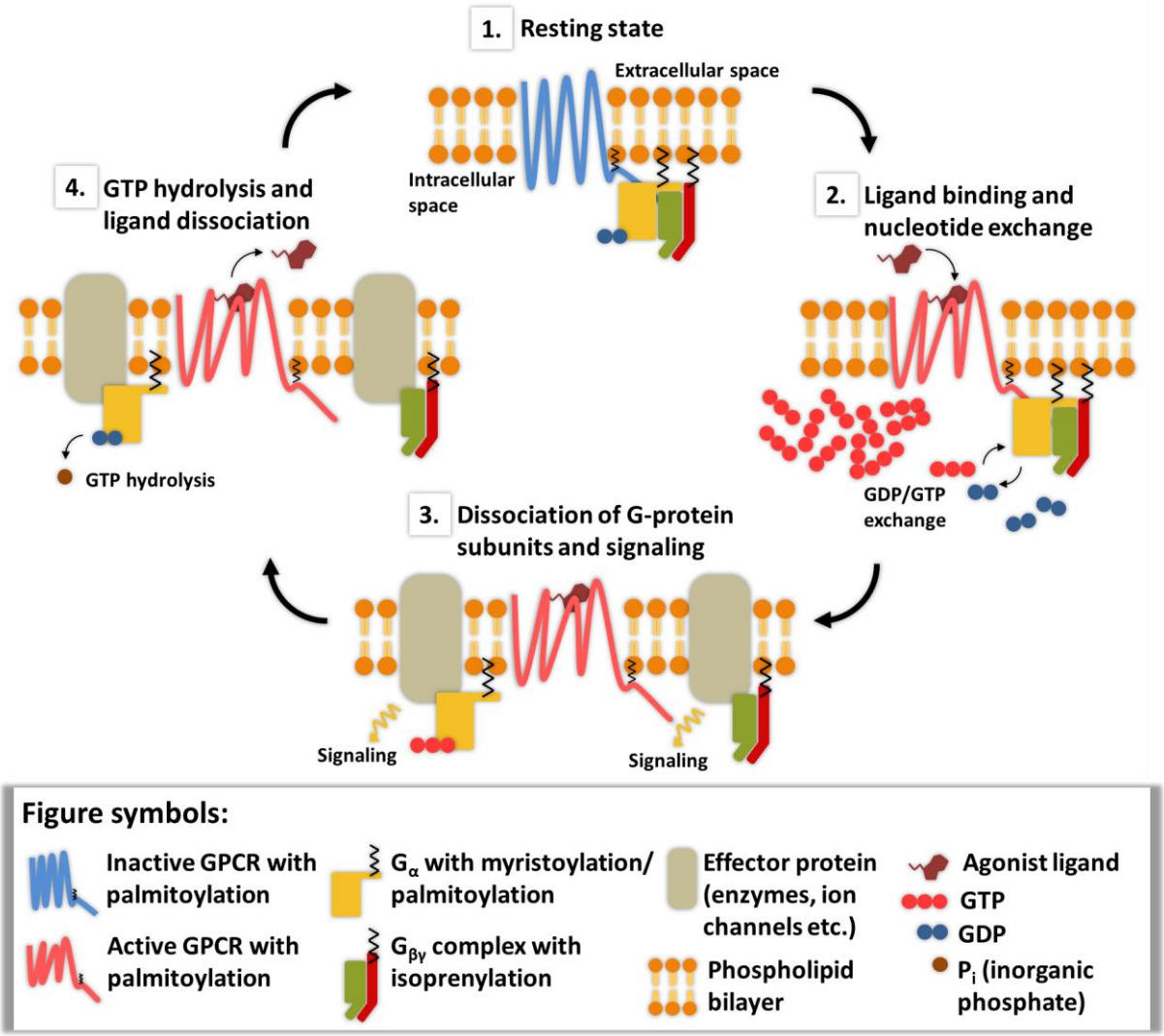

Figure 2 **The G-protein activation/deactivation cycle.** For detailed description see section **1.1.4**. Note the higher levels of GTP in step 2 compared to GDP, this is to insure the GDP/GTP exchange [12]. The hydrolyzed free phosphate ion is referred to as inorganic phosphate; this is to distinguish it from bound phosphates. The basis of the figure was constructed according to the following figure: http://en.wikipedia.org/wiki/File:GPCR_cycle.jpg. The [^{35}S]GTPγS binding assay is illustrated under **Fig. 7** with similar symbols.

1.1.5 The complexity of GPCR signaling

From the 23 encoded human G_{α} proteins four G-protein classes has been described: $G_{\alpha s}$, $G_{\alpha i/o}$, $G_{\alpha q/11}$ and $G_{\alpha 12/13}$ (in case of β and γ there are 6 and 12 G-protein classes) and they can interact with different types of effectors or they can alter their function differently [29]. Stimulation of the $G_{\alpha s}$ subunit activates adenylyl cyclase (AC; [30]), while stimulation of the $G_{\alpha i/o}$ subunit results AC inhibition [31]. Inducing $G_{\alpha q/11}$ activates phospholipase C (PLC; [32]) whereas $G_{\alpha 12/13}$ is involved in the regulation of cell growth [33]. Additionally $G_{\alpha i/o}$ and $G_{\alpha s}$ subunits can go through ADP-ribosylation catalyzed by pertussis (produced by *Bordetella pertussis*) and cholera toxins (produced by the *Vibrio cholerae*) respectively [12,34]. The ADP-ribosylation prevents both G-proteins to function normally, resulting altered AC activity levels compared to normal levels.

The relatively few types of G-protein compared to the vast number of GPCR subfamilies results that G-proteins can interact with many different types of GPCRs, and also many receptors can activate different types of G-protein signaling pathways [12]. The complexity of GPCR signaling is augmented by the large GPCR binding surface of the G-protein [12] which enables it to interact with multiple GPCRs simultaneously. Moreover receptor homo-, and heterodimerization, or even oligomerization is a common phenomenon in the GPCR superfamily [35–37]. Thus it is not surprising that GPCRs can cross-regulate each other's signaling pathways, communicate with one and other, altering each other's physiological responses [29,38–41]. Also there is an emerging concept in GPCR signaling referred to as "biased agonism" or "ligand-directed signaling", which declares that distinct agonists can initiate different active receptor conformational states, which in turn initiates distinct signaling pathways [20,42,43].

1.2 Opioids and cannabinoids and their endogenous systems

1.2.1 Opium poppy and the cannabis plant, opioids and cannabinoids

The usage of the opium poppy (*Papaver somniferum*; **Fig. 5A**) and the cannabis plant (*Cannabis sativa*, *Cannabis indica*, *Cannabis ruderalis*; **Fig. 5B**) as an agricultural plant, medicine or as a recreational drug dates back to ancient history [44,45]. Opium and marijuana are the most known and used recreational drugs derived from the plants. Opium is the dried latex extracted from the ripening pods of the poppy (**Fig. 5A**), while marijuana is the dried flowers and leafs of the female cannabis plant [44,45]. Opium is known for its anesthetic, euphoric and narcotic effects, accompanied by strong withdrawal and addictive effects, while marijuana causes relaxation, increases the appetite and also enhances the enjoyment of tastes, sounds and smells [44,45]. The main psychoactive compound of the opium and marihuana is morphine (**Fig. 5C**) and Δ^9tetrahydracannabinol (THC; **Fig. 5D**) respectively [44,45]. Apart from morphine and THC, there are several other opium poppy and cannabis plant-derived molecules, together with semi- and fully synthetic derivatives which are all together called opioids and cannabinoids respectively (**Fig. 5C** and **D**). Today a lot of effort is being invested into the research of these molecules to maintain or increase the benefits of their natural derivatives while reducing their disadvantages so they can be applied safely for therapeutics.

1.2.2 Opioid and cannabinoid receptors

Opioids and cannabinoids have their specific endogenous receptors: the opioid [46–48] and the cannabinoid receptors [49–51] (**Fig. 3**). Three types of opioid receptors have been determined: μ-,κ- and δ-opioid receptors [52–56] (MOR, KOR, DOR respectively; **Fig. 3**), which were later supplemented by the nociceptin receptor [57]. However the nociceptin receptor is still

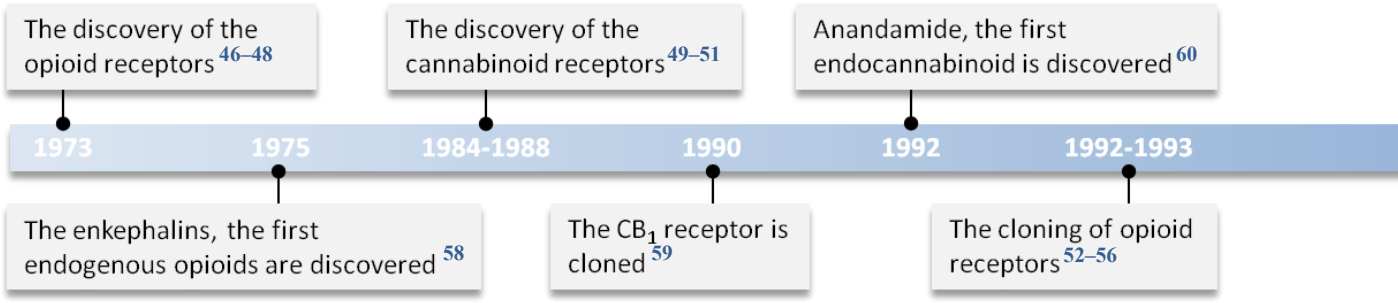

Figure 3 **Milestones in opioid and cannabinoid research I.** The figure is loosely based on the figure in review [44] .

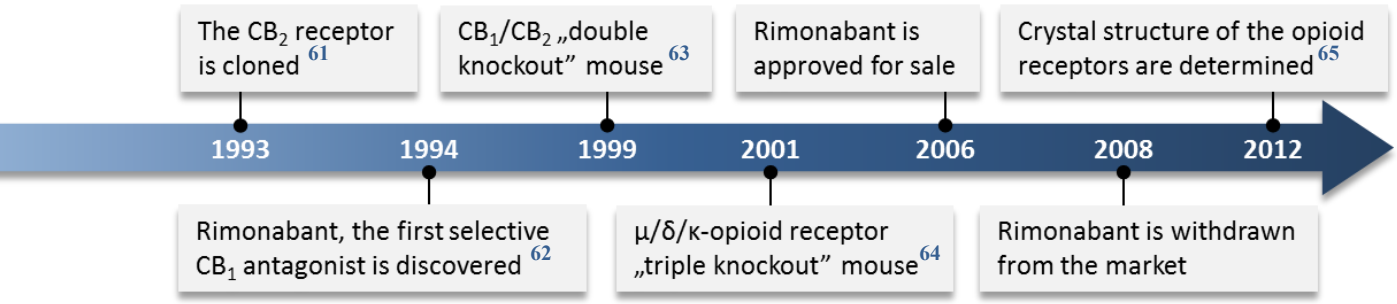

Figure 4 **Milestones in opioid and cannabinoid research II.** The figure is loosely based on the figure in review [44].

being treated separately from "the three classic" opioid receptors, because the semi-synthetic neutral opioid antagonist, naloxone cannot inhibit nociceptin receptor specific binding, unlike the other three opioid receptors binding [45]. The cannabinoid receptor family has two types the type 1 and 2 cannabinoid receptors [59,61] (CB_1, CB_2; **Fig. 3 and 4**), and recently the G-protein coupled receptor 55 along with 119 and 18 (also known as GPR55, GPR119 and GPR18 respectively) are also believed to be cannabinoid receptors [66,67].

Both cannabinoid and opioid receptors belong to the GPCR super family and they mostly couple to $G_{\alpha i/o}$ type G-proteins [68,69], thus they inhibit AC activity [70,71], decrease calcium ion entry [69,72] and increase potassium ion efflux [69,73], which in turn inhibit the presynaptic release of different types of neurotransmitters such as GABA, noradrenaline, acetylcholine or dopamine [74,75]. The cellular actions add up to several important physiological functions which are listed in **Table I** together with the receptors central and peripheral distribution. Important to note that the CB_1 receptor is the most abundant GPCR in the brain, with ten times higher expression levels compared to other GPCRs.

1.2.3 The endogenous opioid and the endocannabinoid system

Besides endogenous opioid and cannabinoid receptors, endogenous opioid and cannabinoid ligands (or endocannabinoids) have also been identified (**Fig. 5C** and **D**). Endogenous opioids are peptide natured neurotransmitters, neuromodulators or even neurohormones [76,77], and the most notable ones are the enkephalins [58] (**Fig. 3**), endorphins [78], dynorphins [79], nociceptin [80] and endomorphins [81]. The endocannabinoids behave as neuromodulators, and are arachidonic acid derivatives [82,83], such as the arachidonoyl ethanolamide (anandamide; **Fig. 4**) [60], 2-arachidonoylglycerol [84] or noladin ether [85]. The endogenous opioids are synthesized from precursor proteins (prepro-opiomelanocortin,

preproenkephalin and preprodynorphin) [86,87], while the endocannabinoids are cleaved from phospholipid membranes or synthesized through the fatty acid synthesis [83]. These systems which comprise the enzymes which synthesize and degrade endogenous opioids and endocannabinoids, together with the receptors, which recognize them, are called the endogenous opioid and endocannabinoid system. Both systems are under strict regulation [83,88], however main difference is that the endocannabinoids are not synthesized in advance and stored in vesicles compared to endogenous opioids [89] or other neuromodulators, instead they are released "on demand" [82,83,90,91].

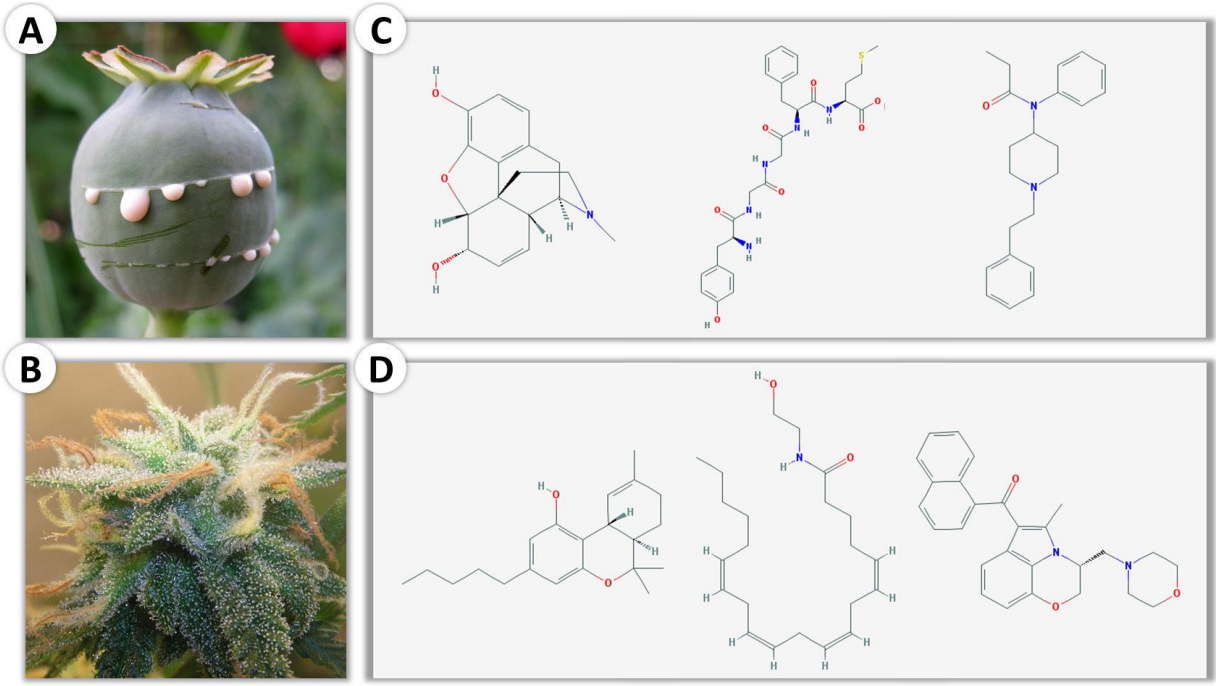

Figure 5 **A: The capsule of the opium poppy (*Papaver somniferum*).** The picture shows the capsule after a fresh incision, with the exuded latex-like raw opium. **B: Female flowering cannabis plant (*Cannabis indica*).** Note the small crystals on the flower, which are highly concentrated with THC. **C: Opioids.** From left to right: morphine (plant derived opium alkaloid), met-enkephalin (endogenous) and fentanyl (fully synthetic). **D: Cannabinoids.** From left to right: THC (plant derived or phytocannabinoid), anandamide (endocannabinoid) and WIN 55,212-2 (fully synthetic). Chemical structures were downloaded from http://www.ncbi.nlm.nih.gov/pccompound/.

1.2.4 Opioid and cannabinoid receptor interactions

It is known that the expression patterns of cannabinoid and opioid receptors overlaps in several parts of the CNS (see **Table I**). In certain forebrain regions, such as caudate putamen, dorsal hippocampus, substantia nigra, and nucleus accumbens, the MOR and CB_1 receptors are not only co-localized, but also co-expressed in the same neurons [92–94]. It has also been shown that these two receptors can be cross-regulated [95] via a direct [96] or indirect interactions [29,97], and they can also form heterodimers [98]. The CB_1 and DOR together with KOR can too allosterically alter each other's activity [97,99–101] and in case of DOR can form heteromers as well [101]. The interaction between these receptors results many overlapping physiological functions such as nociception [101–105], mood regulation [106,107], energy and feeding regulation [108,109], regulation of GI motility [110] or the mediation of ethanol effects [111]. There is also evidence for an interaction between the CB_2 and MOR in the mouse forebrain and brainstem, which was demonstrated by our group [112,113]. However the interaction between opioid and CB_2 receptors needs more detailed studies.

Table I **The distribution and physiological effects of opioid and cannabinoid receptors**

	Opioid receptors	Cannabinoid receptors
Distribution:	**μ:** PAG*, NAcc*, cerebral cortex*, amygdala*, thalamus, SGR, GI. tract **κ:** PAG*, NAcc*, amygdala*, SN* hypothalamus, SGR, GI. tract **δ:** cerebral cortex*, pontine nuclei, amygdala*, olfactory bulbs	**CB_1:** cerebral cortex*, NAcc*, amygdala*, hyppocampus, SN*, basal ganglia, PAG*, cerebellum, GI. tract, pituitary gland, adypocites, Leydig cells, sperms, ovary **CB_2:** macrophages, monocytes, T- and B-cells, neuronal and glial cells of: cerebral cortex, striatum, amygdala, hippocampus, cerebellum, brainstem, spinal cord
Physiological effects:	**μ:** analgesia, miosis, physical dependence, respiratory depression, euphoria, reduced GI. motility **κ:** analgesia, miosis, sedation, dysphoria **δ:** analgesia, euphoria, physical dependence, antidepressent effect	**CB_1:** maintenance of homeostasis, analgesia, appetite control, role in short-term memory and cognition, emotional processing **CB_2:** maintenance of homeostasis, neuroprotection, controlling proliferation, differentiation and survival of neuronal and non-neuronal cells

* denotes the CNS regions where opioid and CB_1 receptors are proved to interact with each other and are co-expressed. The table was constructed based on the following publications: [45,74–76,83,102,114–116]

1.3 Rimonabant

1.3.1 The CB_1 receptor and appetite, Acomplia®

Increased hunger has been long associated with Cannabis use [117–119], also there is extensive evidence that the endocannabinoid system, especially the CB_1 receptor is involved in the control of appetite and feeding (for review see [120]).

SR141716, or rimonabant (**Fig. 6A**) was developed as a highly selective CB_1 antagonist, sponsored by Sanofi Aventis (now Sanofi S.A.) [62], with a K_i of 5.6 nM towards its specific receptor. For comparison, rimonabant binds to CB_2 receptors with >1000 nM K_i. Rimonabant can effectively antagonize most of the effects of different types of CB_1 agonist both *in vivo* and *in vitro* [116,121] and according to preclinical animal, and clinical human studies showed a clear efficacy for the treatment of obesity (for review see: [122,123]). In 2006 The European Commission approved the sale of rimonabant in the European Union and was first introduced in the United Kingdom under the trade name Acomplia® (**Fig. 6B**).

The weight-loss effect of rimonabant is believed to be mostly accomplished through the peripheral CB_1 receptors on adipocytes and hepatocytes, by decreasing lipogenesis (for review see: [120,124]). Rimonabant is also able to pass through the blood-brain-barrier (BBB) [121], therefore it can interact with CB_1 receptors expressed in brain areas which are implicated in the reinforcing effects of natural reinforces such as food (for review see: [120,124]).

1.3.2 The psychiatric side effects and unspecific actions of rimonabant

Interacting with CB_1 receptors that are working together with the reinforcing/reward system might result unspecific actions of rimonabant. Indeed according to Christensen and colleagues [125] during the clinical trials patient were experiencing psychiatric pathographies such as anxiety, depression, mood alterations or suicidal thoughts during 20 mg rimonabant treatment. The psychiatric side effects were also affirmed by the United State Food and Drug Administration's (FDA) briefing document (see web reference [B]), which led to the disapproval of rimonabant marketing authorization in the US. These findings were culminated when four patients committed suicide in the rimonabant group during the study period, which resulted the withdrawal of rimonabant in 2008 by the European Medicines Agency (see web reference [C]).

Many studies revealed that rimonabant can produce effects opposite to cannabinoid agonist *in vivo* and *in vitro*, that is it can behave as an inverse agonist (see section, for review see [123]). It is also believed that its anorectic effect is due this pharmacological property [120,124]. Additionally, before as well as after entering rimonabant to the market there were several publications indicating its non-CB_1 receptor related actions [126,127], partly its inverse agonistic effects [126,128–130] and its dose related side effects [125,131,132]. These reports also established a rather unspecific behavior at higher concentrations (for review see [133,134]). Yet again these unspecific actions can endow rimonabant with promising therapeutical applications in drug dependence (for review see [135]).

1.3.3 Interactions of rimonabant with the opioid system

Rimonabant can interact with other members of the GPCR family, such as opioid receptors (for review see [134]). It has been shown that it can affect the function of MOR through the CB_1 receptor (for review see [135,136]), additionally when studied in behavioral aspects rimonabant reduced opiate self-administration and reward [137–139] and suppress morphine-induced feeding [140]. There are increasing numbers of studies reporting a direct effect of rimonabant on opioid receptors. According to previous direct binding affinity measurements rimonabant is able to bind to all three classic opioid receptors with a relatively high, micromolar concentrations [128,141,142]. It has been also demonstrated that KOR agonist ligand potency can be reduced by rimonabant *in vitro* during agonist-stimulated KOR G-protein activation [143]. Additional *in vitro* assays also excluded a possible allosteric modulatory effect of rimonabant on MOR and DOR [142]. Furthermore, Lockie and co-workers revealed that the opioid system is involved in modulating both the metabolic and mood effects of rimonabant [144].

Also many studies described the effectiveness of combined rimonabant and opioid antagonist treatment. For instance the combination of low dose rimonabant with low dose naloxone/naltrexone can reduce food intake and ethanol intake more effectively than administrating them separately in similar doses (for review see [145,146]).

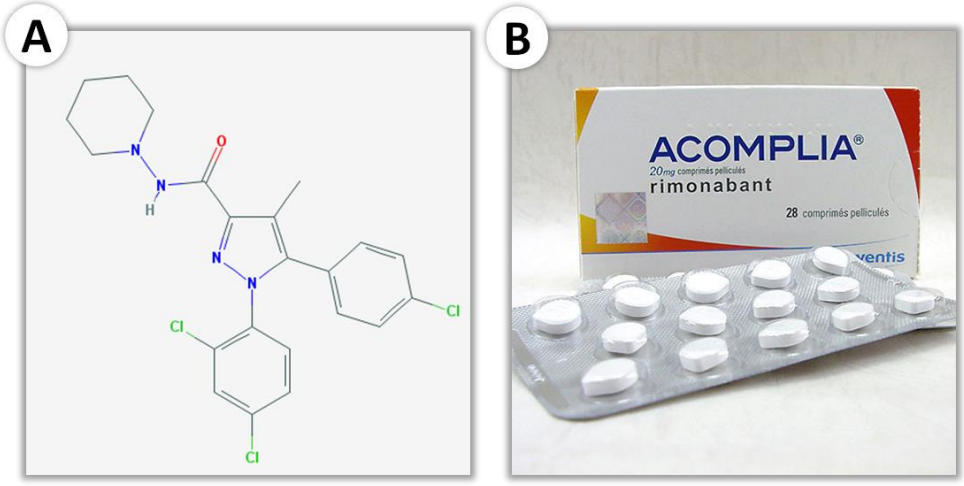

Figure 6 **A**: **The structure of rimonabant**. Systematic name: 5-(4-Chlorophenyl)-1-(2,4-dichloro-phenyl)-4-methyl-N-(piperidin-1-yl)-1H-pyrazole-3-carboxamide. The chemical structure of rimonabant was downloaded from http://www.ncbi.nlm.nih.gov/pccompound/. **B**: **Acomplia® packaging containing 20 mg rimonabant**.

2 AIMS OF THE STUDY

The unspecific behaviour of rimonabant together with its ability to pass through the BBB partly caused its dramatic failure as an authorized anorectic drug (see section **1.3.2**). Additionally the CB_1 receptor is the most widespread GPCR in the brain integrated in different types of neurological pathways such as dopamine pathways [147], which can also explain the psychiatric side effects of rimonabant.

Now it is known that the opioid receptors are also expanded to the unspecific actions of rimonabant (see section **1.3.3**). Most of the studies examining the actions of CB_1 antagonist on opioid receptors are reported to be mediated through CB_1 receptors, but very few studies examine the direct effect of rimonabant on opioid receptors. Herein we clarify whether rimonabant can interact with MOR and DOR directly at the level of ligand-receptor and receptor-G-protein interaction. MOR was chosen because it is one of the most studied opioid receptors, mainly because of their role in pain management [148]. The DOR is relatively studied in a less extent compared to its two other companions, especially to MOR [149]. However, recently there are several studies showing DOR as a potential therapeutic target (for review see [150]). This thesis is part of an overall study, which also investigates the possible direct effect of rimonabant on KOR, however due to page limitations only selections of the results are presented here [151,152].

The aims of the study presented in this thesis were the following:

- To measure the binding affinity of rimonabant towards MOR and the role of the CB_1 receptor in the binding in competition binding assays with MOR specific radioligands performed in wild type and CB_1 knock-out forebrain membranes and in Chinese hamster ovary (CHO) cell membranes overexpressed with rat MORs (CHO-rMOR).

- To characterize the binding capacity of rimonabant on DOR in competition binding assays carried out with DOR specific radioligands accomplished in CHO cell membranes overexpressed with mouse DORs (CHO-mDOR).

- To dock rimonabant into the active and inactive homology model of MOR and also to analyze the docking energies and poses of the compound in docking experiments

- To investigate the effect of rimonabant on DOR mediated G-protein activity in functional [^{35}S]GTPγS binding assays carried out in CHO-mDOR membranes.

- To analyze the impact of rimonabant on DOR mediated G-protein activity after agonist stimulation in functional [^{35}S]GTPγS binding assays accomplished in CHO-mDOR membranes.

- To examine the effect of rimonabant on agonist-stimulated MOR and DOR G-protein activity and the possible role of cannabinoid receptors in the observed actions in the forebrain region in [^{35}S]GTPγS binding assays carried out in wild type and CB_1 or CB_1/CB_2 knock-out mouse forebrain membranes.

3 MATERIALS AND METHODS

3.1 Chemicals

3.1.1 Radiochemicals

[^{3}H]DAMGO (specific activity: 41 Ci/ mmol), [^{3}H]naloxone (specific activity: 31 Ci/ mmol) and [^{3}H]Ile^{5,6}deltorphin II (specific activity: 28 Ci/mmol; [153]) was radiolabeled in the Isotope Laboratory of BRC (Szeged, Hungary). [^{3}H]naltrindole (specific activity: 24 Ci/mmol) was purchased from PerkinElmer (Boston, USA). The radiolabelled GTP analogue, [^{35}S]GTPγS (specific activity: >1000 Ci/mmol) was purchased from the Isotope Institute Ltd. (Budapest, Hungary).

3.1.2 Receptor ligands and fine chemicals

The CB_1 receptor antagonist SR141716 (rimonabant) was acquired from Santa Cruz (Dallas, Texas, USA) and was also provided by SANOFI Research Laboratory (Montpellier, France). The enkephalin analog Tyr-D-Ala-Gly-(NMe)Phe-Gly-ol (DAMGO) was obtained from Bachem Holding AG (Bubendorf, Switzerland). The MOR agonist morphine was obtained from the Alkaloid Chemical Factory (Tiszavasvári, Hungary). The modified DOR specific deltorphin II derivative, Ile^{5,6}deltorphin II was synthesized in the Isotope Laboratory of Biological Research Center (Szeged, Hungary). The DOR specific agonist peptide [D-Pen^{2,5}]-enkephalin hydrate (DPDPE), the DOR antagonist naltrindole, the KOR specific agonist U50488 and the adrenerg receptor agonist L-epinephrine were purchased from Sigma-Aldrich (St. Louis, MO, USA). The opioid antagonist naloxone was kindly provided by the company Endo Laboratories DuPont de Nemours (Wilmington, DE, USA). Ligands were dissolved in ultrapure distilled water, except rimonabant which was dissolved in DMSO. All applied receptor ligands were stored in 1 mM stock solution at -20 ˚C. Tris-HCl, EGTA, NaCl, $MgCl_2$ x $6H_2O$, GDP, the GTP analogue GTPγS were obtained from Sigma-Aldrich (St. Louis, MO, USA). The UltimaGold^{TM} MV aqueous scintillation cocktail was purchased from PerkinElmer (Boston, USA).

3.2 Animals

The CB_1 receptor knockout (CB_1 K.O.) mice and their wild type controls (w.t.) were generated on CD1 background in Dr. Ledent's lab as described in Ledent et al., 1999 [154]. The CB_1 / CB_2 receptor double knockout mice were provided by Dr. Andreas Zimmer's laboratory (University of Bonn, Germany), the lack of both cannabinoid receptors was confirmed in previous studies [63]. The wild type mice were bought from the local animal house of the Biological Research Center (Szeged, Hungary). Both mice genotypes were derived from the C57BL/6J strain. For membrane preparations 6-8 animals were used. All the animals were housed at 21-24 ˚C under a 12:12 light: dark cycle and were provided with water and food *ad libitum*. All housing and experiences were conducted in accordance with the European Communities Council Directives (86/609/ECC) and the Hungarian Act for the Protection of Animals in Research (XXVIII.tv. 32.§).

3.3 Cell lines

Chinese hamster ovary cells (CHO) stably transfected with rat MOR or mouse DOR cDNA (CHO-rMOR and CHO-mDOR respectively) were provided by Dr. Zvi Vogel (Weizmann Institute of Science, Israel). The cell lines were previously characterized by Avidor-Reiss and co-workers together with Ioja and co-workers [155–157]. Parental CHO (pCHO) cell lines were kindly provided by Dr. Melinda Pirity (Biological Research Center, Szeged, Hungary)

CHO-rMOR and CHO-mDOR cells were grown in Dulbecco's modified Eagle's medium (DMEM, Gibco) and in α-minimum essential medium (αMEM, Gibco), respectively. Both media were supplemented with 10% fetal calf serum, 2 mM glutamine, 100 IU/ml penicillin, 100 mg/ml streptomycin, 25 mg/ml fungizone and 0.5 mg/ml geneticin. Parental CHO cells (pCHO) were cultured in F-12 medium with L-glutamine which contained 10% fetal bovine serum. Both CHO cell lines were kept in culture at 37˚C in a humidified atmosphere consisting of 5% CO_2 and 95% air.

3.4 Membrane preparations

3.4.1 Mouse forebrain membrane preparations

Forebrain membrane fractions from CB_1 K.O. and CB_1/ CB_2 K.O. mice and their wild type controls were prepared according to the method previously described [158]. Briefly, mice were decapitated and the brain was quickly removed. The forebrain part was collected and homogenized on ice in 50 mM Tris-HCl buffer (pH 7.4) with a Teflon-glass homogenizer. The homogenate was centrifuged at 18,000 rpm for 20 min at 4˚C and the pellet was resuspended in fresh buffer and incubated for 30 min at 37˚C. This centrifugation step was repeated, and in case of competition binding experiments the final pellet was resuspended in 50 mM Tris-HCl buffer (pH 7.4) containing 0.32 M sucrose and stored at −80˚C until use. For [^{35}S]GTPγS binding assays the final pellet was suspended with ice-cold 50 mM Tris–HCl pH 7.4, 1 mM EGTA, 5 mM $MgCl_2$ (TEM) buffer to obtain the appropriate protein content for the assay (~10 μg/ml).

3.4.2 Cell line membrane preparations

Membranes were prepared from subconfluent cultures. Cells were rinsed three times with PBS and kept in -80 ˚C for one hour. Afterwards the cells were centrifuged at 3000 rpm for 10 minutes. The cells were then suspended in either 50mM Tris-HCl (for competition binding experiments) or TEM (for [^{35}S]GTPγS binding assays) buffer and homogenized with glass/glass homogenizer in ice-bath. Homogenates were centrifuged two times at 18.000 rpm for 20 minutes. The final pellet was resuspended in TEM buffer and stored in aliquots at -80 ˚C until use.

3.5 *In vitro* binding assays

3.5.1 The principles of *in vitro* binding assays

Binding assays allows us to characterize radiolabeled or unlabeled ligands and at the same time we can gather information about the binding capacity or even the functionality of an observed receptor [159,160]. The basis of the assays is to add a radioactive compound to a protein homogenate, membrane fraction, cell culture etc. and then incubate them together in certain conditions until the equilibrium binding is reached. Afterwards the bound and free radioactive ligands can be separated from each other; therefore the amount of bound radioactive ligand can be measured.

During the binding assays with radioactive compounds the radiolabeled molecule can not only bound to its own specific binding site, but also to other non-specific sites such as on cell membranes or other sites of the target protein. This phenomenon is called non-specific binding and it must be subtracted from the measured total binding. To determine the level of non-specific binding, the radioactive ligand must be incubated together with an unlabeled ligand which is highly specific to the same target protein as the radioactive compound (usually it is the unlabeled form of the radioactive ligand). It is important to add the unlabeled ligand in a much higher concentrations than the radioligand itself so that it can be surely "displaced" from its specific binding site by the unlabeled ligand. Accordingly the only detectable radioactivity is due to the non-specific binding of the radioligand.

Important to note that in receptor binding assays a point of reference should be applied, which just only contains the radioactive ligand and the target protein source. This is referred to as total specific binding and it allows comparing when other unlabeled molecules are in the system.

3.5.2 Radioligand competition binding assays

The radioligand competition binding experiment is a type of binding assay, where we apply the radioactive ligand in fixed concentrations in the presence of increasing concentrations of an unlabeled ligand. If the unlabeled ligand has specificity towards the receptor as the radioligand, they will "compete" with each other for the same binding site and the unlabeled ligand will displace the radioligand in a concentration dependent manner. The displacement will be indicated by the reduced detected radioactivity in the sample. This way we can receive binding affinity information about the applied unlabeled ligand, that is why it is called an indirect receptor binding assay, since the informations are gathered through the radioligand. There are two types of radioligand competition binding experiments: homologous and heterologous. In homologous competition binding experiments the radioligand and the unlabeled competitor ligand only differ in the presence of radioactivity, while in case of heterologous competition binding assays the two compounds are chemically distinct as well.

Firstly, in case of CB_1 K.O. forebrain membranes and their wild type controls the frozen aliquots were first centrifuged (18000 rpm, 20 min, 4˚C) to remove sucrose and the pellets, together with pCHO, CHO-rMOR, and CHO-mDOR membranes were suspended in 50 mM Tris-HCl buffer (pH 7.4) to reach the appropriate protein content for the assay (0.2-0.5 mg/ml/tube). Membranes were incubated with gentle shaking at certain conditions depending on the radioligand ([^{3}H]DAMGO: 35˚C for 45 min; [^{3}H]naloxone: 0˚C for 60 min; [^{3}H]Ile^{5,6}deltorphin II: 35˚C for 45 min; [^{3}H]naltrindole: 25 ˚C for 60 min). The final volume of the incubation mixture was 1 ml containing approximately 1 nM of radioligand and increasing (10^{-10} - 10^{-5} M) concentrations of unlabeled rimonabant or DAMGO or Ile^{5,6}deltorphin II, depending on the experiment. The non-specific binding was determined in the presence of 10 μM unlabeled naloxone. The reaction was terminated by rapid filtration under vacuum (Brandel M24R Cell Harvester), and washed three times with ice-cold 50 mM Tris-HCl (pH 7.4) buffer through Whatman GF/C ([^{3}H]DAMGO, [^{3}H]Ile^{5,6}deltorphin II) or GF/B ([^{3}H]naloxone, [^{3}H]naltrindole; which was washed in 3% polyethylenimine for 60 min to reduce non-specific binding) glass fiber filters. The radioactivity of the filters was detected in UltimaGold^{TM} MV aqueous scintillation cocktail with Packard Tricarb 2300TR liquid scintillation counter. The competition binding assays were performed in duplicates and repeated at least three times.

3.5.3 Functional [^{35}S]GTPγS binding assays

During [^{35}S]GTPγS binding assays we monitor the target receptor mediated G-protein activation, namely the GDP → GTP exchange of G_α, in the presence of a certain ligand concentration. The nucleotide exchange is measured by a non-hydrolysable, radioactive GTP analogue called [^{35}S]GTPγS, which contains a sulphur 35 isotope (^{35}S) in the γ phosphate group instead of an oxygen atom. Because of the γ-thiophosphate bound the [^{35}S]GTPγS withstand the GTPase activity of G_α, thus it cannot hydrolyze to GDP and the G-protein cannot reassociate to a heterotrimer (**Fig. 7**, compare with **Fig. 2** and see section **1.1.4**). As a consequence the G_α bound with [^{35}S]GTPγS accumulates and we can measure the incorporated ^{35}S radioactivity in the samples (**Fig. 7**, step 4). If we add an agonist to the experimental system the receptor will be activated resulting a higher GDP → [^{35}S]GTPγS exchange (**Fig. 7**, step 2) with higher radioactivity in the assay compared to the receptors basal activity (see section **1.1.3**). In the presence of an inverse agonist (see section **1.1.3**) the GDP → [^{35}S]GTPγS exchange reaches lower levels compared to basal activity resulting lower radioactivity. In both cases the actions are concentration dependent. Since an antagonist does not alter its target receptors basal activity (see section **1.1.3**) no difference in the nucleotide exchange is detected compared to basal activity. Accordingly the [^{35}S]GTPγS binding assay is capable to distinguish the binding character of a ligand, and also it can give us information about the target receptor mediated G-protein efficacy and the activator ligand potency (see section **3.7**) Worth of note that the total specific binding (which only contains the radioactive molecule) in the [^{35}S]GTPγS binding assay also indicates the basal activity of the target receptors G-protein. In addition the [^{35}S]GTPγS binding assay is more feasible for monitoring G_i type G-proteins [161].

The assays were performed according to previous studies [162,163], with slight modifications. Membrane fractions of pCHO, CHO-rMOR, CHO-mDOR, CB_1 K.O., CB_1/CB_2 K.O. and wild type mouse forebrains were incubated in a final volume of 1 ml at 30˚C for 60 min in Tris-EGTA buffer (pH 7.4) composed of 50 mM Tris-HCl, 1 mM EGTA, 3 mM $MgCl_2$, 100 mM NaCl. The incubation mixture also contained 0.05 nM [^{35}S]GTPγS and 30 μM GDP together with the indicated concentrations of DAMGO, DPDPE, rimonabant, naltrindole, U50488, morphine or L-epinephrine. Non-specific binding was determined in the presence of 10 μM unlabeled GTPγS. Bound and free [^{35}S]GTPγS were separated by vacuum filtration through Whatman GF/B filters, otherwise the filtration process and the detection of

the samples were the same as described under section 3.5.2). The [^{35}S]GTPγS binding experiments were performed in triplicates and repeated at least three times.

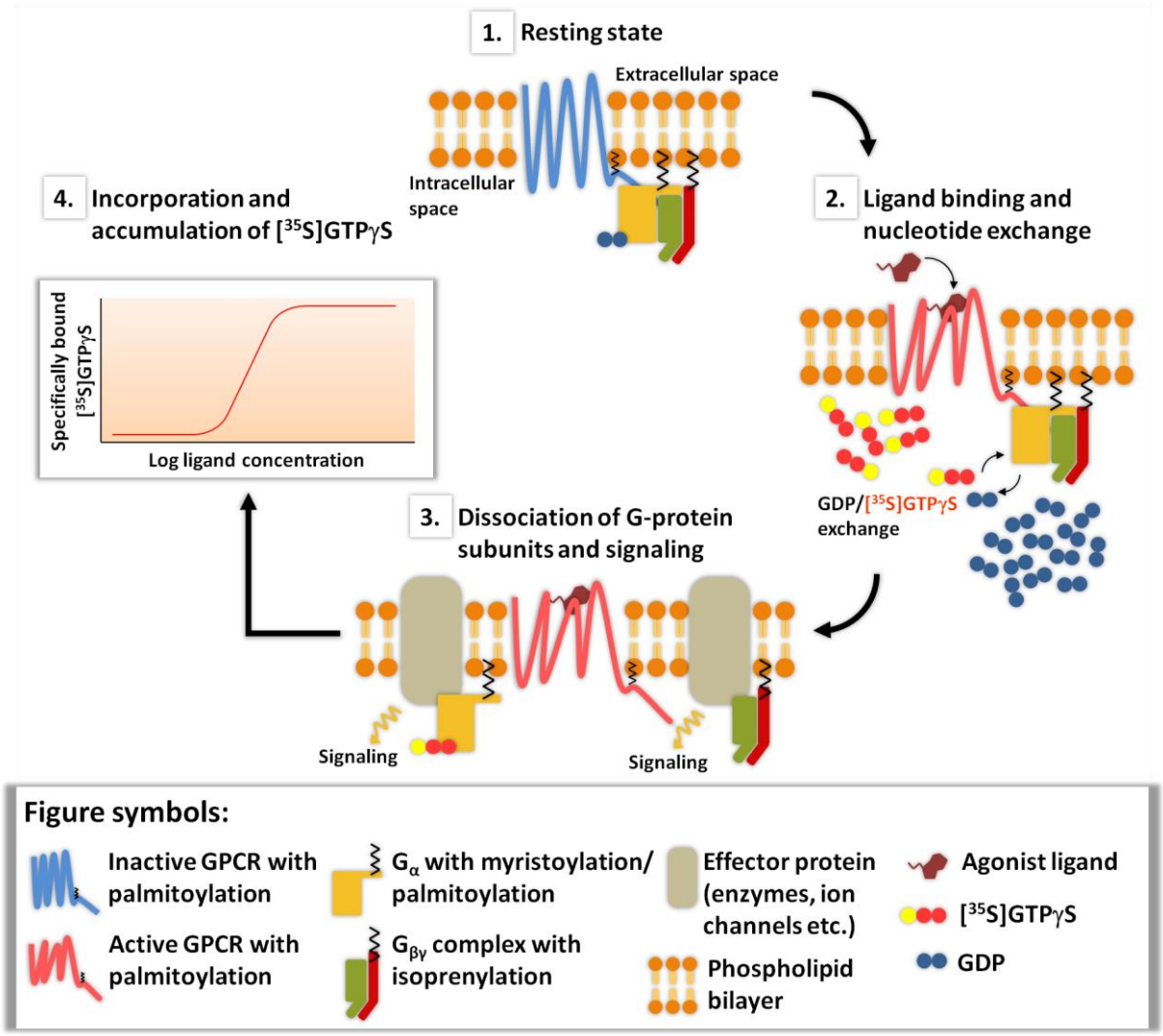

Figure 7 The G-protein activation in the presence of the non-hydrolysable [^{35}S]GTPγS. For detailed description see section 3.5.3. Note the higher levels of GDP in step 2 compared to [^{35}S]GTPγS, this is to insure the initiation of the receptor activation. Compare this figure with Fig. 2.

3.6 Docking experiments

Molecular docking attempts to predict the structure of an intermolecular complex formed between two or more molecules, such as a receptor and a ligand based on their already determined 3D structures (for review see [164,165]). The prediction solves two main problems namely to find the precise orientation and conformation of the ligand (posing) and to calculate the interaction energies between the ligand and the receptor (scoring) [164]. Docking protocols are a combination of a searching algorithm and a scoring function [164]. Basically a search algorithm scans the conformational space for docking, while the scoring function evaluates the strength of intermolecular interactions between the receptor and ligand once the ligand is docked in a certain position [164]. Also the scoring function distinguishes the true binding modes from other alternative ones and classifies which ones are most likely to interact with the receptor based on the established binding free energies (this process is called ranking the ligands) [164]. Genetic algorithm is one of the most favored search algorithms; it applies the theory of genetics and biological evolution in molecular docking [164,166], while most scoring functions are physics-based molecular force fields derived from experimental work as well as quantum mechanical calculations (for review see [167]).

In our docking experiments the 3D coordinates of the active and inactive conformations of MOR prepared by homology modeling were downloaded from the Mosberg group's webpage (see web reference [D]; although the homology model of MOR was prepared for the rat, the part of the sequence modeled was 100% identical to that of mice). The activated receptor model contained the MOR selective agonist, H-Tyr-c(S-Et-S)[D-Cys-Phe-D-Pen]NH_2 (JOM-6; downloaded as: OPRM_RAT_AD_JOM6), and the inactive receptor model contained the κ-opioid antagonist, norbinaltorphimine (nor-BNI; downloaded as: OPRM_RAT_ID_BNI). The 3D coordinates of rimonabant, DAMGO and naloxone were downloaded from the Cactus web site (see web reference [E]) using Avogadro (see web reference [F]), an open source chemical structure editor program. The embedded Openbabel [168] program suite was used to energy minimize the structures with the MMFF94s [169] force field. Ligands and receptors were prepared for docking using the AutoDockTools [170] program suite and then docked by the program AutoDock4 [170]. In AutoDock, the maximum number of energy evaluations, the number of individuals in population and the number of Lamarckian Genetic Algorithm runs were 25000000, 350 and 20, respectively to achieve an exhaustive search for the docked poses. The size of the grid docking box was 50 Å and centered at the middle of the binding pocket. Each docking started with a random translation, rotation and

torsional modification of the ligands. The receptors were kept rigid in the docking calculations because the limitation in the number of the flexible torsional angles prevented to treat the whole binding pocket and the ligands flexible simultaneously. In addition, the docking calculations were repeated by using the flexible ring method, a specific feature of AutoDock. The calculations resulted in the estimated docking free energies in kcal/mol.

3.7 Data analysis

All experimental data were presented as means ± S.E.M. and if the ligands were added in increasing concentration they were presented in the function of the applied ligand concentration in a logarithmic scale. Data were fitted with the professional curve fitting program, GraphPad Prism 5.0 (GraphPad Prism Software Inc., San Diego, CA), using non-linear regression.

In the competition binding assays the inhibition of the specifically bound [^{3}H]DAMGO, [^{3}H]Ile^{5,6}deltorphin II, [^{3}H]naloxone and [^{3}H]naltrindole was given in percentage, the total specific binding and the minimum level of non-specific binding was defined as 100% and 0% respectively. Data were fitted with the 'One site competition' or in the case of [^{3}H]naloxone or [^{3}H]naltrindole displacement studies the 'Two sites-Fit logIC50' fitting equation was applied to determine the concentration of the competitor ligands that displaced 50% of the radioligand (IC_{50}; **Fig. 8A**). The IC_{50} value characterizes the affinity of the unlabeled ligand towards the target receptor; the lower the IC_{50} value is, the higher the affinity of the unlabeled ligand towards the observed receptor, since it can produce the 50 % inhibition in lower concentrations. Additionally in competition binding experiments performed in pCHO cell membranes the bound [^{3}H]Ile^{5,6}deltorphin II was represented in cpm (counts per minute) since there was no specific binding observed in these experiments (see **Fig. 10**).

In the [^{35}S]GTPγS binding assays the 'Sigmoid dose-response' fitting was used to determine the maximal stimulation or efficacy (E_{max}) of the receptors G-protein (**Fig. 8B**) and the potency (EC_{50}) of the stimulating ligand (**Fig. 8B**). The EC_{50} value indicates the affinity property of the applied ligand and it is analogous to the IC_{50} value. Stimulation was given in percents of the specific [^{35}S]GTPγS binding observed over or under the basal activity, which was settled as 100%.

Statistical analyses were performed by GraphPad Prism 5.0. In case of two data sets unpaired t-test with two-tailed P value statistical analysis was used, while in the case of three or more data sets One-way ANOVA with Bonferroni's Multiple Comparison post hoc test was performed to determine the significance level. Since both the competitor and stimulator ligands were presented in the logarithm form, the curve fitting program could only calculate S.E.M. for the logarithm form of IC_{50} ($logIC_{50}$) and EC_{50} ($logEC50$) values. At the same time their antilogarithm form were also shown in the figures for better understanding. Significance was accepted at the $P < 0.05$ level.

During docking experiments the lowest docking free energies obtained were used to rank the ability of the ligands to bind to the receptor. Additionally, the energy balance of the receptor activation process was calculated for each ligand, subtracting the docking energy of the ligand-active receptor complex from that of the ligand-inactive receptor complex ("receptor activation energy"). This value was used to characterize the agonistic-antagonistic nature of rimonabant. The docking poses of rimonabant were analyzed and visualized by the program Chimera [10].

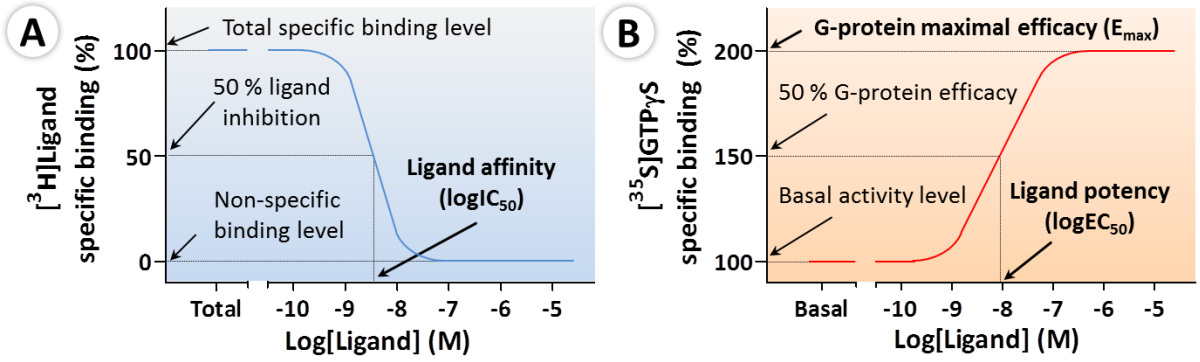

Figure 8 **A: The parameters of competition binding curves. B: The parameters of sigmoid dose-response curves of [^{35}S]GTPγS binding assays.** The important parameters such as $logIC_{50}$, E_{max} and $logEC_{50}$ are indicated in bold; the other parameters are also represented because they are necessary for the calculations of $logIC_{50}$ or $logEC_{50}$ values. "Total" and "Basal" on the X axis refers to the points which did not contain unlabeled ligands only the radioactive compounds and also represents the total specific binding of the radioactive molecule or the basal activity of the receptor (**B**). The gap in the X-axis indicates the scale between the most diluted point and the point where no unlabeled ligands were added ("Total" and "Basal"). For more details see section **3.7**.

4 RESULTS

4.1 Direct binding affinity measurements

4.1.1 Direct binding of rimonabant towards MOR in radioligand competition binding assays performed in wild type and CB_1 K.O. mouse forebrain membranes

The direct binding affinity of rimonabant towards MOR was analyzed in competition binding assays with the highly MOR selective tritiated peptide agonist DAMGO ([^{3}H]DAMGO) using membranes prepared from wild type (w.t.) and CB_1 knock-out (CB_1 K.O.) mice forebrain. The competing ligands were unlabeled DAMGO (as a control) or rimonabant added in increasing concentrations.

Our results demonstrate that rimonabant reduced [^{3}H]DAMGO specific binding both in wild type and CB_1 K.O. mice only at the highest, micromolar concentrations (**Fig. 9**). Even at this concentration the reduction of MOR specific binding was very small, 20 % compared to total specific binding (=100 %). The binding capacity of rimonabant remained unaltered in CB_1 K.O. mice forebrain membranes. As a result the IC_{50} values of rimonabant were in the micromolar range both wild type and CB_1 K.O. mouse forebrain membranes (**Fig. 9**). For comparison the MOR specific DAMGO possessed a binding affinity in the nanomolar range as expected. Important to note that the affinity of DAMGO was not altered significantly when the CB_1 receptor was not present in the forebrain membranes (**Fig. 9**).

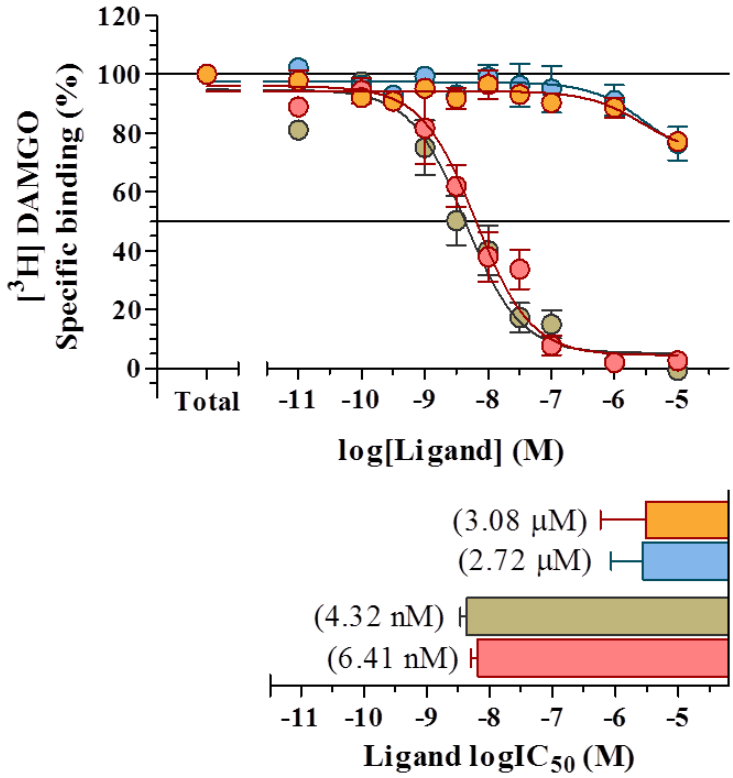

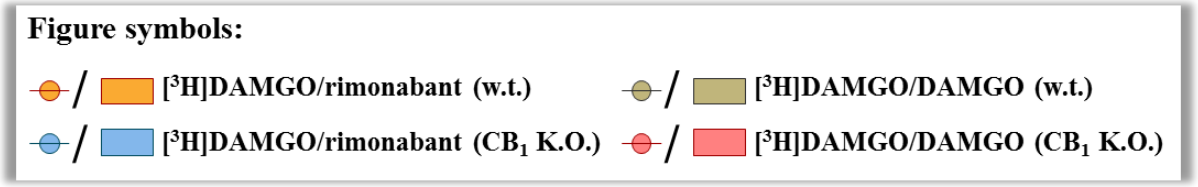

Figure 9 **Direct binding affinity measurements of rimonabant towards MOR in competition binding experiments in wild type and CB_1 K.O. mouse forebrain membranes.** The figures represent the specifically bound fixed concentrations of [^{3}H]DAMGO in percentage in the presence of increasing (10^{-10}-10^{-5} M) concentrations of unlabeled rimonabant and DAMGO (for control). The calculated $logIC_{50}$ (the measurement of ligand binding capacity) of unlabeled rimonabant and DAMGO are also indicated in column diagrams. Points and columns represent means ± S.E.M. for at least three experiments performed in duplicate. Total and non specific binding was settled as 100% and 0% respectively. The antilogarithm form of $logIC_{50}$ (IC_{50}) values are presented in brackets. For additional figure information see **Fig. 8A**.

4.1.2 Direct binding of rimonabant towards MOR and DOR in radioligand competition binding assays performed in CHO-rMOR or CHO-mDOR cell membranes

To investigate the direct binding affinity of rimonabant towards MOR more thoroughly we performed our radioligand competition binding assays in membrane fractions of CHO cells overexpressing rat MOR (CHO-rMOR) to insure a better receptor-ligand interaction. In physiological conditions CHO cell lines express neither MORs nor CB_1 receptors [128,171], that is why they are suitable for the overexpression of these receptors. At the same time we analyzed the binding properties of rimonabant towards DOR straightforwardly in CHO cell membranes overexpressing mouse DOR (CHO-mDOR). The presence of DOR specific binding in untransfected CHO cell lines will be discussed above. The equilibrium competition binding experiments were carried out again with [^{3}H]DAMGO and with the DOR selective tritiated agonist Ile^{5,6}deltorphin II ([^{3}H]Ile^{5,6}deltorphin II). Additionally radiolabeled opioid receptor specific antagonists were also applied, namely the tritiated opioid receptor specific naloxone ([^{3}H]naloxone) and the DOR specific naltrindole ([^{3}H]naltrindole).

In parental (untransfected) CHO cell lines (pCHO) no significant displacement was observed between [^{3}H]Ile^{5,6}deltorphin II and unlabeled Ile^{5,6}deltorphin II (**Fig. 10**), therefore the points could not be fitted with non-linear regression. Additionally similar [^{3}H]Ile^{5,6}deltorphin II binding values were detected in the presence of unlabeled Ile^{5,6}deltorphin II and 10 μM naloxone (**Fig. 10**), which is applied for the calculation of non-specific binding (see section **3.5.2**). Thus the detected bound [^{3}H]Ile^{5,6}deltorphin II was due to non-specific binding, hence we can conclude that in CHO cell lines DORs are not expressed physiologically.

According to our competition binding assays performed in CHO-rMOR, rimonabant reduced [^{3}H]DAMGO total specific binding (100%) in the micromolar range ($3x10^{-7}$- 10^{-5} M; **Fig. 11A**) and at the highest applied concentrations the reduction approximately reached the non-specific binding level (0%; **Fig. 11A**). As a result rimonabant bound to the MOR with a 1.74 μM IC_{50} value (**Fig. 11A**). [^{3}H]Ile^{5,6}deltorphin II total specific binding was also inhibited only when rimonabant was present in micromolar concentrations, however at the highest concentrations the total specific binding of the radioligand was only inhibited approximately 50% (**Fig. 11B**). Nevertheless the IC_{50} value of rimonabant again resulted in the micromolar range (2.8 μM) during DOR binding (**Fig. 11B**).

Interestingly rimonabant showed a markedly different binding character when radiolabeled opioid receptor antagonists were applied in the assays: the total specific binding

of both tritiated opioid antagonists were firstly reduced when rimonabant was present in the nanomolar range (10^{-10}-10^{-9} M), which was followed by a short plateau phase. Finally in the micromolar range the total specific binding of the opioid antagonists were again decreased to the similar level as seen in the case of the radioactive opioid agonists (**Fig. 11A** and **B**). The "two phase" inhibition suggests a higher and a lower affinity binding site on both MOR and DOR, which can be both occupied by rimonabant with a subnanomolar (high affinity binding site) and micromolar (low affinity binding site) IC_{50} value (**Fig. 11A** and **B**). Moreover rimonabant significantly inhibited MOR antagonist binding more effectively in the micromolar range compared to MOR agonist binding (1.74 μM vs. 0.18 μM; $P < 0.01$, unpaired t test, two-tailed P value; **Fig. 11A**).

Thus in the micromolar range rimonabant can affect the ligand binding of MOR and DOR directly, moreover rimonabant can also inhibit specific antagonist binding in the nanomolar range with very high affinity.

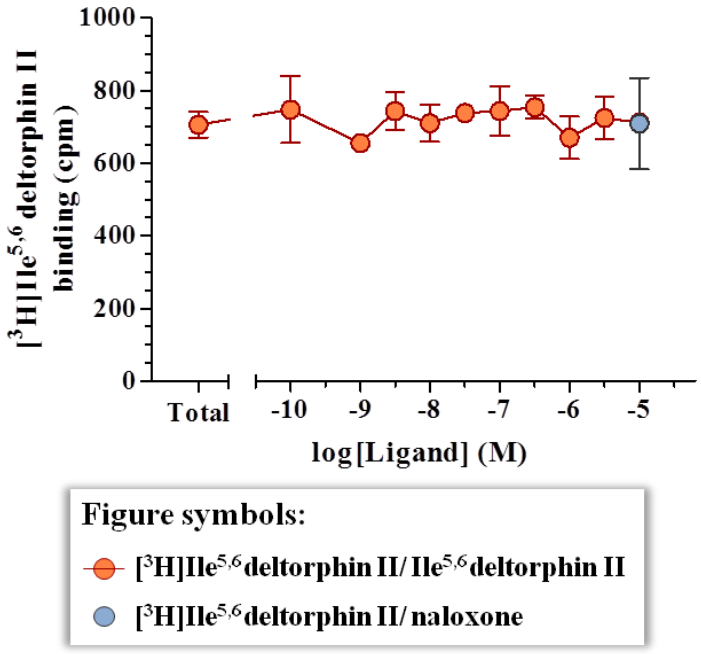

Figure 10 **DOR specific ligand binding in pCHO cell membranes**. Bound [^{3}H]Ile^{5,6}deltorphin II in counts per minute (cpm) in fixed concentrations in the presence of increasing (10^{-10}-10^{-5} M) concentrations of unlabeled Ile^{5,6}deltorphin II and 10 μM naloxone in pCHO cell membranes. Points and columns represent means ± S.E.M. for at least three experiments performed in duplicate. For additional figure information see **Fig. 8A**.

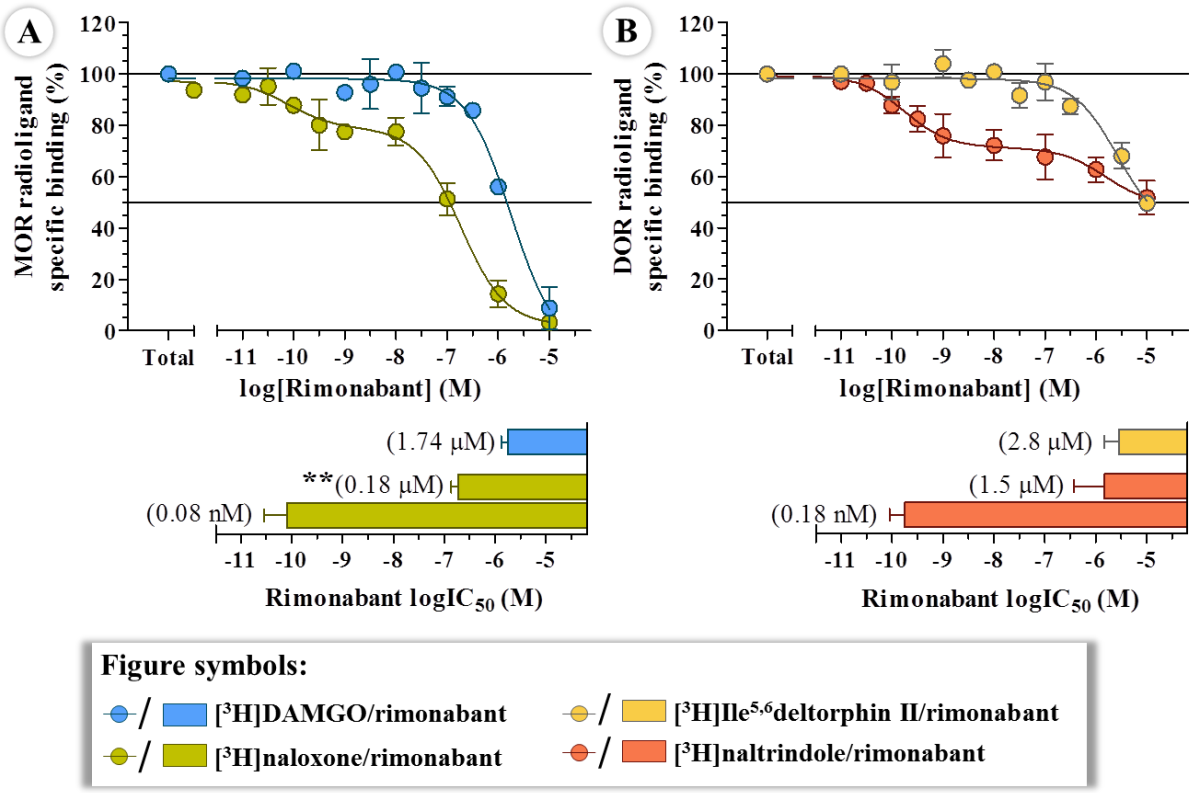

Figure 11 Direct binding affinity measurements of rimonabant towards MOR and DOR in competition binding experiments in CHO-rMOR (A) and CHO-mDOR (B) membranes. The figure shows the percentage of specifically bound fixed concentrations of [^{3}H]DAMGO/[^{3}H]naloxone or [^{3}H]Ile^{5,6}deltorphin II/[^{3}H]naltrindole in percentage in the presence of increasing (10^{-10}-10^{-5} M) concentrations of unlabeled rimonabant in CHO-rMOR (**A**) or CHO-mDOR (**B**) membrane fractions. The calculated logIC_{50} (ligand binding capacity) of unlabeled rimonabant is also indicated. Points and columns represent means ± S.E.M. for at least three experiments performed in duplicate. The two columns close to each other indicate the logIC_{50} values of rimonabant for the high and low affinity binding sites. Total and non specific binding was settled as 100% and 0% respectively. The antilogarithm form of logIC_{50} (IC_{50}) values are presented in brackets. * indicates the significant reduction of rimonabant logIC_{50} value in [^{3}H]naloxone displacement compared to [^{3}H]DAMGO displacement (unpaired t-test, two-tailed P value). **: P <0.01. For additional figure information see **Fig. 8A**.

4.1.3 Docking experiments with rimonabant to inactive and active MOR homology model

To underpin our competition binding assay results performed in CHO-rMOR cell lines, we carried out docking calculations. Docking, a particular field of molecular modeling is a widely used tool to simulate the preferred orientations of a ligand in the binding site. Rimonabant was docked to the homology models of the inactive and active state of the MOR. The MOR agonist DAMGO and the opioid antagonist naloxone were also docked to the receptor models for control. Because DAMGO contains an N-MePhe (N-methylphenylalanine) in its sequence, there is a possibility that it adopts a *cis* Gly^3-N-$MePhe^4$ peptide bond [172]. According to this, DAMGO was docked both in all-*trans* form and with a *cis* Gly^3-N-$MePhe^4$ peptide bond (*cis*-DAMGO). Since the applied active and inactive MOR homology models already contained JOM-6 and nor-BNI, respectively, these ligands were also docked to the receptor models to cross validate our docking experiments. Each ligand was docked to both receptor conformations to compare their preference for the specific state of MOR.

In the first calculation the receptors were rigid and the ligands were flexible except that the aliphatic rings of the ligands were kept in the conformation obtained by the energy minimization (**Fig. 12A**). As expected during our docking experiments JOM-6 and nor-BNI achieved the same docking poses as published previously [161]. Even though rimonabant is a highly specific CB_1 receptor antagonist, the ligand bound to the active state of MOR with surprisingly low docking energies (**Fig. 12A**). Moreover, rimonabant bound to the inactive state of MOR with a much lower docking energy, resulting a positive receptor activation energy unlike DAMGO, *cis*-DAMGO and JOM-6 (**Fig. 12A**). In fact the receptor activation energy of rimonabant was very similar to that of the antagonist naloxone (**Fig. 12A**). In the second calculation the possibility of applying flexible aliphatic rings during the experiments did not improve the docking energies in general (**Fig. 12B**).

As an important difference between the binding modes, rimonabant docked to the inactive and active state of the receptor by the opposite ends (**Fig. 13A** and **B**). Also a hydrogen bond occurs between Thr218 (T218) in the TM7 domain and the hydrazide group of rimonabant (**Fig. 13C**) in the inactive state of the binding pocket, while no hydrogen bonds were observed in the binding pocket of the active receptor.

Summarizing the results of our docking calculations, we observed that rimonabant binds to the active conformation of MOR with a surprisingly low energy similar to the agonist

DAMGO. However, the docking energies were even lower in the inactive state of the MOR suggesting that rimonabant has a preference for the inactive state of MOR. These findings raise the possibility that rimonabant acts as an antagonist on MOR. Nevertheless, only the inactive state gives the opportunity to form a hydrogen bond between rimonabant and one of the residues in the binding pocket.

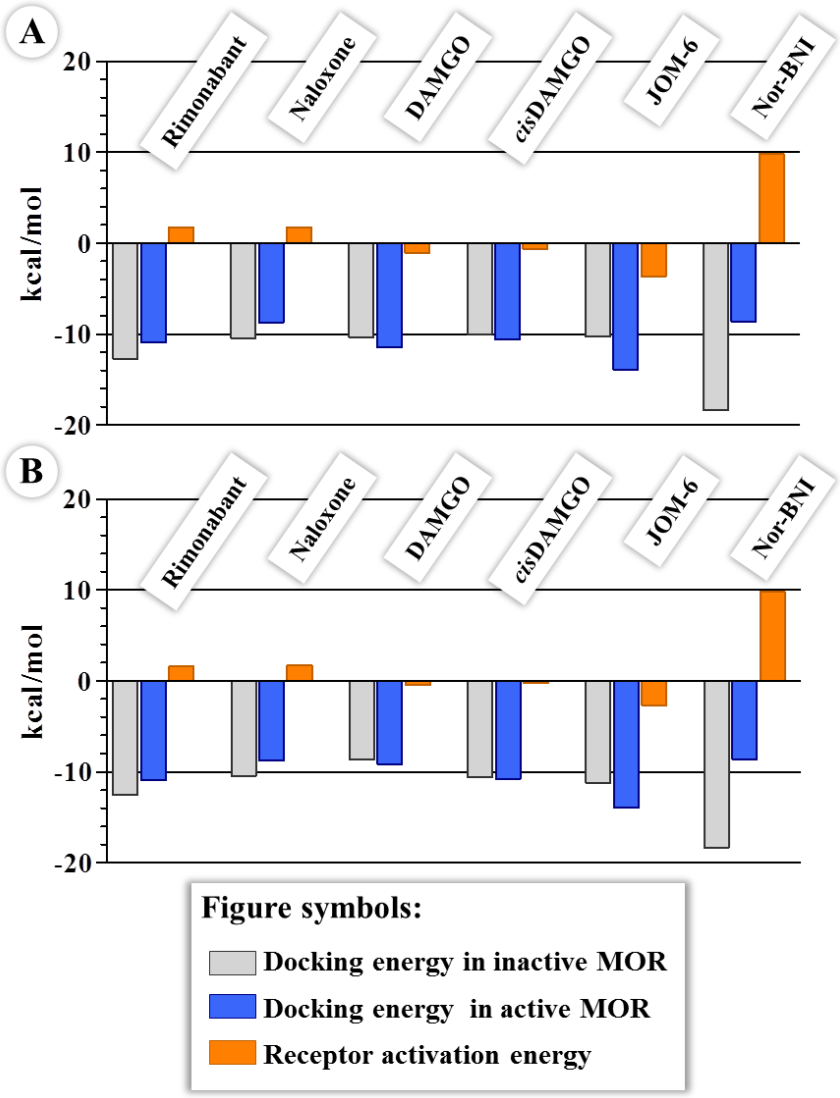

Figure 12 Docking energies and the calculated receptor activation energy of rimonabant compared to the indicated ligands in docking experiments accomplished with rigid receptor, rigid ring (A) and rigid receptor, flexible ring (B) in inactive and active MOR. The 3D coordinates of the inactive and active conformations of MOR, and the preparations of the ligands for docking are described under section **3.6**. Receptor activation energy was calculated by subtracting the docking energy of the activated MOR from that of the inactive MOR. The data are represented in kcal/mol.

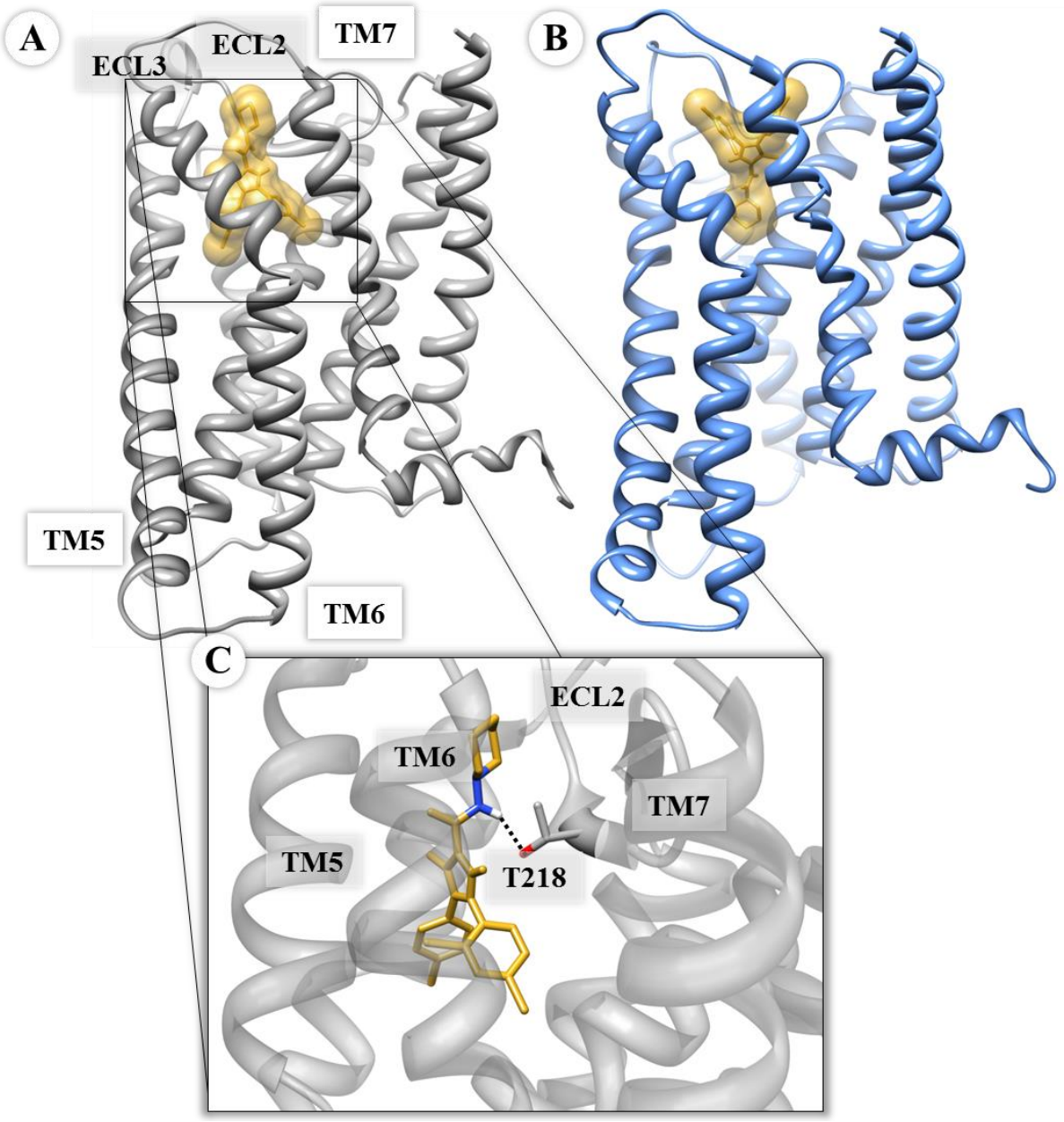

Figure 13 The docking pose of rimonabant in the inactive (A) and active (B) MOR, and the hydrogen bond between rimonabant and T218 (C). Rimonabant is indicated in yellow (the nitrogen and hydrogen atoms of the hydrazide group are shown in blue and white, respectively). The hydrogen bond is highlighted with a black dotted line; the hydrogen acceptor (oxygen) is shown in red on T218. The essential extracellular loops (ECL) and transmembrane regions (TM) are indicated on the inactive conformation of MOR for clarity. The docking poses were analyzed and visualized by the program Chimera.

4.2 MOR and DOR mediated G-protein activity measurements

4.2.1 The effect of rimonabant on DOR G-protein basal activity in [^{35}S]GTPγS binding assays, in CHO-mDOR and pCHO cell membranes

Further on we examined whether the DOR mediated G-protein basal activity can be altered by rimonabant, that is whether it can exert its inverse agonistic effect on DOR. The experiments were accomplished in functional [^{35}S]GTPγS binding experiments, with a non-hydrolysable radiolabeled GTP analog, [^{35}S]GTPγS. The assays were performed in CHO-mDOR and pCHO cell membranes, to avoid interaction of DORs with other opioid and cannabinoid receptors, and also to see clearly the direct actions of rimonabant on DOR G-protein coupling.

According to our results rimonabant significantly decreased the DORs basal activity (100%, **Fig. 14A**), with an efficacy (E_{max}) of 48.1% and with a potency (EC_{50}) of 1.3 μM (**Fig. 14A**). Thus rimonabant may behave as an inverse agonist at DOR.

To investigate whether the inverse agonistic effect of rimonabant on DOR is indeed DOR related, we measured the specifically bound [^{35}S]GTPγS when 10 μM rimonabant was incubated together with 1 μM of the DOR specific antagonist naltrindole, again in CHO-mDOR cell membranes (**Fig. 14B**). Our results pointed out that naltrindole failed to reverse the inverse agonistic effect of rimonabant (**Fig. 14B**), therefore DOR is not involved in this action. For comparison, naltrindole significantly inhibited DPDPE-stimulated [^{35}S]GTPγS binding (**Fig. 14B**). Also the MOR agonist morphine and the KOR agonist U50488, together with naltrindole failed to alter the G-protein basal activity of DOR significantly (**Fig. 14B**). This confirms the lack of both MOR and KOR in the CHO-mDOR cell membranes, and the pure antagonistic character of naltrindole. Additionally rimonabant also significantly decreased G-protein basal activity in pCHO cell membranes (**Fig. 14C**), which did not contain DORs (DPDPE did not alter basal activity, see **Fig. 14C**), which underpins the non-DOR related inverse agonistic effect of rimonabant.

These results were in accordance with previous studies with CHO-MOR cell membranes in similar experimental conditions [128,171].

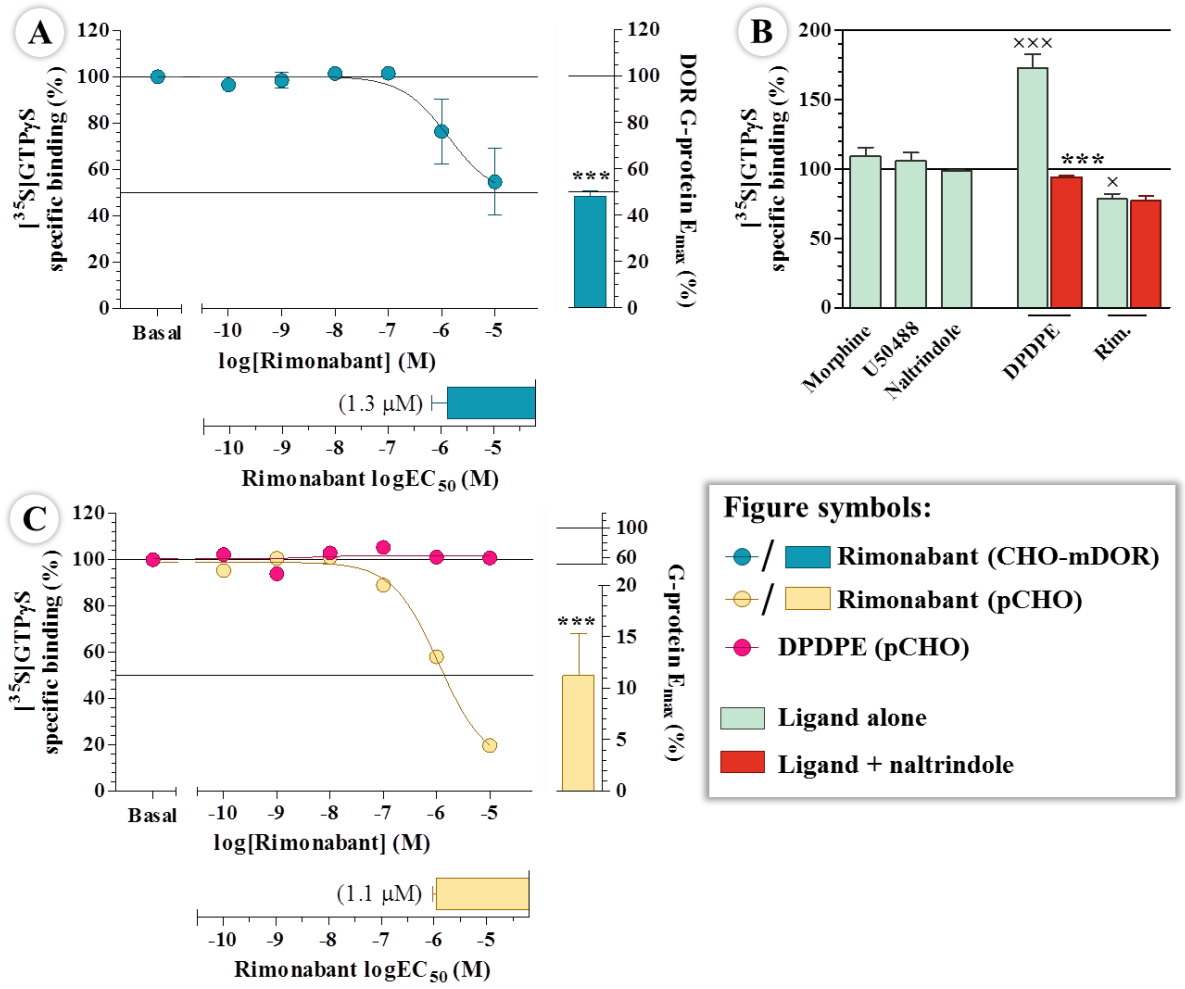

Figure 14 The effect of rimonabant on DOR G-protein basal activity in ligand-modulated [^{35}S]GTPγS binding assays, in CHO-mDOR (A and B) and in pCHO (C) cell membranes. A and C represents the specifically bound [^{35}S]GTPγS in percentage in the presence of increasing concentrations (10^{-10}-10^{-5} M) of rimonabant or DPDPE in CHO-mDOR (A) or pCHO cell membranes (C). The calculated E_{max} (G-protein maximal efficacy) and $logEC_{50}$ (ligand potency) values are also presented in column diagrams. * denotes the significant alterations of DOR G-protein E_{max} value (unpaired t-test, two-tailed P value) compared to basal activity (100%) in the presence of rimonabant. In case of C the error bars are shorter than the points itself. B represents specifically bound [^{35}S]GTPγS in percentage in the presence of 10 μM of the indicated ligands alone or together with 1 μM naltrindole in CHO-mDOR cell membranes. × indicates the significant alterations in specifically bound [^{35}S]GTPγS (One-way ANOVA, Bonferroni's Multiple Comparison post hoc test), compared to basal activity in the presence of rimonabant or DPDPE. * indicates the significant reduction in the specifically bound [^{35}S]GTPγS during DPDPE stimulation in the presence of NTI compared to DPDPE alone. Total (=basal activity) and non specific binding was settled as 100% and 0% respectively. Points and columns represent means ± S.E.M. for at least three experiments performed in triplicate. ×××, ***: P <0.001; ×: P < 0.05. For additional figure information see **Fig. 8B**.

4.2.2 The effect of rimonabant on DOR G-protein activation in DPDPE-stimulated [^{35}S]GTPγS binding, in CHO-mDOR cell membranes

In the next step we examined whether rimonabant at micromolar concentration range has any effect on DORs G-protein activation during receptor stimulation. The experiments were again accomplished in functional [^{35}S]GTPγS binding experiments using CHO-mDOR cell membranes. The receptor was stimulated with the enkephalin analogue DOR specific agonist DPDPE, which activated the DOR the most effectively compared to our other DOR activator ligand candidates (data not shown).

DPDPE stimulated the DOR with a potency (EC_{50}) of 12.4 nM and the receptors G-protein had a maximal stimulation or efficacy (E_{max}) of 285.6 % during DPDPE stimulated receptor activation (**Fig. 15**). Rimonabant in 1 and 10 μM concentrations significantly decreased the DORs G-protein efficacy (**Fig. 15**) and also the potency of DPDPE but only in 10 μM concentrations (**Fig. 15**).

Thus rimonabant inhibited the DPDPE-induced maximal G-protein stimulation of the DOR and also the potency of the stimulator ligand in the micromolar range when no cannabinoid or other opioid receptors were present in the experimental system.

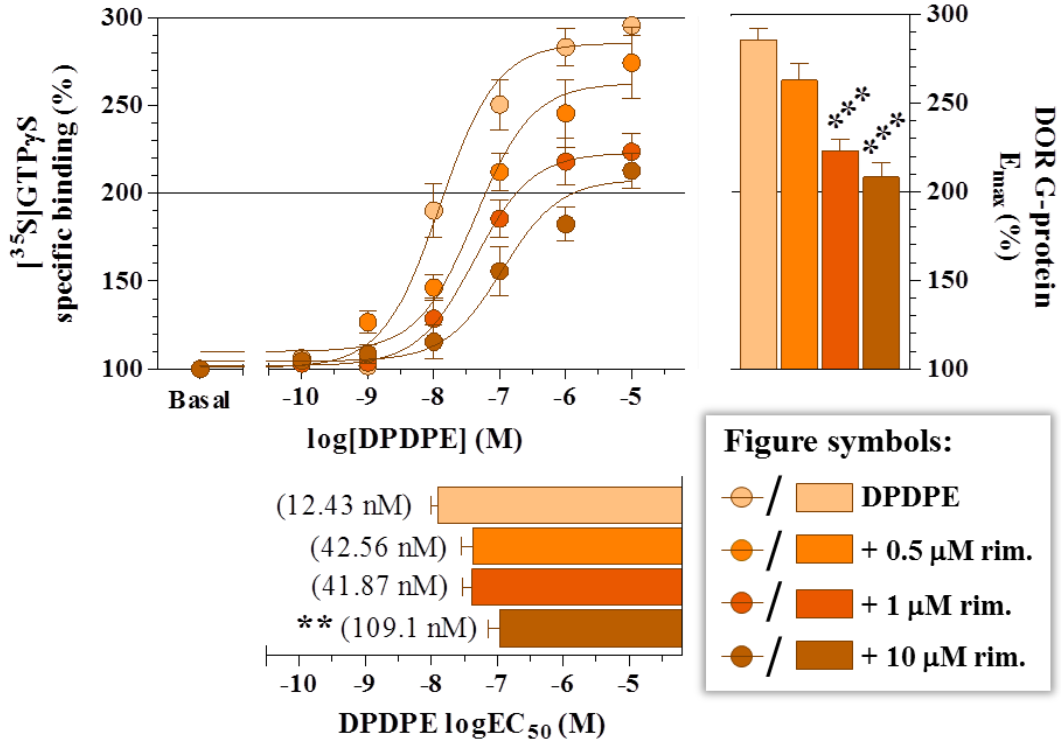

Figure 15 The effect of rimonabant on DOR G-protein activation in DPDPE-stimulated [^{35}S]GTPγS binding, in CHO-mDOR cell membranes. The figure represents the specifically bound [^{35}S]GTPγS in percentage in the presence of increasing concentrations (10^{-10}-10^{-5} M) of DPDPE in the absence or presence of the indicated rimonabant concentrations. The calculated E_{max} (G-protein maximal efficacy) value of DOR G-protein and $logEC_{50}$ (ligand potency) value of DPDPE are also indicated. Points and columns represent means ± S.E.M. for at least three experiments performed in triplicate. * indicates the significant reduction in E_{max} and $logEC_{50}$ values in the presence of rimonabant compared to DPDPE alone (One-way ANOVA, Bonferroni's Multiple Comparison post hoc test). The DOR basal activity level was settled as 100%. The antilogarithm form of $logEC_{50}$ (EC_{50}) values are presented in brackets. ***: $P < 0.001$; **: $P < 0.01$. For additional figure information see **Fig. 8B**.

4.2.3 The effect of rimonabant on MOR and DOR G-protein activation in agonist-stimulated [^{35}S]GTPγS binding, in wild type and CB_1 and CB_1/CB_2 receptor double knock-out mouse forebrain membranes

To underpin our opioid receptor G-protein activation results, we accomplished the assays in mouse forebrain membranes. In this brain region both opioid and cannabinoid receptors are expressed in eligible amount [114,173,174]. Therefore agonist stimulated MOR and DOR G-protein activity can be studied when the receptors are expressed in physiological conditions and when cannabinoid and other opioid receptors are present, thus interactions may occur between them. The investigations were also performed in CB_1 and CB_1/CB_2 double knock-out mice (CB_1 K.O. and CB_1/CB_2 K.O. respectively), because previously our group demonstrated an interaction between the CB_2 receptor and MOR in mice forebrain [113]. Since the inhibitory actions of rimonabant occurred from 1 μM in the cell membranes, we carried out our further experiments with this concentration.

In wild type (w.t.) mouse forebrain membranes the maximal efficacy (E_{max}) of MOR during DAMGO-stimulation was significantly decreased in the presence of rimonabant together with the potency (EC_{50}) of DAMGO (**Fig. 16**). In CB_1 knockout animals the maximal efficacy of MOR mediated G-protein was also significantly diminished by rimonabant (**Fig. 16**), whereas the potency of DAMGO remained unaltered (**Fig. 16**). The lack of both cannabinoid receptors did not modulate the inhibitory effect of rimonabant on MOR G-protein activity (**Fig. 17A**), thus we can rule out the role of CB_1 and CB_2 receptors in the observed effects of rimonabant upon MOR function.

During DPDPE-stimulated DOR G-protein activation, the presence of rimonabant produced a significant attenuation in the maximal efficacy of DORs G-protein activity (**Fig. 17B**) and in the potency of the stimulatory ligand (**Fig. 17B**) similar to that in the wild type mouse forebrain membranes. The reduced maximal efficacy of the receptor and the potency of the activating ligand - similar to that of MOR - were also established in the CB_1/CB_2 K.O. mouse forebrain when rimonabant was present (**Fig. 17B**).

Further on we wanted to verify that the inhibitory actions of rimonabant are not due to the unspecific inverse agonistic effect discussed previously under section **4.2.1**. To exclude this possibility we applied L-epinephrine, which is a non-selective endogenous adrenergic receptor agonist. With L-epinephrine we stimulated adrenergic receptors (AR) in [^{35}S]GTPγS binding assays performed in CB_1/CB_2 K.O. mouse forebrain membranes. ARs are highly expressed in the forebrain structures and can coupled to $G_{i/o}$ type G-proteins such as the α_2

type receptors [175], therefore they can be monitored by L-epinephrine-stimulated [^{35}S]GTPγS binding assays (see section **3.5.3**). In addition there is evidence that α_2 ARs are expressed physiologically in CHO cell lines (see web reference [G]), also it has been previously reported that rimonabant is able to inhibit α_2 adrenergic receptor binding in micromolar concentrations. Therefore the non-CB_1 mediated inverse agonistic effect of rimonabant can be mediated through α_2 ARs.

L-epinephrine activated its specific receptor with 31.6 nM potency (**Fig. 18**) and the coupled G-protein had a 166.8% maximal efficacy during the activation (**Fig. 18**). In the presence of 10 μM rimonabant neither of the parameters changed significantly (E_{max}: 162%; EC_{50}: 26.7 nM; **Fig. 18**), thus the inhibitory actions of rimonabant are not due its non-specific inverse agonistic actions.

To summarize the [^{35}S]GTPγS binding experiments performed in forebrain membranes, we can conclude that rimonabant in the micromolar range *in vitro* inhibits agonist-stimulated MOR and DOR G-protein efficacy and ligand potency. Thus the inhibitory actions of rimonabant cannot only occur when both receptors are overexpressed in cell lines, but also when they are expressed in physiological conditions. Further on in case of both opioid receptors the reduced G-protein efficacy together with the decreased DPDPE potency was independent from cannabinoid receptors.

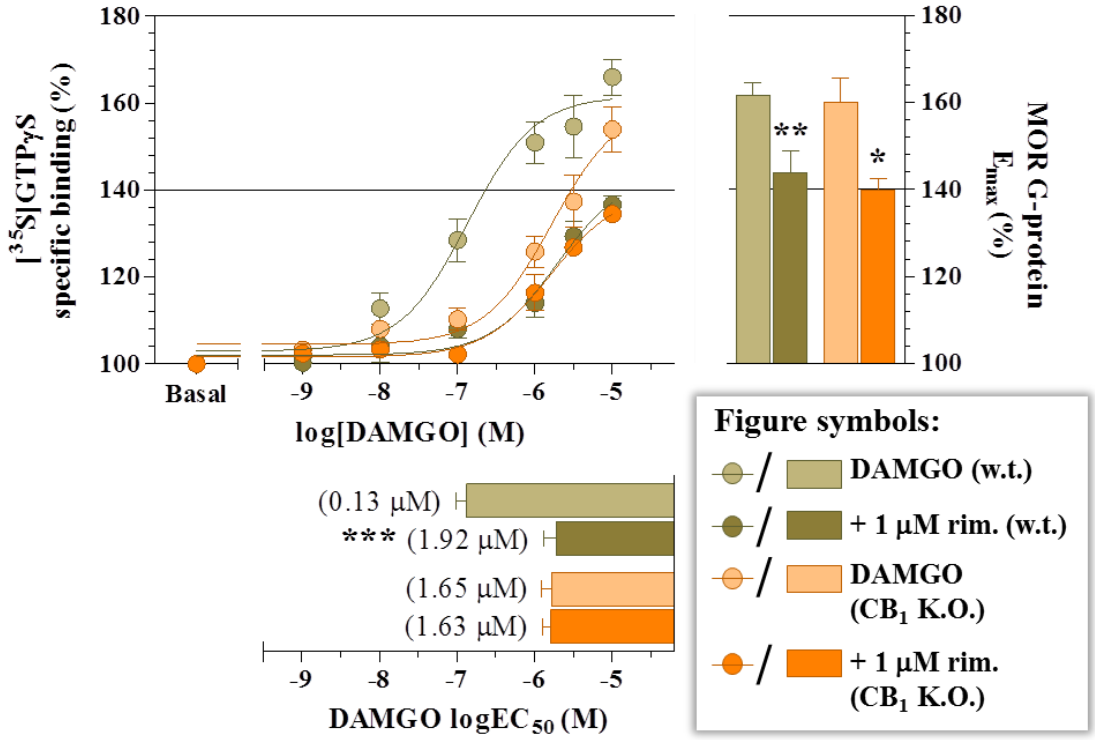

Figure 16 The effect of rimonabant on MOR G-protein activation in DAMGO-stimulated [^{35}S]GTPγS binding, in wild type and CB_1 knock-out mouse forebrain membranes. The figure represents the specifically bound [^{35}S]GTPγS in percentage in the presence of increasing concentrations (10^{-9}-10^{-5} M) of DAMGO in the absence or presence of 1 μM rimonabant. The calculated E_{max} (maximal efficacy) value of MOR G-protein and $logEC_{50}$ (ligand potency) value of DAMGO are also indicated in column diagrams. Points and columns represent means ± S.E.M. for at least three experiments performed in triplicate. * indicates the significant reduction in E_{max} and $logEC_{50}$ values in the presence of rimonabant compared to DAMGO alone in wild type or in CB_1 receptor knock-out mouse (unpaired t-test, two-tailed P value). The MOR basal activity level was settled as 100%. The antilogarithm form of $logEC_{50}$ (EC_{50}) values are presented in brackets. ***: $P < 0.001$; **: $P < 0.01$; *: $P < 0.05$. For additional figure information see **Fig. 8B**.

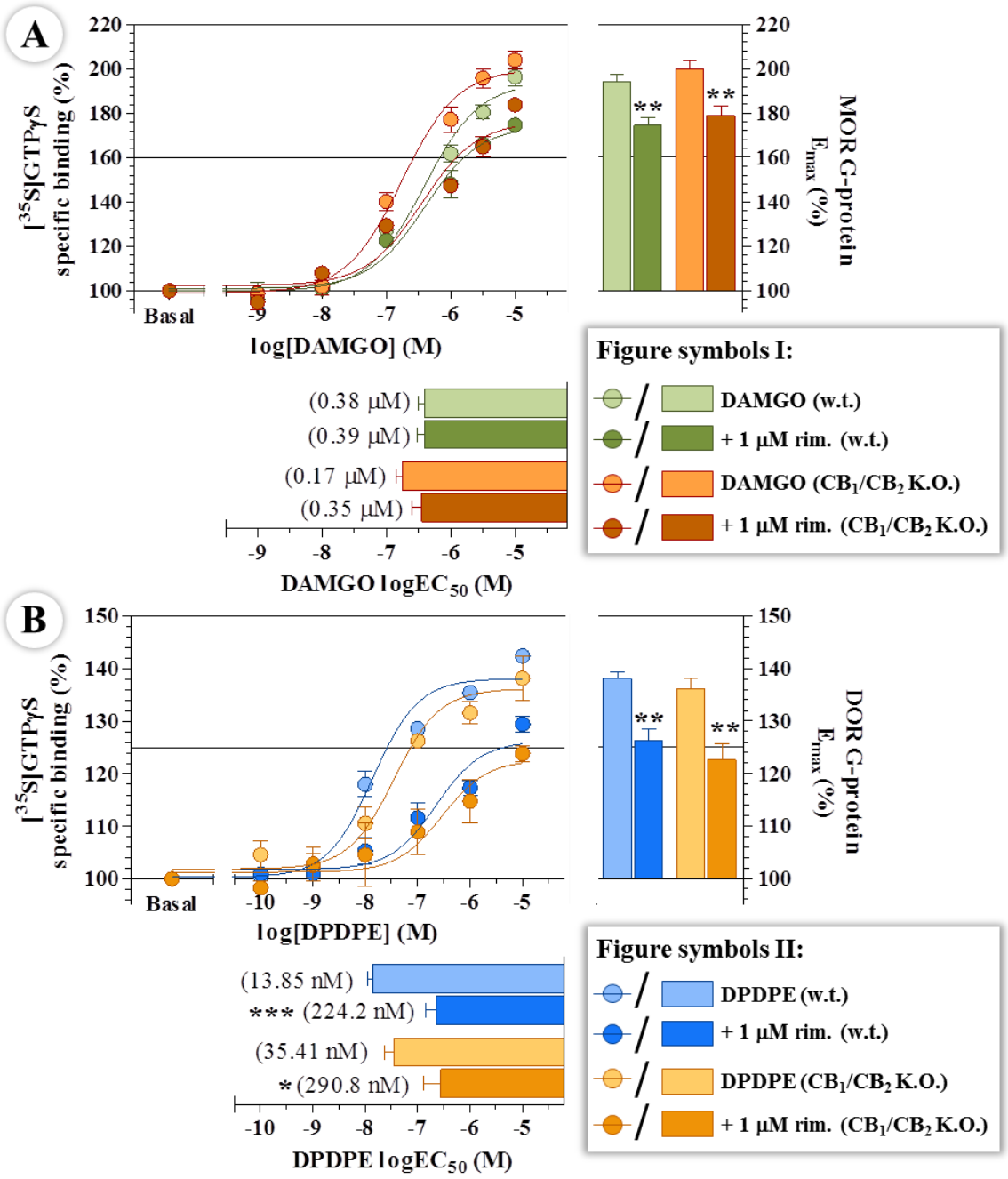

Figure 17 The effect of rimonabant on MOR and DOR G-protein activation in (A) DAMGO- and (B) DPDPE-stimulated [^{35}S]GTPγS binding, in wild type and CB_1/CB_2 knock-out mouse forebrain membranes. The figure represents the specifically bound [^{35}S]GTPγS in percentage in the presence of increasing concentrations (10^{-10}-10^{-5} M) of DAMGO (**A**) or DPDPE (**B**) in the absence or presence of 1 μM rimonabant. The calculated E_{max} (maximal efficacy) value of MOR (**A**) and DOR (**B**) G-protein and $logEC_{50}$ (ligand potency) value of DAMGO (**A**) and DPDPE (**B**) are also indicated. Points and columns represent means ± S.E.M. for at least three experiments performed in triplicate. * indicates the significant reduction in E_{max} and $logEC_{50}$ values in the presence of rimonabant compared to DAMGO or DPDPE alone in wild type or in CB_1/CB_2 receptor double knock-out mouse (unpaired t-test, two-tailed P value). The receptor basal activity level was settled as 100%. The antilogarithm form of $logEC_{50}$ (EC_{50}) values are presented in brackets. ***: $P < 0.001$; **: $P < 0.01$; *: $P < 0.05$. For additional figure information see **Fig. 8B**.

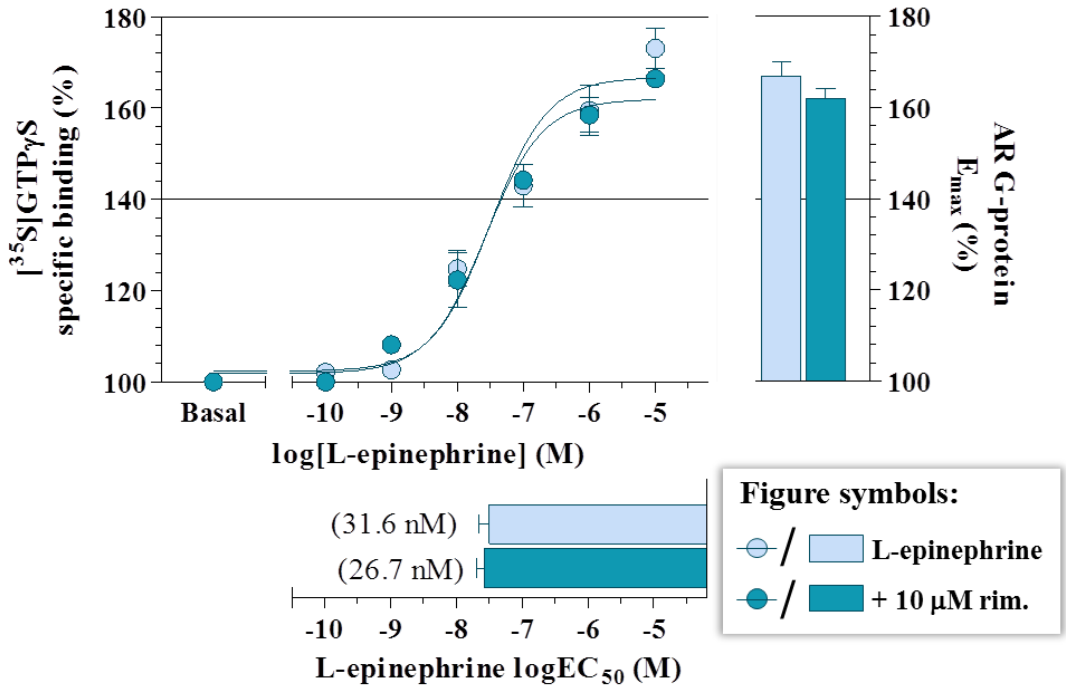

Figure 18 The effect of rimonabant on AR G-protein activation in L-epinephrine-stimulated [^{35}S]GTPγS binding, in CB_1/CB_2 knock-out mouse forebrain membranes. The figure represents the specifically bound [^{35}S]GTPγS in percentage in the presence of increasing concentrations (10^{-10}-10^{-5} M) of L-epinephrine in the absence or presence of 10 µM rimonabant. The calculated E_{max} (maximal efficacy) value of AR G-protein and $logEC_{50}$ (ligand potency) value L-epinephrine are also indicated in column diagrams. Points and columns represent means ± S.E.M. for at least three experiments performed in triplicate. AR basal activity was settled as 100%. The antilogarithm form of $logEC_{50}$ (EC_{50}) values are presented in brackets. AR: adrenergic receptor. For additional figure information see **Fig. 8B**.

5 DISCUSSION

Rimonabant was the first CB_1 receptor antagonist/inverse agonist to be developed, and it is still a perfect tool for antagonizing CB_1 related effects (for review see [123]). Later it turned out that rimonabant had several non-cannabinoid related effects such as decreasing alcohol intake, opiate self-administration and increasing smoking cessation (for review see [135]). There is also evidence that rimonabant can interact with several GPCRs and ion channels (for review see [134]).

This study focuses on the interaction between rimonabant and the MOR and DOR. The interaction was studied at ligand-receptor level in competition binding experiments and docking experiments, and at the receptor-G-protein level in functional [^{35}S]GTPγS binding assays.

In our competition binding experiments performed with mouse forebrain membranes rimonabant could only displace [^{3}H]DAMGO in the highest concentrations, and even at that level it could only cause a minor decrease in the specific binding of the radiolabeled MOR agonist. The lack of CB_1 receptor did not affect the binding characteristics of either ligand, as we got comparable results in CB_1 knockouts as well. We also carried out equilibrium competition binding experiments in CHO-rMOR cell membranes to measure the ligand-receptor interaction more precisely. [^{3}H]DAMGO was fully displaced from its receptor in CHO-rMOR cell membranes by rimonabant, but only in higher concentrations, which resulted a similar micromolar affinity for the compound. Other publications also reported micromolar affinity for rimonabant on MOR in similar experimental conditions [128,141,142]. On the other hand rimonabant was able to displace [^{3}H]naloxone with a significantly lower logIC_{50} value compared to [^{3}H]DAMGO. In CHO-mDOR cell membranes rimonabant decreased only 50% of both the DOR agonist [^{3}H]Ile^{5,6}deltorphin II and the DOR antagonist [^{3}H]naltrindole total specific binding. For comparison in Kathmann and co-workers study rimonabant inhibited [^{3}H]naltrindole binding by only 20% [142], which can be partly explained by the different experimental conditions applied during the assay (incubation time and temperature, final volume etc.) and by the applied cell lines. Additionally in case of both DOR specific radioligands rimonabant reached an IC_{50} value in the micromolar range, similar to our competition binding experiments performed in CHO-rMOR cell membranes. As reported in previous studies rimonabant also bound with an IC_{50} in the micromolar range to other

members of the GPCR family, such as adrenergic and 5-HT_6 receptors or to ion channels, like calcium, sodium and potassium channels (for review see [134]).

Interestingly a higher affinity binding site for rimonabant was measured in the displacement of both [^{3}H]naloxone and [^{3}H]naltrindole: rimonabant also displaced the antagonist [^{3}H]naloxone and [^{3}H]naltrindole in the subnanomolar range with a very high affinity, which did not occur during the displacement of the agonist [^{3}H]Ile^{5,6}deltorphin II and [^{3}H]DAMGO. The high and low affinity binding sites are common in GPCRs [176], and previously our group had demonstrated it on opioid receptors, including on the MOR [177]. It is known that antagonists stabilize the receptors in the inactive state, thus they prefer the inactive receptor form, while agonists prefer the active receptor state, since they stabilize the active form [4,18] (see section **1.1.3**). Accordingly in our competition binding experiments rimonabant may behave as an antagonist, since it displaced the radioactive opioid receptor antagonists (which probably maintains the MOR or DOR to the inactive state) from the higher affinity binding site, which did not occur during the displacement of the radiolabeled opioid agonist (which probably stabilized the MOR or DOR in the active state).

Further on we investigated the binding capabilities of rimonabant towards the MOR in *in silico* docking calculations. Docking calculations gives the opportunity to gather information about the receptor-ligand complex, such as the estimate of binding energy, the possible intermolecular interactions, orientations or the occurring energy alterations, which are hard to achieve in *in vitro* studies. According to our calculations rimonabant accommodated to both receptor conformations with a low docking energy (which was unexpectedly low in the case of the active state), but with a high energy expense for the activated receptor compared to the inactive one, suggesting an antagonistic character for the ligand. This is supported by our finding that only the inactive state gives the possibility for a hydrogen bond between rimonabant and a residue in the binding pocket of MOR. As for the docking calculations for the DOR, it is under progress.

It is well known that G-proteins have a constitutive activity (for review see [178]) which can be further modified upon ligand binding (see section **1.1.3**). In turn the altered basal activity initiates different types of signaling cascades [40]. For further investigations we examined the impact of rimonabant on the basal activity of the DORs G-protein, which can give us valuable information about the binding character of rimonabant on DOR. MOR was investigated in this aspect with similar methods previously by Cinar and Szűcs [128] and later Seely and co-workers [171]. According to their studies rimonabant decreased G-protein basal activity in CHO-MOR cells, however in both cases the effect was not MOR specific, since it

was not reversed by naloxone and it also occurred in untransfected cell lines. In our [^{35}S]GTPγS binding assays the inverse agonistic effect of rimonabant was unrelated to DOR, and also confirmed the non-CB_1 mediated inverse agonistic effect. Therefore the agonistic (since rimonabant did not enhance DOR G-protein basal activity) and inverse agonistic character of rimonabant at DOR can be excluded as it is pertained to the MOR. As regard to the non-CB_1 related inverse agonistic effect of rimonabant, it has been proven to be pertussis toxin sensitive and it was demonstrated in different types of brain tissues in several other publications so far [126,128–130].

Since rimonabant affected the MORs and DORs ligand binding, it raises the possibility that it can also interfere with the receptors G-protein activation during MOR and DOR specific agonist stimulation. In case of DOR the investigations initiated again in CHO-mDOR cell lines. The MOR was previously studied in CHO cell lines overexpressed with MOR in similar experimental conditions again by Cinar and Szűcs [128] and afterwards by Seely et al [171]. MOR DAMGO-induced maximal stimulation was slightly, but not significantly reduced in the presence of 10 μM rimonabant [128] and also the potency of the agonist morphine stimulatory ligand was decreased in the presence of the same rimonabant concentration [171]. These findings indicate an antagonistic behaviour for rimonabant on MOR [171]. In our DPDPE-induced DOR G-protein activity measurements, rimonabant inhibited the maximal stimulation of the DORs G-protein and also the potency of the stimulator ligand significantly. Moreover the inhibition occurred in the micromolar concentration range, similarly as in direct affinity measurements in CHO-mDOR cell membranes and as in the previously reported MOR G-protein activity results.

The CHO cell line with homogeneous population of overexpressed MOR or DOR is a useful tool to investigate the direct interaction between rimonabant and these two opioid receptors, since there is no cannabinoid or other opioid receptors in the system which can interact with them, thus the direct effect of rimonabant can be measured more accurately. However as it was discussed under section **1.1.5**, in physiological conditions GPCR receptors often communicate with each other via overlapping signaling pathways or more even via heterodimerization [29,35,38,41], which in addition alters there functionality [37,41]. Taking this into consideration we investigated the impact of rimonabant on MOR and DOR G-protein activation in mouse forebrain, where the cannabinoid and opioid receptors are expressed in adequate quantity [74,75,114,179]. According to our results, in 1 μM concentrations the attenuated efficacy of MOR and DOR G-protein and the reduced potency of the stimulatory ligands also occurred in the presence of rimonabant, when the receptors were expressed in physiological

conditions. Moreover the decreased maximal MOR G-protein efficacy was also observed when the CB_1 receptors were not expressed in the forebrain; therefore it is a CB_1 receptor independent action, at least in the forebrain region. In previous MOR G-protein studies ten times higher concentrations of rimonabant significantly altered the potency of DAMGO CB_1 receptor independently, but did not change the maximal stimulation over basal activity of the MOR [128].

Despite that CB_2 is mostly present in non-neuronal peripheral tissues, increasing amount of data shows its neuronal and non-neuronal presence in the CNS [180,181]. Previously our group also showed a CB_2 mediated noladin ether influence on forebrain MOR G-protein activation [113] as well as an inhibitory role of a CB_2 antagonist (SR144528) at MOR activity in brainstem [112]. To examine whether the CB_2 receptor has a role (if any) in the observed changes in MOR G-protein stimulation, in the next step we performed the DAMGO-stimulated [^{35}S]GTPγS binding experiments on CB_1/CB_2 double knockout mice forebrain. According to our data, particularly that rimonabant decreased MOR signaling in the same extent in double knockouts as in controls, the role of the CB_2 can also be excluded. These results were however expected since rimonabant has a very poor affinity for the CB_2 receptor [62]. Additionally the significantly reduced DOR G-protein maximal efficacy and DPDPE potency was also unaltered when neither cannabinoid receptors were present in the forebrain. Thus our [^{35}S]GTPγS binding experiments conducted in mouse forebrain membranes highlighted a cannabinoid receptor independent MOR and DOR function.

To make certain that the observed actions of rimonabant are not due to the non-CB_1 related inverse agonistic effect, we examined L-epinephrine-induced G-protein activity in the presence of rimonabant in CB_1/CB_2 receptor double knock-out mouse forebrain membranes. The α_2 AR is known to be expressed physiologically in CHO cell lines and it is present in high levels in certain forebrain regions, in addition there is evidence that rimonabant can bind to this type of AR with micromolar affinity. According to our results rimonabant did not have any effect on adrenergic receptor G-protein maximal activity or L-epinephrine potency during L-epinephrine stimulation even at a very high, 10 μM concentrations. Therefore it strengthens our findings that the decreased agonist mediated MOR and DOR G-protein activation by rimonabant is an antagonistic mechanism and henceforth excludes the unspecific inverse agonistic effect.

Thus according to our binding studies rimonabant can directly inhibit MOR and DOR specific agonist binding in micromolar concentrations and antagonist binding in subnanomolar concentrations independently from other opioid or cannabinoid receptors. Our

G-protein activity measurements also pointed out that rimonabant in micromolar concentrations can also inhibit agonist-stimulated MOR and DOR G-protein efficacy and potency again separately from other opioid and cannabinoid receptors. The mechanism behind these actions are possibly due to the antagonistic character of rimonabant towards the MOR and DOR, which possibility is confirmed by our results, together with other previous reports in many levels: (1) the reduced specific binding of the MOR and DOR antagonist in the subnanomolar concentration range, (2) rimonabant favored the inactive MOR receptor conformation, (3) rimonabant on its own did not enhanced the basal activity of either of the investigated opioid receptors, therefore it did not behave as an agonist towards them, (4) the inverse agonistic character can also be excluded since it was neither a MOR nor DOR specific action, (5) the reduced potency of the stimulator ligand in our and other reported results and (6) the reduced E_{max} value of the MOR and DOR G-protein during agonist stimulation. Further on the allosteric effect can also be excluded since Kathmann and co-workers demonstrated previously that rimonabant did not show any allosteric properties on either MOR or DOR in dissociation kinetic studies [142]. Although our results rules out the possibility of rimonabant exerting its observed effects through cannabinoid receptors, opioid receptors (apart from MOR or DOR) or even adrenergic receptors; other direct or indirect interactions might occur between MOR or DOR and other GPCRs. However this possibility is shadowed by the fact that rimonabant reduced MOR and DOR specific binding and G-protein function in similar concentrations. The direct antagonistic behaviour of rimonabant on MOR was also confirmed by Seely and co-workers with non-receptor assay methods [171]: rimonabant blocked morphine attenuated intracellular cAMP levels in intact CHO cells overexpressed with human MOR and also reduced morphine analgesia in mouse tail-flick tests.

After chronic rimonabant treatment the plasma protein level of the compound in humans is reported to be in the mid nanomolar range [128,142,182], which is ten times lower than the inhibitory concentration range of rimonabant observed in MOR and DOR agonist binding and agonist stimulated G-protein activation. However there is no data referring to the bioavailability of rimonabant or the tissue distribution during chronic treatment. Additionally rimonabant is a highly hydrophobic molecule, thus it can deposit in the fat tissue and easily penetrate through the BBB [121], also it has a long half-life (6-9 days with normal BMI and 16 days with higher than 30 kg/m^2, see web reference [H]), because of its high plasma protein binding, which is almost 100% (see web reference [H]). Therefore it is possible that rimonabant may reach micromolar concentrations in peripheral tissues or even in the brain during chronic treatment. Being aware of these informations the inhibitory actions of rimonabant on MOR

and DOR function observed in the micromolar range might have pharmacological relevance. If so the antagonistic behavior of rimonabant on DOR could partially explain the psychiatric side effects of the compound during chronic treatments, since DOR antagonists are proved to cause anxiogenic and depressive-like behaviour [183,184]. It is worth to note that the mediatory role of KOR in the mood related side effects of rimonabant has been demonstrated previously [144]. On the other hand the very low, subnanomolar inhibitory concentration range of rimonabant during MOR and DOR antagonists specific binding can also have pharmacological relevance, however these binding sites were exiguous in case of both receptors (about 20% of the total binding site population) and did not affect either of the receptors G-protein activity during agonist stimulation at this concentration level.

Due to the limited footage of the thesis, it is only focusing on *in vitro* and *in silico* studies. However by the part of this study agonist stimulated MOR G-protein activity measurements were also performed after acute, low dose i.p. rimonabant treatment in mice forebrains. Similarly to the *in vitro* studies the compound inhibited maximal MOR G-protein efficacy independently from CB_1 receptors [152], albeit the exact mechanisms and interactions involved in the effects of our *in vivo* data are more difficult to interpret. The KOR is also part of this overall study, however data are not yet published, but the manuscript is very close to submission. According to these data rimonabant also behaves as an antagonist towards the KOR. In addition administering the compound acutely, i.p., in low dose also reduced the KOR maximal G-protein activity and KOR protein expression rate CB_1 receptor independently in mice forebrains. The low dose treatment reduced anxiety-like behaviour in mice as well.

This overall study does not question the true high affinity of rimonabant towards the CB_1 receptor; it is still a perfect tool to antagonize CB_1 mediated effects (for review see [123]), which was the original purpose of the compounds development [62]. This study aimed to clarify the possible direct mechanisms between rimonabant and the opioid receptors, which had a growing number of literatures in the past few years. We think that the results reported in this thesis together with other published and yet unpublished data regarding to this overall study elucidates that rimonabant, although in relatively high concentrations, but can directly target opioid receptors.

6 SUMMARY

- Rimonabant **inhibited** MOR and DOR specific **agonist binding** in **micromolar** concentrations and MOR and DOR specific **antagonist binding** in **micro-** and **subnanomolar** concentrations. In both cases the inhibition was **independent** from cannabinoid receptors and other opioid receptors.

- Docking computational studies showed a favorable binding position of rimonabant to the **inactive conformational state of MOR**, combined with a **possibility of a hydrogen bond** between rimonabant and a residue in the inactive binding pocket of MOR.

- In G-protein activity measurements we demonstrated that rimonabant has an inverse agonistic action **independent from DOR**, which confirms the non-CB_1 related inverse agonistic effect of rimonabant.

- During DOR **agonist stimulation** rimonabant **inhibited** DOR G-protein activity and DOR agonist potency in **micromolar** concentrations in membranes of **CHO cell lines transfected with DOR**.

- **Micromolar** concentrations of rimonabant also **inhibited** MOR and DOR mediated G-protein activity and DOR agonist potency in **mouse forebrain** membranes **independently** from both cannabinoid receptors in agonist stimulated G-protein activity measurements.

- Our results pointed out an **antagonistic binding character** for rimonabant towards MOR and DOR, which finding is also confirmed by subsequent reports.

7 CONCLUDING REMARKS

We can certainly claim that rimonabant had a huge impact on cannabinoid receptor research as well as on the pharmaceutical industry. For the first time rimonabant gave the researchers the possibility to selectively antagonize the effects of CB_1 receptors, however this ability was later shadowed by its inverse agonistic and unspecific actions (for review see [123,134]). Taranabant [185], a highly selective CB_1 receptor inverse agonist was also a clinical candidate for the treatment of obesity, with a more safer pharmacological profile compared to rimonabant [141]. However the trials were stopped because it had also produced strong psychiatric side-effects [186]. The rimonabant analogue AM251 [187] has also been proven being involved in MOR related effects [188,189], moreover it was described as an antagonist for MOR [171]. Thus examining the currently available CB_1 receptor antagonists/inverse agonists, it is unlikely that the opioid receptors are their possible therapeutic targets. Partly because of their relatively low affinity towards these receptors and partly because the psychiatric side effects of these compounds are possibly mediated through these receptors [144]. Reducing the BBB penetration of these compounds is a possible way to reduce their undesired psychiatric side effects and they are already under development (for review see [190]). At the same time it can possibly make the CB_1 receptors again a promising target for anti-obesity agents. As described in section **1.3.3** low dose combined treatment with opioid antagonists have promising therapeutic applications, partly due to the applied lower concentrations, which lowers the risk of possible side effects. Other interesting approaches are the construction of MOR agonist and CB_1 receptor antagonist bivalent ligands, which than can target both receptors at the same time. For instance according to the study of Le Naour and co-workers the morphine and rimonabant bivalent ligand had potent analgesic effect and at the same time it was devoid of tolerance [191]. Very recently hybrid molecules derived from fentanyl (a highly MOR selective agonist [192]) and rimonabant has been developed and showed antagonist behaviour towards MOR and CB_1 receptor both *in vivo* and *in vitro* [193]. Thus combining opioid and cannabinoid ligands either in a monovalent or a bivalent form can be a possible approach for future therapeutic applications.

8 REFERENCES

1. Fredriksson, R. **The G-Protein-Coupled Receptors in the Human Genome Form Five Main Families. Phylogenetic Analysis, Paralogon Groups, and Fingerprints**. *Mol Pharmacol* 63**,** 1256–72 (2003).

2. Fredriksson, R. **The Repertoire of G-Protein-Coupled Receptors in Fully Sequenced Genomes**. *Mol Pharmacol* 67**,** 1414–25 (2005).

3. Perez, D. M. **From plants to man: the GPCR "tree of life".** *Mol Pharmacol* 67**,** 1383–4 (2005).

4. Rosenbaum, D. M., Rasmussen, S. G. F. & Kobilka, B. K. **The structure and function of G-protein-coupled receptors.** *Nature* 459**,** 356–63 (2009).

5. Venkatakrishnan, a J., Deupi, X., Lebon, G., Tate, C. G., Schertler, G. F. & Babu, M. M. **Molecular signatures of G-protein-coupled receptors.** *Nature* 494**,** 185–94 (2013).

6. Salon, J., Lodowski, D. & Palczewski, K. **The significance of G protein-coupled receptor crystallography for drug discovery**. *Pharmacol Rev* 63**,** 901–37 (2011).

7. Hermans, E. **Biochemical and pharmacological control of the multiplicity of coupling at G-protein-coupled receptors.** *Pharmacol Ther* 99**,** 25–44 (2003).

8. Kobilka, B. K. **Structural insights into adrenergic receptor function and pharmacology.** *Trends Pharmacol Sci* 32**,** 213–8 (2011).

9. Overington, J. P., Al-Lazikani, B. & Hopkins, A. L. **How many drug targets are there?** *Nat Rev Drug Discov* 5**,** 993–6 (2006).

10. Pettersen, E. F., Goddard, T. D., Huang, C. C., Couch, G. S., Greenblatt, D. M., Meng, E. C. & Ferrin, T. E. **UCSF Chimera--a visualization system for exploratory research and analysis.** *J Comput Chem* 25**,** 1605–12 (2004).

11. Smotrys, J. E. & Linder, M. E. **Palmitoylation of intracellular signaling proteins: regulation and function.** *Annu Rev Biochem* 73**,** 559–87 (2004).

12. Oldham, W. M. & Hamm, H. E. **Heterotrimeric G protein activation by G-protein-coupled receptors.** *Nat Rev Mol Cell Biol* 9**,** 60–71 (2008).

13. Tate, C. G. & Schertler, G. F. X. **Engineering G protein-coupled receptors to facilitate their structure determination.** *Curr Opin Struct Biol* 19**,** 386–95 (2009).

14. Lefkowitz, R. J. **Historical review: a brief history and personal retrospective of seven-transmembrane receptors.** *Trends Pharmacol Sci* 25**,** 413–22 (2004).

15. Samama, P., Cotecchia, S., Costa, T. & Lefkowitz, R. J. **A mutation-induced activated state of the beta 2-adrenergic receptor. Extending the ternary complex model.** *J Biol Chem* 268**,** 4625–36 (1993).

16. Dror, R. O., Arlow, D. H., Maragakis, P., Mildorf, T. J., Pan, A. C., Xu, H., Borhani, D. W., Shaw, D. E., Drora, R. O., Arlowa, D. H., Maragakisa, P., Mildorfa, T. J., Pana, A. C., Xua, H., David W. Borhania, A. & Shawa, D. E. **Activation mechanism of the β2-adrenergic receptor.** *Proc Natl Acad Sci U S A* 108**,** 18684–9 (2011).

17. Kahsai, A. W., Xiao, K., Rajagopal, S., Ahn, S., Shukla, A. K., Sun, J., Oas, T. G. & Lefkowitz, R. J. **Multiple ligand-specific conformations of the β2-adrenergic receptor.** *Nat Chem Biol* 7**,** 692–700 (2011).

18. Strange, P. G. **Mechanisms of inverse agonism at G-protein-coupled receptors**. *Trends Pharmacol Sci* 23**,** 89–95 (2002).

19. Milligan, G. **Constitutive activity and inverse agonists of G protein-coupled receptors: a current perspective.** *Mol Pharmacol* 64**,** 1271–6 (2003).

20. Kenakin, T. **Inverse, protean, and ligand-selective agonism: matters of receptor conformation**. *FASEB J* 15**,** 598–11 (2001).

21. Spiegel, A. M. **Defects in G protein-coupled signal transduction in human disease.** *Annu Rev Physiol* 58**,** 143–70 (1996).

22. De Ligt, R. A., Kourounakis, A. P. & IJzerman, A. P. **Inverse agonism at G protein-coupled receptors: (patho)physiological relevance and implications for drug discovery.** *Br J Pharmacol* 130**,** 1–12 (2000).

23. Arvanitakis, L., Geras-Raaka, E., Varma, A., Gershengorn, M. C. & Cesarman, E. **Human herpesvirus KSHV encodes a constitutively active G-protein-coupled receptor linked to cell proliferation.** *Nature* 385**,** 347–50 (1997).

24. Rosenkilde, M. M. & Schwartz, T. W. **Potency of ligands correlates with affinity measured against agonist and inverse agonists but not against neutral ligand in constitutively active chemokine receptor.** *Mol Pharmacol* 57**,** 602–9 (2000).

25. Schmidt, C. J., Thomas, T. C., Levine, M. A. & Neer, E. J. **Specificity of G protein beta and gamma subunit interactions.** *J Biol Chem* 267**,** 13807–10 (1992).

26. Ayoub, M. A., Al-Senaidy, A. & Pin, J.-P. **Receptor-G protein interaction studied by bioluminescence resonance energy transfer: lessons from protease-activated receptor 1.** *Front Endocrinol (Lausanne)* 3**,** doi: 10.3389/fendo.2012.00082 (2012).

27. Oldham, W. M., Van Eps, N., Preininger, A. M., Hubbell, W. L. & Hamm, H. E. **Mechanism of the receptor-catalyzed activation of heterotrimeric G proteins.** *Nat Struct Mol Biol* 13**,** 772–7 (2006).

28. Oldham, W. M. & Hamm, H. E. **Structural basis of function in heterotrimeric G proteins.** *Q Rev Biophys* 39**,** 117–66 (2006).

29. Hur, E. M. & Kim, K. T. **G protein-coupled receptor signalling and cross-talk: achieving rapidity and specificity.** *Cell Signal* 14**,** 397–405 (2002).

30. Kilts, J. D., Gerhardt, M. A., Richardson, M. D., Sreeram, G., Mackensen, G. B., Grocott, H. P., White, W. D., Davis, R. D., Newman, M. F., Reves, J. G., Schwinn, D. A. & Kwatra, M. M.

Beta(2)-adrenergic and several other G protein-coupled receptors in human atrial membranes activate both G(s) and G(i). *Circ Res* 87**,** 705–9 (2000).

31. Cordeaux, Y., Nickolls, S. A., Flood, L. A., Graber, S. G. & Strange, P. G. **Agonist regulation of D(2) dopamine receptor/G protein interaction. Evidence for agonist selection of G protein subtype.** *J Biol Chem* 276**,** 28667–75 (2001).

32. Chen, Z. & Minneman, K. P. **Recent progress in alpha1-adrenergic receptor research.** *Acta Pharmacol Sin* 26**,** 1281–7 (2005).

33. Wang, D., Tan, Y., Kreitzer, G. E., Nakai, Y., Shan, D., Zheng, Y. & Huang, X.-Y. **G proteins G12 and G13 control the dynamic turnover of growth factor-induced dorsal ruffles.** *J Biol Chem* 281**,** 32660–7 (2006).

34. West, R. E., Moss, J., Vaughan, M., Liu, T. & Liu, T. Y. **Pertussis toxin-catalyzed ADP-ribosylation of transducin. Cysteine 347 is the ADP-ribose acceptor site.** *J Biol Chem* 260**,** 14428–30 (1985).

35. Rozenfeld, R. & Devi, L. A. **Exploring a role for heteromerization in GPCR signalling specificity.** *Biochem J* 433**,** doi: 10.1042/BJ20100458 (2011).

36. Fonseca, J. & Lambert, N. **Instability of a class A G protein-coupled receptor oligomer interface**. *Mol Pharmacol* 75**,** 1296–9 (2009).

37. Birdsall, N. J. M. **Class A GPCR heterodimers: evidence from binding studies.** *Trends Pharmacol Sci* 31**,** 499–508 (2010).

38. González-Maeso, J. **GPCR oligomers in pharmacology and signaling.** *Mol Brain* 4**,** doi: 10.1186/1756–6606–4–20. (2011).

39. Selbie, L. A. & Hill, S. J. **G protein-coupled- receptor cross-talk : the fine-tuning of multiple pathways**. *Trends Pharmacol Sci* 19**,** 87–93 (1998).

40. Hamm, H. **The many faces of G protein signaling**. *J Biol Chem* 273**,** 669–72 (1998).

41. Jordan, B. & Devi, L. **G-protein-coupled receptor heterodimerization modulates receptor function**. *Nature* 399**,** 697–700 (1999).

42. Kenakin, T. **Functional selectivity and biased receptor signaling.** *J Pharmacol Exp Ther* 336**,** 296–302 (2011).

43. Reiter, E., Ahn, S., Shukla, A. K. & Lefkowitz, R. J. **Molecular mechanism of β-arrestin-biased agonism at seven-transmembrane receptors.** *Annu Rev Pharmacol Toxicol* 52**,** 179–97 (2012).

44. Murray, R. M., Morrison, P. D., Henquet, C. & Di Forti, M. **Cannabis, the mind and society: the hash realities.** *Nat Rev Neurosci* 8**,** 885–95 (2007).

45. Brownstein, M. J. **A brief history of opiates , opioid peptides , and opioid receptors**. 90**,** 5391–3 (1993).

46. Pert, C. B. & Snyder, S. H. **Opiate receptor: demonstration in nervous tissue.** *Science (80-)* 179**,** 1011–4 (1973).

47. Simon, E. J., Hiller, J. M. & Edelman, I. **Stereospecific binding of the potent narcotic analgesic (3H) Etorphine to rat-brain homogenate.** *Proc Natl Acad Sci U S A* 70**,** 1947–9 (1973).

48. Terenius, L. **Characteristics of the "receptor" for narcotic analgesics in synaptic plasma membrane fraction from rat brain.** *Acta Pharmacol Toxicol* 33**,** 377–84 (1973).

49. Devane, W. A., Dysarz, F. A., Johnson, M. R., Melvin, L. S. & Howlett, A. C. **Determination and characterization of a cannabinoid receptor in rat brain.** *Mol Pharmacol* 34**,** 605–13 (1988).

50. Howlett, A. C. & Fleming, R. M. **Cannabinoid inhibition of adenylate cyclase. Pharmacology of the response in neuroblastoma cell membranes.** *Mol Pharmacol* 26**,** 532–8 (1984).

51. Howlett, A. C., Qualy, J. M. & Khachatrian, L. L. **Involvement of Gi in the inhibition of adenylate cyclase by cannabimimetic drugs.** *Mol Pharmacol* 29**,** 307–13 (1986).

52. Kieffer, B. L., Befort, K., Gaveriaux-Ruff, C. & Hirth, C. G. **The delta-opioid receptor: isolation of a cDNA by expression cloning and pharmacological characterization.** *Proc Natl Acad Sci U S A* 89**,** 12048–52 (1992).

53. Minami, M., Toya, T., Katao, Y., Maekawa, K., Nakamura, S., Onogi, T., Kaneko, S. & Satoh, M. **Cloning and expression of a cDNA for the rat kappa-opioid receptor.** *FEBS Lett* 329**,** 291–5 (1993).

54. Yasuda, K., Raynor, K., Kong, H., Breder, C. D., Takeda, J., Reisine, T. & Bell, G. I. **Cloning and functional comparison of kappa and delta opioid receptors from mouse brain.** *Proc Natl Acad Sci U S A* 90**,** 6736–40 (1993).

55. Chen, Y., Mestek, A., Liu, J., Hurley, J. A. & Yu, L. **Molecular cloning and functional expression of a mu-opioid receptor from rat brain.** *Mol Pharmacol* 44**,** 8–12 (1993).

56. Evans, C. J., Keith, D. E., Morrison, H., Magendzo, K. & Edwards, R. H. **Cloning of a delta opioid receptor by functional expression.** *Science* 258**,** 1952–5 (1992).

57. RK, Reinscheid Ardati A, Monsma FJ Jr, C. O. **ORL1, a novel member of the opioid receptor family. Cloning, functional expression and localization.** *FEBS Lett* 341**,** 33–8 (1996).

58. Hughes, J., Smith, T. W., Kosterlitz, H. W., Fothergill, L. A., Morgan, B. A. & Morris, H. R. **Identification of two related pentapeptides from the brain with potent opiate agonist activity.** *Nature* 258**,** 577–80 (1975).

59. Matsuda, L. A., Lolait, S. J., Brownstein, M. J., Young, A. C. & Bonner, T. I. **Structure of a cannabinoid receptor and functional expression of the cloned cDNA.** *Nature* 346**,** 561–4 (1990).

60. Devane, W. A., Hanus, L., Breuer, A., Pertwee, R. G., Stevenson, L. A., Griffin, G., Gibson, D., Mandelbaum, A., Etinger, A. & Mechoulam, R. **Isolation and structure of a brain constituent that binds to the cannabinoid receptor.** *Science* 258**,** 1946–9 (1992).

61. Munro, S., Thomas, K. L. & Abu-Shaar, M. **Molecular characterization of a peripheral receptor for cannabinoids.** *Nature* 365**,** 61–5 (1993).

62. Rinaldi-Carmona, M., Barth, F., Héaulme, M., Shire, D., Calandra, B., Congy, C., Martinez, S., Maruani, J., Néliat, G. & Caput, D. **SR141716A, a potent and selective antagonist of the brain cannabinoid receptor.** *FEBS Lett* 350**,** 240–4 (1994).

63. Járai, Z., Wagner, J. A., Varga, K., Lake, K. D., Compton, D. R., Martin, B. R., Zimmer, a M., Bonner, T. I., Buckley, N. E., Mezey, E., Razdan, R. K., Zimmer, A. & Kunos, G. **Cannabinoid-induced mesenteric vasodilation through an endothelial site distinct from CB1 or CB2 receptors.** *Proc Natl Acad Sci U S A* 96**,** 14136–41 (1999).

64. Simonin, F., Slowe, S., Becker, J. A., Matthes, H. W., Filliol, D., Chluba, J., Kitchen, I. & Kieffer, B. L. **Analysis of [3H]bremazocine binding in single and combinatorial opioid receptor knockout mice.** *Eur J Pharmacol* 414**,** 189–95 (2001).

65. Cox, B. M. **Recent developments in the study of opioid receptors.** *Mol Pharmacol* 83**,** 723–8 (2013).

66. Brown, A. J. **Novel cannabinoid receptors.** *Br J Pharmacol* 152**,** 567–75 (2007).

67. McHugh, D., Hu, S. S. J., Rimmerman, N., Juknat, A., Vogel, Z., Walker, J. M. & Bradshaw, H. B. **N-arachidonoyl glycine, an abundant endogenous lipid, potently drives directed cellular migration through GPR18, the putative abnormal cannabidiol receptor.** *BMC Neurosci* 11**,** doi: 10.1186/1471–2202–11–44 (2010).

68. Burford, N. T., Wang, D. & Sadée, W. **G-protein coupling of mu-opioid receptors (OP3): elevated basal signalling activity.** *Biochem J* 348**,** 531–7 (2000).

69. Demuth, D. G. & Molleman, A. **Cannabinoid signalling.** *Life Sci* 78**,** 549–63 (2006).

70. Johnson, P. S., Wang, J. B., Wang, W. F. & Uhl, G. R. **Expressed mu opiate receptor couples to adenylate cyclase and phosphatidyl inositol turnover.** *Neuroreport* 5**,** 507–9 (1994).

71. Bidaut-Russell, M., Devane, W. A. & Howlett, A. C. **Cannabinoid receptors and modulation of cyclic AMP accumulation in the rat brain.** *J Neurochem* 55**,** 21–6 (1990).

72. Bourinet, E., Soong, T. W., Stea, A. & Snutch, T. P. **Determinants of the G protein-dependent opioid modulation of neuronal calcium channels.** *Proc Natl Acad Sci U S A* 93**,** 1486–91 (1996).

73. Ivanina, T., Varon, D., Peleg, S., Rishal, I., Porozov, Y., Dessauer, C. W., Keren-Raifman, T. & Dascal, N. **Galphai1 and Galphai3 differentially interact with, and regulate, the G protein-activated K+ channel.** *J Biol Chem* 279**,** 17260–8 (2004).

74. Howlett, a C., Barth, F., Bonner, T. I., Cabral, G., Casellas, P., Devane, W. a, Felder, C. C., Herkenham, M., Mackie, K., Martin, B. R., Mechoulam, R. & Pertwee, R. G. **International Union of Pharmacology. XXVII. Classification of cannabinoid receptors.** *Pharmacol Rev* 54**,** 161–202 (2002).

75. Mansour, A., Fox, C., Akil, H. & Watson, S. **Opioid-receptor mRNA expression in the rat CNS: anatomical and functional implications**. *Trends Neurosci* 18**,** 22–9 (1995).

76. Koneru, A., Satyanarayana, S. & Rizwan, S. **Endogenous opioids: their physiological role and receptors**. *Glob J Pharmacol* 3**,** 149–53 (2009).

77. Fichna, J., Gach, K., Piestrzeniewicz, M., Burgeon, E., Poels, J., Broeck, J. Vanden & Janecka, A. **Functional characterization of opioid receptor ligands by aequorin luminescence-based calcium assay.** *J Pharmacol Exp Ther* 317**,** 1150–4 (2006).

78. Li, C. H. & Chung, D. **Isolation and structure of an untriakontapeptide with opiate activity from camel pituitary glands.** *Proc Natl Acad Sci U S A* 73**,** 1145–8 (1976).

79. Goldstein, A., Fischli, W., Lowney, L. I., Hunkapiller, M. & Hood, L. **Porcine pituitary dynorphin: complete amino acid sequence of the biologically active heptadecapeptide.** *Proc Natl Acad Sci U S A* 78**,** 7219–23 (1981).

80. Meunier, J. C., Mollereau, C., Toll, L., Suaudeau, C., Moisand, C., Alvinerie, P., Butour, J. L., Guillemot, J. C., Ferrara, P. & Monsarrat, B. **Isolation and structure of the endogenous agonist of opioid receptor-like ORL1 receptor.** *Nature* 377**,** 532–5 (1995).

81. Zadina, J. E., Hackler, L., Ge, L. J. & Kastin, A. J. **A potent and selective endogenous agonist for the mu-opiate receptor.** *Nature* 386**,** 499–502 (1997).

82. Bisogno, T. **Endogenous cannabinoids: structure and metabolism.** *J Neuroendocrinol* 20**,** 1–9 (2008).

83. Rodríguez de Fonseca, F., Del Arco, I., Bermudez-Silva, F. J., Bilbao, A., Cippitelli, A. & Navarro, M. **The endocannabinoid system: physiology and pharmacology.** *Alcohol Alcohol* 40**,** 2–14 (2005).

84. Di Marzo, V. & Fontana, A. **Anandamide, an endogenous cannabinomimetic eicosanoid: "killing two birds with one stone".** *Prostaglandins Leukot Essent Fatty Acids* 53**,** 1–11 (1995).

85. Hanus, L., Abu-Lafi, S., Fride, E., Breuer, A., Vogel, Z., Shalev, D. E., Kustanovich, I. & Mechoulam, R. **2-arachidonyl glyceryl ether, an endogenous agonist of the cannabinoid CB1 receptor.** *Proc Natl Acad Sci U S A* 98**,** 3662–5 (2001).

86. Kakidani, H., Furutani, Y., Takahashi, H., Noda, M., Morimoto, Y., Hirose, T., Asai, M., Inayama, S., Nakanishi, S. & Numa, S. **Cloning and sequence analysis of cDNA for porcine beta-neo-endorphin/dynorphin precursor.** *Nature* 298**,** 245–9 (1982).

87. Noda, M., Furutani, Y., Takahashi, H., Toyosato, M., Hirose, T., Inayama, S., Nakanishi, S. & Numa, S. **Cloning and sequence analysis of cDNA for bovine adrenal preproenkephalin.** *Nature* 295**,** 202–6 (1982).

88. Johanning, K., Juliano, M. A., Juliano, L., Lazure, C., Lamango, N. S., Steiner, D. F. & Lindberg, I. **Specificity of prohormone convertase 2 on proenkephalin and proenkephalin-related substrates.** *J Biol Chem* 273**,** 22672–80 (1998).

89. Fichna, J., Janecka, A., Costentin, J. & Do Rego, J.-C. **The endomorphin system and its evolving neurophysiological role.** *Pharmacol Rev* 59**,** 88–123 (2007).

90. Basavarajappa, B. S. **Critical enzymes involved in endocannabinoid metabolism.** *Protein Pept Lett* 14**,** 237–46 (2007).

91. Alexander, S. P. H. & Kendall, D. A. **The complications of promiscuity: endocannabinoid action and metabolism.** *Br J Pharmacol* 152**,** 602–23 (2007).

92. Pickel, V. M., Chan, J., Kash, T. L., Rodríguez, J. J. & MacKie, K. **Compartment-specific localization of cannabinoid 1 (CB1) and mu-opioid receptors in rat nucleus accumbens.** *Neuroscience* 127**,** 101–12 (2004).

93. Rodriguez, J. J., Mackie, K. & Pickel, V. M. **Ultrastructural localization of the CB1 cannabinoid receptor in mu-opioid receptor patches of the rat Caudate putamen nucleus.** *J Neurosci* 21**,** 823–33 (2001).

94. Salio, C., Fischer, J., Franzoni, M. F., Mackie, K., Kaneko, T. & Conrath, M. **CB1-cannabinoid and mu-opioid receptor co-localization on postsynaptic target in the rat dorsal horn.** *Neuroreport* 12**,** 3689–92 (2001).

95. Schoffelmeer, A. N. M., Hogenboom, F., Wardeh, G. & De Vries, T. J. **Interactions between CB1 cannabinoid and mu opioid receptors mediating inhibition of neurotransmitter release in rat nucleus accumbens core.** *Neuropharmacology* 51**,** 773–81 (2006).

96. Rios, C., Gomes, I. & Devi, L. A. **Mu opioid and CB1 cannabinoid receptor interactions: reciprocal inhibition of receptor signaling and neuritogenesis.** *Br J Pharmacol* 148**,** 387–95 (2006).

97. Berrendero, F., Mendizabal, V., Murtra, P., Kieffer, B. L. & Maldonado, R. **Cannabinoid receptor and WIN 55 212-2-stimulated [35S]-GTPgammaS binding in the brain of mu-, delta- and kappa-opioid receptor knockout mice**. *Eur J Neurosci* 18**,** 2197–2202 (2003).

98. Hojo, M., Sudo, Y., Ando, Y., Minami, K., Takada, M., Matsubara, T., Kanaide, M., Taniyama, K., Sumikawa, K. & Uezono, Y. **Mu-opioid receptor forms a functional heterodimer with cannabinoid CB1 receptor: electrophysiological and FRET assay analysis.** *J Pharmacol Sci* 108**,** 308–19 (2008).

99. Urigüen, L., Berrendero, F., Ledent, C., Maldonado, R. & Manzanares, J. **Kappa- and delta-opioid receptor functional activities are increased in the caudate putamen of cannabinoid CB1 receptor knockout mice.** *Eur J Neurosci* 22**,** 2106–10 (2005).

100. Rozenfeld, R., Bushlin, I., Gomes, I., Tzavaras, N., Gupta, A., Neves, S., Battini, L., Gusella, G. L., Lachmann, A., Ma'ayan, A., Blitzer, R. D. & Devi, L. A. **Receptor heteromerization expands the repertoire of cannabinoid signaling in rodent neurons.** *PLoS One* 7**,** doi:10.1371/journal.pone.0029239 (2012).

101. Bushlin, I., Gupta, A., Stockton, S. D., Miller, L. K. & Devi, L. A. **Dimerization with cannabinoid receptors allosterically modulates delta opioid receptor activity during neuropathic pain.** *PLoS One* 7**,** doi:10.1371/journal.pone.0049789 (2012).

102. Pertwee, R. G. **Cannabinoid receptors and pain.** *Prog Neurobiol* 63**,** 569–611 (2001).

103. Maldonado, R. & Valverde, O. **Participation of the opioid system in cannabinoid-induced antinociception and emotional-like responses**. *Eur Neuropsychopharmacol* 13**,** 401–410 (2003).

104. Bie, B. & Pan, Z. Z. **Trafficking of central opioid receptors and descending pain inhibition.** *Mol Pain* 3**,** doi:10.1186/1744–8069–3–37 (2007).

105. Lichtman, A. H., Cook, S. A. & Martin, B. R. **Investigation of brain sites mediating cannabinoid-induced antinociception in rats: evidence supporting periaqueductal gray involvement.** *J Pharmacol Exp Ther* 276**,** 585–93 (1996).

106. Bambico, F. R., Katz, N., Debonnel, G. & Gobbi, G. **Cannabinoids elicit antidepressant-like behavior and activate serotonergic neurons through the medial prefrontal cortex.** *J Neurosci* 27**,** 11700–11 (2007).

107. Filliol, D., Ghozland, S., Chluba, J., Martin, M., Matthes, H. W., Simonin, F., Befort, K., Gavériaux-Ruff, C., Dierich, a, LeMeur, M., Valverde, O., Maldonado, R. & Kieffer, B. L. **Mice deficient for delta- and mu-opioid receptors exhibit opposing alterations of emotional responses.** *Nat Genet* 25**,** 195–200 (2000).

108. Tallett, a J., Blundell, J. E. & Rodgers, R. J. **Endogenous opioids and cannabinoids: system interactions in the regulation of appetite, grooming and scratching.** *Physiol Behav* 94**,** 422–31 (2008).

109. Cota, D., Tschöp, M. H., Horvath, T. L. & Levine, A. S. **Cannabinoids, opioids and eating behavior: the molecular face of hedonism?** *Brain Res Rev* 51**,** 85–107 (2006).

110. Carai, M. a M., Colombo, G., Gessa, G. L., Yalamanchili, R., Basavarajappa, B. S., Basavarajppa, B. S. & Hungund, B. L. **Investigation on the relationship between cannabinoid CB1 and opioid receptors in gastrointestinal motility in mice.** *Br J Pharmacol* 148**,** 1043–50 (2006).

111. Manzanares, J., Ortiz, S., Oliva, J. M., Pérez-Rial, S. & Palomo, T. **Interactions between cannabinoid and opioid receptor systems in the mediation of ethanol effects.** *Alcohol Alcohol* 40**,** 25–34 (2005).

112. Páldy, E., Bereczki, E., Sántha, M., Wenger, T., Borsodi, A., Zimmer, A. & Benyhe, S. **CB(2) cannabinoid receptor antagonist SR144528 decreases mu-opioid receptor expression and activation in mouse brainstem: role of CB(2) receptor in pain.** *Neurochem Int* 53**,** 309–16 (2008).

113. Páldyová, E., Bereczki, E., Sántha, M., Wenger, T., Borsodi, A. & Benyhe, S. **Noladin ether, a putative endocannabinoid, inhibits mu-opioid receptor activation via CB2 cannabinoid receptors.** *Neurochem Int* 52**,** 321–8 (2008).

114. Sim, L. J. & Childers, S. R. **Anatomical distribution of mu, delta, and kappa opioid- and nociceptin/orphanin FQ-stimulated [35S]guanylyl-5'-O-(gamma-thio)-triphosphate binding in guinea pig brain.** *J Comp Neurol* 386**,** 562–72 (1997).

115. Pertwee, R. G. & Howlett, A. C. **International Union of Basic and Clinical Pharmacology. LXXIX. Cannabinoid receptors and their ligands: beyond CB1 and CB2**. *Pharmacol Rev* 62**,** 588–631 (2010).

116. Pagotto, U., Marsicano, G., Cota, D., Lutz, B. & Pasquali, R. **The emerging role of the endocannabinoid system in endocrine regulation and energy balance.** *Endocr Rev* 27**,** 73–100 (2006).

117. Birch, E. A. **The use of indian hemp in the treatment of chronic chloral and chronic opium poisoning**. *Lancet* 1**,** 625 (1889).

118. Donovan, M. **On the physical and medicinal qualities of Indian hemp (Cannabis Indica); with observations on the best mode of administration, and cases illustrative of its powers**. *Dublin J Med Sci* 26**,** 368–402 (1845).

119. Touw, M. **The religious and medicinal uses of Cannabis in China, India and Tibet.** *J Psychoactive Drugs* 13**,** 23–34 (1981).

120. Xie, S. & Furjanic, M. **The endocannabinoid system and rimonabant: a new drug with a novel mechanism of action involving cannabinoid CB1 receptor antagonism - or inverse agonism - as potential obesity treatment and other therapeutic use.** *J Clin Pharm Ther* 32**,** 209–31 (2007).

121. Rinaldi-Carmona, M., Barth, F. & Héaulme, M. **Biochemical and pharmacological characterisation of SR141716A, the first potent and selective brain cannabinoid receptor antagonist**. *Life Sci* 56**,** 1941–7 (1995).

122. Christopoulou, F. D. & Kiortsis, D. N. **An overview of the metabolic effects of rimonabant in randomized controlled trials: potential for other cannabinoid 1 receptor blockers in obesity.** *J Clin Pharm Ther* 36**,** 10–8 (2011).

123. Pertwee, R. G. **Inverse agonism and neutral antagonism at cannabinoid CB1 receptors.** *Life Sci* 76**,** 1307–24 (2005).

124. Padwal, R. S. & Majumdar, S. R. **Drug treatments for obesity: orlistat, sibutramine, and rimonabant.** *Lancet* 369**,** 71–7 (2007).

125. Christensen, R., Kristensen, P. K., Bartels, E. M., Bliddal, H. & Astrup, A. **Efficacy and safety of the weight-loss drug rimonabant: a meta-analysis of randomised trials.** *Lancet* 370**,** 1706–13 (2007).

126. Breivogel, C. S., Griffin, G., Di Marzo, V. & Martin, B. R. **Evidence for a new G protein-coupled cannabinoid receptor in mouse brain.** *Mol Pharmacol* 60**,** 155–63 (2001).

127. Hough, L. B., Svokos, K. & Nalwalk, J. W. **Non-opioid antinociception produced by brain stem injections of improgan: significance of local, but not cross-regional, cannabinoid mechanisms.** *Brain Res* 1247**,** 62–70 (2009).

128. Cinar, R. & Szücs, M. **CB1 receptor-independent actions of SR141716 on G-protein signaling: coapplication with the mu-opioid agonist Tyr-D-Ala-Gly-(NMe)Phe-Gly-ol unmasks novel, pertussis toxin-insensitive opioid signaling in mu-opioid receptor-Chinese hamster ovary cells.** *J Pharmacol Exp Ther* 330**,** 567–74 (2009).

129. MacLennan, S. J., Reynen, P. H., Kwan, J. & Bonhaus, D. W. **Evidence for inverse agonism of SR141716A at human recombinant cannabinoid CB1 and CB2 receptors.** *Br J Pharmacol* 124**,** 619–22 (1998).

130. Sim-Selley, L. J., Brunk, L. K. & Selley, D. E. **Inhibitory effects of SR141716A on G-protein activation in rat brain.** *Eur J Pharmacol* 414**,** 135–43 (2001).

131. Beyer, C. E., Dwyer, J. M., Piesla, M. J., Platt, B. J., Shen, R., Rahman, Z., Chan, K., Manners, M. T., Samad, T. a, Kennedy, J. D., Bingham, B. & Whiteside, G. T. **Depression-like phenotype following chronic CB1 receptor antagonism.** *Neurobiol Dis* 39**,** 148–55 (2010).

132. Mitchell, P. B. & Morris, M. J. **Depression and anxiety with rimonabant**. *Lancet* 370**,** 1671–2 (2007).

133. Raffa, R. B. & Ward, S. J. **CB1-independent mechanisms of Δ^9-THCV, AM251 and SR141716 (rimonabant).** *J Clin Pharm Ther* 37**,** 260–5 (2012).

134. Pertwee, R. G. **Receptors and channels targeted by synthetic cannabinoid receptor agonists and antagonists**. *Curr Med Chem* 17**,** 1360–81 (2010).

135. Le Foll, B. & Goldberg, S. R. **Cannabinoid CB 1 Receptor Antagonists as Promising New Medications for Drug Dependence**. *J Pharmacol Exp Ther* 312**,** 875–83 (2005).

136. Robledo, P., Berrendero, F., Ozaita, A. & Maldonado, R. **Advances in the field of cannabinoid--opioid cross-talk.** *Addict Biol* 13**,** 213–24 (2008).

137. Braida, D., Pozzi, M., Parolaro, D. & Sala, M. **Intracerebral self-administration of the cannabinoid receptor agonist CP 55,940 in the rat: interaction with the opioid system.** *Eur J Pharmacol* 413**,** 227–34 (2001).

138. Fattore, L., Spano, S., Cossu, G., Deiana, S., Fadda, P. & Fratta, W. **Cannabinoid CB(1) antagonist SR 141716A attenuates reinstatement of heroin self-administration in heroin-abstinent rats.** *Neuropharmacology* 48**,** 1097–104 (2005).

139. Navarro, M., Carrera, M. R., Fratta, W., Valverde, O., Cossu, G., Fattore, L., Chowen, J. A., Gomez, R., del Arco, I., Villanua, M. A., Maldonado, R., Koob, G. F. & Rodriguez de Fonseca, F. **Functional interaction between opioid and cannabinoid receptors in drug self-administration.** *J Neurosci* 21**,** 5344–50 (2001).

140. Verty, A. N. A., Singh, M. E., McGregor, I. S. & Mallet, P. E. **The cannabinoid receptor antagonist SR 141716 attenuates overfeeding induced by systemic or intracranial morphine.** *Psychopharmacology (Berl)* 168**,** 314–23 (2003).

141. Fong, T. M., Shearman, L. P., Stribling, D. S., Shu, J., Lao, J., Huang, C. R.-R., Xiao, J. C., Shen, C.-P., Tyszkiewicz, J., Strack, A. M., DeMaula, C., Hubert, M.-F., Galijatovic-Idrizbegovic, A., Owen, R., Huber, A. C. & Lanning, C. L. **Pharmacological efficacy and safety profile of taranabant in preclinical species**. *Drug Dev Res* 70**,** 349–62 (2009).

142. Kathmann, M., Flau, K., Redmer, A., Tränkle, C. & Schlicker, E. **Cannabidiol is an allosteric modulator at mu- and delta-opioid receptors.** *Naunyn Schmiedebergs Arch Pharmacol* 372**,** 354–61 (2006).

143. Walentiny, D., Vann, R. & Warner, J. **Kappa opioid mediation of cannabinoid effects of the potent hallucinogen, salvinorin A, in rodents**. *Psychopharmacology (Berl)* 210**,** 275–84 (2010).

144. Lockie, S. H., Czyzyk, T. A., Chaudhary, N., Perez-Tilve, D., Woods, S. C., Oldfield, B. J., Statnick, M. A. & Tschöp, M. H. **CNS opioid signaling separates cannabinoid receptor 1-mediated effects on body weight and mood-related behavior in mice.** *Endocrinology* 152**,** 3661–7 (2011).

145. Gallate, J. E., Mallet, P. E. & McGregor, I. S. **Combined low dose treatment with opioid and cannabinoid receptor antagonists synergistically reduces the motivation to consume alcohol in rats.** *Psychopharmacology (Berl)* 173**,** 210–6 (2004).

146. Kirkham, T. C. & Williams, C. M. **Synergistic efects of opioid and cannabinoid antagonists on food intake**. *Psychopharmacology (Berl)* 153**,** 267–70 (2001).

147. Melis, T., Succu, S., Sanna, F., Boi, A., Argiolas, A. & Melis, M. R. **The cannabinoid antagonist SR 141716A (Rimonabant) reduces the increase of extra-cellular dopamine release in the rat nucleus accumbens induced by a novel high palatable food.** *Neurosci Lett* 419**,** 231–5 (2007).

148. Pasternak, G. & Pan, Y.-X. **Mu opioid receptors in pain management.** *Acta Anaesthesiol Taiwan* 49**,** 21–5 (2011).

149. Pradhan, A. A., Smith, M. M. L., Kieffer, B. L. & Evans, C. J. **Ligand-directed signalling within the opioid receptor family.** *Br J Pharmacol* 167**,** 960–9 (2012).

150. Pradhan, A. A., Befort, K., Nozaki, C., Gavériaux-Ruff, C. & Kieffer, B. L. **The delta opioid receptor: an evolving target for the treatment of brain disorders.** *Trends Pharmacol Sci* 32**,** 581–90 (2011).

151. Zádor, F., Kocsis, D., Borsodi, A. & Benyhe, S. **Micromolar concentrations of rimonabant directly inhibits delta opioid receptor specific ligand binding and agonist-induced G-protein activity.** *Neurochem Int* 67**,** 14–22 (2014).

152. Zádor, F., Ötvös, F., Benyhe, S., Zimmer, A. & Páldy, E. **Inhibition of forebrain μ-opioid receptor signaling by low concentrations of rimonabant does not require cannabinoid receptors and directly involves μ-opioid receptors.** *Neurochem Int* 61**,** 378–88 (2012).

153. Nevin, S. T., Kabasakal, L., Otvös, F., Töth, G. & Borsodi, A. **Binding characteristics of the novel highly selective delta agonist, [3H]IIe5,6deltorphin II.** *Neuropeptides* 26**,** 261–5 (1994).

154. Ledent, C., Valverde, O., Cossu, G., Petitet, F., Aubert, J. F., Beslot, F., Böhme, G. A., Imperato, A., Pedrazzini, T., Roques, B. P., Vassart, G., Fratta, W. & Parmentier, M. **Unresponsiveness to cannabinoids and reduced addictive effects of opiates in CB1 receptor knockout mice.** *Science* 283**,** 401–4 (1999).

155. Ioja, E., Tóth, G., Benyhe, S., Tourwe, D., Péter, A., Tömböly, C. & Borsodi, A. **Opioid receptor binding characteristics and structure-activity studies of novel tetrapeptides in the TIPP (Tyr-Tic-Phe-Phe) series.** *Neurosignals* 14**,** 317–28 (2005).

156. Ioja, E., Tourwé, D., Kertész, I., Tóth, G., Borsodi, A. & Benyhe, S. **Novel diastereomeric opioid tetrapeptides exhibit differing pharmacological activity profiles.** *Brain Res Bull* 74**,** 119–29 (2007).

157. Avidor-Reiss, T., Bayewitch, M., Levy, R., Matus-Leibovitch, N., Nevo, I. & Vogel, Z. **Adenylylcyclase supersensitization in mu-opioid receptor-transfected Chinese hamster ovary cells following chronic opioid treatment**. *J Biol Chem* 270**,** 29732–8 (1995).

158. Benyhe, S., Farkas, J., Tóth, G. & Wollemann, M. **Met5-enkephalin-Arg6-Phe7, an endogenous neuropeptide, binds to multiple opioid and nonopioid sites in rat brain.** *J Neurosci Res* 48**,** 249–58 (1997).

159. Schütz, W. **The pharmacological basis of receptor binding.** *Wien Klin Wochenschr* 103**,** 438–42 (1991).

160. Strange, P. G. **Use of the GTPγS ([35S]GTPγS and Eu-GTPγS) binding assay for analysis of ligand potency and efficacy at G protein-coupled receptors.** *Br J Pharmacol* 161**,** 1238–49 (2010).

161. Pogozheva, I. D., Przydzial, M. J. & Mosberg, H. I. **Homology modeling of opioid receptor-ligand complexes using experimental constraints.** *AAPS J* 7**,** 434–48 (2005).

162. Traynor, R., Nahorski, R., Traynor, J. R. & Nahorski, S. R. **Modulation by mu-opioid agonists of guanosine-5'-O-(3-[35S]thio)triphosphate binding to membranes from human neuroblastoma SH-SY5Y cells.** *Mol Pharmacol* 47**,** 848–54 (1995).

163. Sim, L. J., Selley, D. E. & Childers, S. R. **In vitro autoradiography of receptor-activated G proteins in rat brain by agonist-stimulated guanylyl 5'-[gamma-[35S]thio]-triphosphate binding.** *Proc Natl Acad Sci USA* 92**,** 7242–46 (1995).

164. Sousa, S. F., Fernandes, P. A. & Ramos, M. J. **Protein-ligand docking: current status and future challenges.** *Proteins* 65**,** 15–26 (2006).

165. Van Dijk, A. D. J., Boelens, R. & Bonvin, A. M. J. J. **Data-driven docking for the study of biomolecular complexes.** *FEBS J* 272**,** 293–312 (2005).

166. Morris, G. M., Goodsell, D. S., Halliday, R. S., Huey, R., Hart, W. E., Belew, R. K. & Olson, A. J. **Automated docking using a Lamarckian genetic algorithm and an empirical binding free energy function**. *J Comput Chem* 19**,** 1639–62 (1998).

167. Mackerell, A. D. **Empirical force fields for biological macromolecules: overview and issues.** *J Comput Chem* 25**,** 1584–604 (2004).

168. O'Boyle, N. M., Banck, M., James, C. A., Morley, C., Vandermeersch, T. & Hutchison, G. R. **Open Babel: An open chemical toolbox.** *J Cheminform* 3**,** doi: 10.1186/1758–2946–3–33 (2011).

169. Halgren, T. A. **MMFF VI. MMFF94s option for energy minimization studies**. *J Comput Chem* 20**,** 720–29 (1999).

170. Morris, G. M., Huey, R., Lindstrom, W., Sanner, M. F., Belew, R. K., Goodsell, D. S. & Olson, A. J. **AutoDock4 and AutoDockTools4: automated docking with selective receptor flexibility.** *J Comput Chem* 30**,** 2785–91 (2009).

171. Seely, K. a, Brents, L. K., Franks, L. N., Rajasekaran, M., Zimmerman, S. M., Fantegrossi, W. E. & Prather, P. L. **AM-251 and rimonabant act as direct antagonists at mu-opioid receptors: implications for opioid/cannabinoid interaction studies.** *Neuropharmacology* 63**,** 905–15 (2012).

172. Misicka, A., Verheyden, P. M. F. & Binst, G. Van. **Equilibrium of the cis-trans isomerisation of the peptide bond with N-alkyl amino acids measured by 2D NMR**. *Lett Pept Sci* 5**,** 375–7 (1998).

173. Svízenská, I., Dubový, P. & Sulcová, A. **Cannabinoid receptors 1 and 2 (CB1 and CB2), their distribution, ligands and functional involvement in nervous system structures - a short review.** *Pharmacol Biochem Behav* 90**,** 501–11 (2008).

174. Lever, J. R. **PET and SPECT imaging of the opioid system : receptors, radioligands and avenues for drug discovery and development**. *Curr Pharm Des* 13**,** 33–49 (2007).

175. Cottingham, C. & Wang, Q. **A2 adrenergic receptor dysregulation in depressive disorders: implications for the neurobiology of depression and antidepressant therapy.** *Neurosci Biobehav Rev* 36**,** 2214–25 (2012).

176. Baker, J. G. & Hill, S. J. **Multiple GPCR conformations and signalling pathways: implications for antagonist affinity estimates.** *Trends Pharmacol Sci* 28**,** 374–81 (2007).

177. Krizsan, D., Varga, E., Hosztafi, S., Benyhe, S., Szucs, M. & Borsodi, A. **Irreversible blockade of the high and low affinity (3H) naloxone binding sites by C-6 derivatives of morphinane-6-ones.** *Life Sci* 48**,** 439–51 (1991).

178. Seifert, R. & Wenzel-Seifert, K. **Constitutive activity of G-protein-coupled receptors: cause of disease and common property of wild-type receptors.** *Naunyn Schmiedebergs Arch Pharmacol* 366**,** 381–416 (2002).

179. Gong, J.-P., Onaivi, E. S., Ishiguro, H., Liu, Q.-R., Tagliaferro, P. A., Brusco, A. & Uhl, G. R. **Cannabinoid CB2 receptors: immunohistochemical localization in rat brain.** *Brain Res* 1071**,** 10–23 (2006).

180. Van Sickle, M. D., Duncan, M., Kingsley, P. J., Mouihate, A., Urbani, P., Mackie, K., Stella, N., Makriyannis, A., Piomelli, D., Davison, J. S., Marnett, L. J., Di Marzo, V., Pittman, Q. J., Patel, K. D. & Sharkey, K. a. **Identification and functional characterization of brainstem cannabinoid CB2 receptors.** *Science* 310**,** 329–32 (2005).

181. Ross, R. A., Coutts, A. A., McFarlane, S. M., Anavi-Goffer, S., Irving, a J., Pertwee, R. G., MacEwan, D. J. & Scott, R. H. **Actions of cannabinoid receptor ligands on rat cultured sensory neurones: implications for antinociception.** *Neuropharmacology* 40**,** 221–32 (2001).

182. Henness, S., Robinson, D. M. & Lyseng-Williamson, K. A. **Rimonabant.** *Drugs* 66**,** 2109–19; discussion 2120–1 (2006).

183. Saitoh, A., Kimura, Y., Suzuki, T., Kawai, K., Nagase, H. & Kamei, J. **Potential anxiolytic and antidepressant-like activities of SNC80, a selective delta-opioid agonist, in behavioral models in rodents.** *J Pharmacol Sci* 95**,** 374–80 (2004).

184. Perrine, S. A., Hoshaw, B. A. & Unterwald, E. M. **Delta opioid receptor ligands modulate anxiety-like behaviors in the rat.** *Br J Pharmacol* 147**,** 864–72 (2006).

185. Lin, L. S., Lanza, T. J. Jr., Jewell, J. P., Liu, P., Shah, S. K., Qi, H., Tong, X., Wang, J., Xu, S. S., Fong, T. M., Shen, C. P., Lao J., Xiao, J.C., Shearman, L. P., Stribling, D.S., Rosko, K., Strack, A., Marsh, D.J., Feng, Y., Kumar, S., Samuel, K., , W. K. **Discovery of N-[(1S,2S)-3-(4-Chlorophenyl)-2- (3-cyanophenyl)-1-methylpropyl]-2-methyl-2- {[5-(trifluoromethyl)pyridin-2-yl]oxy}propanamide (MK-0364), a novel, acyclic cannabinoid-1 receptor inverse agonist for the treatment of obesity.** *J Med Chem* 49**,** 7584–7 (2006).

186. Kipnes, M. S., Hollander, P., Fujioka, K., Gantz, I., Seck, T., Erondu, N., Shentu, Y., Lu, K., Suryawanshi, S., Chou, M., Johnson-Levonas, A. O., Heymsfield, S. B., Shapiro, D., Kaufman, K. D. & Amatruda, J. M. **A one-year study to assess the safety and efficacy of the CB1R inverse agonist taranabant in overweight and obese patients with type 2 diabetes.** *Diabetes Obes Metab* 12**,** 517–31 (2010).

187. Gatley, S. J., Gifford, A. N., Volkow, N. D., Lan, R. & Makriyannis, A. **123I-labeled AM251: a radioiodinated ligand which binds in vivo to mouse brain cannabinoid CB1 receptors.** *Eur J Pharmacol* 307**,** 331–8 (1996).

188. Da Fonseca Pacheco, D., Klein, A., de Castro Perez, A., da Fonseca Pacheco, C. M., de Francischi, J. N. & Duarte, I. D. G. **The mu-opioid receptor agonist morphine, but not agonists at delta- or kappa-opioid receptors, induces peripheral antinociception mediated by cannabinoid receptors.** *Br J Pharmacol* 154**,** 1143–9 (2008).

189. Trang, T., Sutak, M. & Jhamandas, K. **Involvement of cannabinoid (CB1)-receptors in the development and maintenance of opioid tolerance.** *Neuroscience* 146**,** 1275–88 (2007).

190. Lee, H.-K., Choi, E. B. & Pak, C. S. **The current status and future perspectives of studies of cannabinoid receptor 1 antagonists as anti-obesity agents.** *Curr Top Med Chem* 9**,** 482–503 (2009).

191. Le Naour, M., Akgün, E., Yekkirala, A., Lunzer, M. M., Powers, M. D., Kalyuzhny, A. E. & Portoghese, P. S. **Bivalent ligands that target μ opioid (MOP) and cannabinoid1 (CB1) receptors are potent analgesics devoid of tolerance.** *J Med Chem* 56**,** 5505–13 (2013).

192. Montero, A., Goya, P., Jagerovic, N., Callado, L. F., Meana, J. J., Girón, R., Goicoechea, C. & Martín, M. I. **Guanidinium and aminoimidazolinium derivatives of N-(4-piperidyl)propanamides as potential ligands for mu opioid and I2-imidazoline receptors: synthesis and pharmacological screening.** *Bioorg Med Chem* 10**,** 1009–18 (2002).

193. Jagerovic, N., Fernández-Fernández, C., Erdozain, A. M., Girón, R., Sánchez, E., López-Moreno, J. A., Morales, P., Rodríguez de Fonseca, F., Goya, P., Meana, J. J., Martín, M. I., Callado, L. F. & Fernández Ruiz, J. **Combining rimonabant and fentanyl in a single entity: preparation and pharmacological results**. *Drug Des Devel Ther* 8**,** 263–77 (2014).

9 WEB REFERENCES

A: http://www.nobelprize.org/nobel_prizes/chemistry/laureates/2012/

B: http://www.fda.gov/ohrms/dockets/ac/07/briefing/2007-4306b1-01-sponsor-backgrounder.pdf

C: http://www.ema.europa.eu/docs/en_GB/document_library/Press_release/2009/11/WC500014774.pdf

D: http://www.mosberglab.phar.umich.edu/resources/

E: http://cactus.nci.nih.gov/chemical/structure

F: http://avogadro.openmolecules.net/wiki/Main_Page

G: http://www.tumor-gene.org/cgi-bin/GPCR/by_cell_line.cgi

H: http://www.drugbank.ca/drugs/DB06155

Note: all web references were last accessed in the year 2014. In case of web reference "**D**" the homology models which we used in our docking studies unfortunately are not available anymore in this webpage.

10 ACKNOWLEDGEMENTS

I am very grateful to my supervisor Dr. Sándor Benyhe for giving me the opportunity to fulfill this work in his laboratory and for his kind support, guidance and useful advice throughout my studies.

I am deeply thankful to Dr. Eszter Páldy - from who I inherited this project - for supporting and supervising me alongside her own project in abroad independently from our group. Her accuracy in the scientific field will always be a guide for me.

I am sincerely thankful to Prof. Anna Borsodi for arranging the initial steps of valuable cooperations for me, without it this work would not have reached its current form.

I am very grateful to the Isotope laboratory for synthesizing and providing me the necessary radioactive and unlabeled opioid ligands.

I would like to thank Prof. Tibor Wenger and Prof. György M. Nagy (Department of Human Morphology and Developmental Biology, SOTE) for providing me the CB_1 K.O. mice and their wild type controls.

I would also like to thank Prof. Andreas Zimmer (University of Bonn, Germany) for providing me the CB_1/CB_2 K.O. mice.

I am very grateful to Dr. Zvi Vogel (Weizmann Institute of Science, Israel) and Dr. Melinda Pirity (Institute of Genetics, Biological Research Center, Szeged) for providing us the μ- and δ-opioid receptor transfected CHO cell lines and parental CHO cell lines respectively. Also I would like to thank Erzsébet Kusz (Institute of Bochemistry, Biological Research Center, Szeged) and Gergő Kovács (Institute of Genetics, Biological Research Center, Szeged) for the growing of the cell lines.

I am very grateful to Dr. Ferenc Ötvös for performing the docking calculations.

I am thankful for Béláné Papp for the initial help in the acquirement of laboratory technics and I am deeply grateful to Zsuzsa Canjavec and Ildikó Némethné for the technical guidance and support. I would also like to thank Dóra Kocsis for the participation in the δ-opioid receptor study and for her further technical assistance.

I am also grateful to other former (Judit Szokolainé, Gabriella Szőllősiné) and present colleagues in the Opioid Research Group, especially to Reza Samavati for his support and scientific advice.

I would also like to thank Prof. Mária Wollemann for the critical reading of my manuscripts and this thesis. Her up to date knowledge in the scientific field will always be exemplary for me.

I would like to thank the Biochemistry Institute of the Biological Research Centre for giving me the 3 year fellowship to carry on this study.

Finally I would like to thank my family and my partner Petra for their patience and support. I am especially grateful to my father for his valuable advice and for always looking through my publications and this thesis as well.

This study was supported by funds from the National Development Agency (NFÜ, Budapest, Hungary; grant number: TÁMOP-4.2.2A-11/1KONV-2012-0024 and TÁMOP-4.2.2A-11/1KONV-2012-0052), OTKA 108518 and CK-78566 and finally from the Dr. Rollin D. Hotchkiss Foundation.

APPENDICES

Appendix A: **Summary of the Ph.D. thesis in Hungarian**

Appendix B: **Off-prints of thesis related publications**

Appendix A: Summary of the Ph.D. thesis in Hungarian

Rimonabant: egy CB_1 receptor antagonista, mely direkt kölcsönhatásba lép a μ- és δ-opioid receptorral

Ph.D. értekezés összefoglalója

BEVEZETÉS

Opioid és kannabinoid receptorok és interakciójuk

A kannabinoid receptoroknak (CB_1 és CB_2) és a klasszikus opioid receptoroknak (μ-, κ- és δ-opioid receptorok; sorrendben MOR, KOR, DOR) számos közös jellemzőjük van: a G-fehérje kapcsolt receptor családhoz tartoznak (GPCR), az esetek többségében az ún. $G_{\alpha i/o}$ típusú G-fehérjéhez kapcsolódnak és preszinaptikusan gátolják a különböző neurotranszmitterek felszabadulását. Bizonyos előagyi régiókban az opioid és CB_1 receptorok nemcsak együtt lokalizálódnak, hanem együtt is expresszálódnak akár ugyanazon idegsejten is. Az is bebizonyosodott, hogy képesek indirekt vagy direkt módon egymás működését szabályozni, sőt heterodimert formálni. Ezen interakciók számos átfedő élettani funkciót eredményezhetnek, mint például a fájdalom, a hangulat, az energiaháztartás, a táplálkozás és a bélrendszer működésének szabályozása vagy az alkohol hatásainak közvetítése.

A rimonabant és kapcsolata az opioid rendszerrel

A rimonabant volt az első CB_1 receptorra kifejlesztett szelektív antagonista, amely hatékony étvágycsökkentő hatása miatt kereskedelmi forgalomba is került. Azonban 2 évvel a bevezetését követően visszavonták a forgalmazását a krónikus szedés esetén fellépő erős pszichiátriai mellékhatásai, például súlyos depresszió, szorongás és öngyilkosság gondolata miatt. A rimonabant engedélyezése előtt illetve azt követően számos közlemény rávilágított a gyógyszer nem CB_1-receptor-specifikus hatásaira. Ezek a hatások magas koncentráció alkalmazásakor voltak megfigyelhetők, és a rimonabant később leírt inverz agonista hatásával is magyarázhatók voltak.

Egyre több adat van arra vonatkozóan, hogy a rimonabant képes módosítani az opioid rendszer működését. Bebizonyosodott, hogy a rimonabant által közvetített metabolikus hatásokat és kedélyállapot változásokat az opioid rendszer is képes befolyásolni. Ismert az is, hogy a rimonabant mindhárom klasszikus opioid receptorhoz kötődik relatíve nagy, mikromoláris koncentrációban.

CÉLKITŰZÉSEK

A rimonabant, engedélyezett étvágycsökkentő gyógyszerként bekövetkezett, kudarcát részben a nem specifikus hatásai okozták, részben pedig az, hogy képes a vér-agy-gáton áthatolni. Ma már ismert, hogy a rimonabant nem CB_1 receptor által közvetített hatásai az opioid rendszerre is kiterjednek. Azonban a tanulmányok többsége a rimonabant opioid rendszerre gyakorolt hatását leginkább CB_1 receptor által közvetített hatásként írja le és csak kevés irodalmi adat van a rimonabant opioid receptorokra gyakorolt direkt hatására vonatkozóan. Nem ismert például, hogy a rimonabant milyen hatásmechanizmussal kötődik az opioid receptorokhoz (agonista, vagy antagonista karakterű), illetve az opioid receptorok által közvetített G-fehérje aktivációról is csak kevés információ áll rendelkezésre. Munkánk során ezért ezen direkt hatást vizsgáltuk meg részletesen a MOR-ra és DOR-ra fókuszálva. A MOR-ra azért esett a választás, mert a legintenzívebben kutatott opioid receptor típus, a DOR pedig - hozzá képest - általánosságban kevésbé tanulmányozott, ugyanakkor számos adat demonstrálja, hogy ígéretes terápiás célpont lehet. Kísérleteinkben a ligand-receptor és a receptor-G-fehérje kölcsönhatása szintjén vizsgáltuk:

- A CB_1 receptor szerepét a rimonabant a MOR-hoz való kötődésében
- A rimonabant kötési tulajdonságait MOR-hoz és DOR-hoz, MOR-t és DOR-t túlexpresszáló kínai hörcsög ovárium sejteken (Chinese hamster ovary; CHO)
- A rimonabant dokkolását a MOR aktív és inaktív homológ modelljeihez
- A rimonabant hatását a DOR bazális aktivitására
- A rimonabant hatását a MOR és a DOR által közvetített G-fehérje aktivációra agonista stimuláció során
- A kannabinoid receptorok lehetséges szerepét ezen hatásokban

A direkt affinitási vizsgálatokat kompetíciós kötési tesztekkel végeztük, opioid receptor specifikus radioligandok segítségével, míg a MOR és DOR közvetített G-fehérje aktivációs méréseket funkcionális [^{35}S]GTPγS kötési tesztekkel vizsgáltuk.

MÓDSZEREK

Radioligand kompetíciós kötési tesztek

A radioligand kompetíciós kötési tesztek során állandó koncentrációjú radioaktívan jelölt szelektív MOR vagy DOR ligandok specifikus kötéseinek változását vizsgáltuk növekvő koncentrációjú jelöletlen rimonabant jelenlétében. A kapott radioligandok specifikus kötési értékeit kiértékelve görbeillesztő program segítségével, közvetve információt kaphatunk a jelöletlen ligand affinitásáról.

Funckcionális [^{35}S]GTPγS kötési teszt

A G-fehérje aktivációs kísérletek során a $G_{\alpha i/o}$ GDP/GTP kicserélődését monitorozzuk egy radioaktívan jelölt, nem hidrolizáló [^{35}S]GTPγS GTP analóggal. Ha növekvő koncentrációban aktiváljuk a receptort egy adott liganddal, akkor a specifikusan kötött [^{35}S]GTPγS mennyisége információt ad a vizsgált receptor által közvetített G-fehérje maximális aktivitásáról és a receptort aktiváló ligand potenciáljáról. Továbbá megállapítható a receptorhoz kötő ligand agonista, vagy antagonista karaktere is.

Dokkolási kísérletek

A dokkolási kísérletek lehetőséget adnak arra, hogy a ligand-receptor komplexről atomi szintű információkat gyűjtsünk, mint például a molekulák között lehetséges kölcsönhatások, orientációk, valamint dokkolási energiák, melyekről az általunk végzett *in vitro* kísérletek nem adnak választ.

EREDMÉNYEK ÖSSZEFOGLALÁSA

A ligand-receptor kölcsönhatás szintjén végzett kísérletek:

- A rimonabant **CB_1 receptortól függetlenül gátolta** a **MOR agonista** ligand kötődését **mikromoláris koncentrációban,** egér előagyban.
- A rimonabant MOR-ral és DOR-ral transzfektált sejtvonal membránpreparátumon is **gátolta** a **MOR és DOR specifikus agonista** ligandok kötődését **mikromoláris koncentrációban**, míg a **MOR és DOR antagonista** ligandok specifikus kötődését nem csak **mikromoláris** hanem **szubnanomoláris** koncentrációkban is **csökkentette**. A gátló hatás mindkét esetben **kannabinoid receptoroktól függetlenül** ment végbe, mivel a CHO sejtekben fiziológiás körülmények között CB_1 és CB_2 receptorok nem expresszálódnak.

- A dokkolási kísérletek eredményei alapján a rimonabant az **inaktív**, tehát az **antagonisták által stabilizált MOR konformációt preferálta**. Az eredményt a rimonabant és a MOR **inaktív** kötőzsebének egyik aminosava közötti **hidrogén kötés kialakulásának lehetősége** is megerősíti.

Receptor-G-fehérje kölcsönhatás szintjén végzett kísérletek:

- A rimonabant önmagában **inverz agonista** hatást mutatott**,** azonban ez a DOR-t nem expresszáló vad típusú CHO sejtvonalon is érvényesült, így ez **nem tekinthető DOR közvetített hatásnak**.
- A DOR-ral transzfektált CHO sejtvonalon végzett kísérletek alapján a DOR aktiválása során a rimonabant **mikromoláris koncentrációban gátolta a receptor közvetített G-fehérje aktivitását** és az **aktiváló ligand potenciálját**.
- A rimonabant MOR és DOR stimulációja során egér előagyban is **gátolta a MOR és a DOR által közvetített G-fehérje aktivitást,** valamint **csökkentette** a **DOR agonista ligand potenciálját is mindkét kannabinoid receptortól függetlenül, mikromoláris koncentrációban**.

KONKLÚZIÓ

A CB_1 receptor antagonista rimonabant direkt módon, kannabinoid receptoroktól függetlenül gátolja a MOR és DOR működését mikromoláris koncentrációban. Eredményeink alapján arra következtethetünk, hogy a gátló hatás antagonista jellegű, melyet a más kutatócsoportok által közölt eredmények is alátámasztanak.

A viszonylag magas effektív koncentráció miatt kérdés, hogy a MOR és DOR terápiás célpontok lehetnek-e a rimonabant számára? A kompetíciós kötési tesztek alapján a rimonabant ugyan rendkívül alacsony koncentrációban gátolta az antagonista ligandok kötődését, de ez a gátlás meglehetősen kismértékű volt és a G-fehérje aktivációs vizsgálatok során már nem volt megfigyelhető ugyanabban a koncentráció tartományban. Ígéretes eredményeket mutat azonban a rimonabant-opioid hibrid ligandok fejlesztése, mely rendkívül új terület fejlődéséhez véleményünk szerint az itt demonstrált eredmények is hozzájárulhatnak.

Appendix B: Off-prints of thesis related publications

I.

Zádor, F., Ötvös, F., Benyhe, S., Zimmer, A., Páldy, E. **Inhibition of forebrain μ-opioid receptor signaling by low concentrations of rimonabant does not require cannabinoid receptors and directly involves μ-opioid receptors.** *Neurochem Int* 61, 378-88 (2012).

(2.66 impact factor)

Neurochemistry International 61 (2012) 378–388

Contents lists available at SciVerse ScienceDirect

Neurochemistry International

journal homepage: www.elsevier.com/locate/nci

Inhibition of forebrain μ-opioid receptor signaling by low concentrations of rimonabant does not require cannabinoid receptors and directly involves μ-opioid receptors

Ferenc Zádor [a], Ferenc Ötvös [a], Sándor Benyhe [a,*], Andreas Zimmer [b], Eszter Páldy [a,1]

[a] Institute of Biochemistry, Biological Research Centre, Hungarian Academy of Sciences, Temesvari krt. 62, H-6726 Szeged, Hungary
[b] Institute of Molecular Psychiatry, University of Bonn, Sigmund-Freud-Street 25, 53105 Bonn, Germany

ARTICLE INFO

Article history:
Received 21 December 2011
Received in revised form 12 April 2012
Accepted 10 May 2012
Available online 18 May 2012

Keywords:
Rimonabant
CB_1 cannabinoid receptor
μ-Opioid receptor
[^{35}S]GTPγS binding
Radioligand binding
Docking
CB_1 receptor knockout mouse
CB_1/CB_2 receptor double knockout mouse
Forebrain

ABSTRACT

Increasing number of publications shows that cannabinoid receptor 1 (CB_1) specific compounds might act in a CB_1 independent manner, including rimonabant, a potent CB_1 receptor antagonist. Opioids, cannabinoids and their receptors are well known for their overlapping pharmacological properties. We have previously reported a prominent decrease in μ-opioid receptor (MOR) activity when animals were acutely treated with the putative endocannabinoid noladin ether (NE). In this study, we clarified whether the decreased MOR activation caused by NE could be reversed by rimonabant in CB_1 receptor deficient mice. In functional [^{35}S]GTPγS binding assays, we have elucidated that 0.1 mg/kg of intraperitoneal (i.p.) rimonabant treatment prior to that of NE treatment caused further attenuation on the maximal stimulation of Tyr-D-Ala-Gly-(NMe)Phe-Gly-ol (DAMGO), which is a highly specific MOR agonist. Similar inhibitory effects were observed when rimonabant was injected i.p. alone and when it was directly applied to forebrain membranes. These findings are cannabinoid receptor independent as rimonabant caused inhibition in both CB_1 single knockout and CB_1/CB_2 double knockout mice. In radioligand competition binding assays we highlighted that rimonabant fails to displace effectively [^{3}H]DAMGO from MOR in low concentrations and is highly unspecific on the receptor at high concentrations in CB_1 knockout forebrain and in their wild-type controls. Surprisingly, docking computational studies showed a favorable binding position of rimonabant to the inactive conformational state of MOR, indicating that rimonabant might behave as an antagonist at MOR. These findings were confirmed by radioligand competition binding assays in Chinese hamster ovary cells stably transfected with MOR, where a higher affinity binding site was measured in the displacement of the tritiated opioid receptor antagonist naloxone. However, based on our *in vivo* data we suggest that other, yet unidentified mechanisms are additionally involved in the observed effects.

1. Introduction

Cannabinoids mediate their effects via activating at least two types of cannabinoid receptors, CB_1 and CB_2 both G protein-coupled (for review, see Howlett, 1998). CB_1 cannabinoid receptor is the most abundant G-protein coupled receptor (GPCR) type in the brain with 10 times higher expression levels than other GPCRs. In the central nervous system, the distribution of CB_1 receptors greatly varies between different parts of the brain and in different neuronal cell types. They are widely expressed in several forebrain regions including the olfactory bulbs (Herkenham et al., 1991), all regions of the cerebral neocortex (Egertová and Elphick, 2000; Glass et al., 1997; Herkenham et al., 1991; Matsuda et al., 1990), the hippocampal formations (Herkenham et al., 1991; Jansen et al., 1992), the subcortical regions (Breivogel et al., 1997; Herkenham et al., 1991; Julian et al., 2003; Matsuda et al., 1990; Robbe et al., 2001), among others. CB_2 receptors are predominantly expressed in immune and hematopoietic cells. However, there are many recent publications showing that CB_2 receptors are also present in some central and peripheral neurons (Beltramo et al., 2006; Ross et al., 2001; Skaper et al., 1996; Van Sickle et al., 2005), however, the role of the neuronal CB_2 receptors has still to be established.

Rimonabant, which was the first selective and orally active CB_1 antagonist (Rinaldi-Carmona et al., 1994), together with many other CB_1 and CB_2 antagonists behave as an inverse agonist rather than as a neutral antagonist (for review see Pertwee, 2005)

* Corresponding author. Address: Institute of Biochemistry, Biological Research Centre, Hungarian Academy of Sciences, P.O. Box 521, H-6701 Szeged, Hungary. Tel.: +36 62 432 099; fax: +36 62 433 432.
E-mail address: benyhe@brc.hu (S. Benyhe).
[1] Present address: Pharmacology Institute, University of Heidelberg, Im Neuenheimer Feld 366, 69120 Heidelberg, Germany.

0197-0186/$ - see front matter © 2012 Elsevier Ltd. All rights reserved.
http://dx.doi.org/10.1016/j.neuint.2012.05.015

indicating that CB_1 and CB_2 receptors can exist in a constitutively active stage. It was the first CB_1 antagonist to be approved for the treatment of obesity (Padwal and Majumdar, 2007), but was withdrawn from the market in 2008 as it was found to cause strong psychiatric disorders. Before, as well as after entering rimonabant to the market there were several publications indicating its non-CB_1 receptor related actions (Breivogel et al., 2001; Hough et al., 2009) and its dose related side effects (Beyer et al., 2010; Christensen et al., 2007; Mitchell and Morris, 2007), suggesting rather unspecific behavior at higher concentrations (reviewed in Raffa and Ward, 2011).

It is well known that cannabinoid receptor system shares several features with the μ-opioid receptor (MOR) system. Both receptor types are GPCR, mainly coupled to the inhibitory $G_{i/o}$ proteins (Burford et al., 2000; Demuth and Molleman, 2006). At this level they might even functionally interact (Canals and Milligan, 2008; Rios et al., 2006). The expression patterns of CB_1 and MOR overlaps in several parts of the CNS. In certain forebrain regions, such as caudate putamen, dorsal hippocampus, substantia nigra and nucleus accumbens, the MOR and CB_1 receptors are not only co-localized, but also co-expressed in the same neurons (Pickel et al., 2004; Rodriguez et al., 2001; Salio et al., 2001). It has also been shown that these two receptor subtypes can be cross-regulated (Schoffelmeer et al., 2006) via a direct (Rios et al., 2006) or indirect interactions (Hur and Kim, 2002). When studied in behavioral aspects rimonabant reduced opiate self-administration and reward (Braida et al., 2001; Fattore et al., 2005; Navarro et al., 2001) and suppress morphine-induced feeding (Verty et al., 2003).

Previously we have shown that the putative endocannabinoid noladin ether (NE; Hanus et al., 2001) is capable of attenuating the functional activity of MOR in mouse forebrain and this effect can be partially reversed by a CB_2 antagonist (Páldyová et al., 2008). Now we clarified whether the decreased MOR activity caused by NE, which is rather acting at CB_1 receptors than at CB_2, could be reversed by rimonabant as well as we addressed to investigate the effect of rimonabant on the MOR G protein-activation alone, without NE. Recently, it is believed that rimonabant applied at high concentrations acts on a CB_1 receptor independent manner involving MORs (Cinar and Szücs, 2009), among others (Begg et al., 2005; Gibson et al., 2008; Pertwee et al., 2010; Savinainen et al., 2003). We designed our [^{35}S]GTPγS binding experiments in a way to use low concentrations of rimonabant that we either injected intraperitoneally (alone or in combination with NE) or we directly added to CB_1 wild type ($CB_1^{+/+}$) and CB_1 knockout ($CB_1^{-/-}$) mice forebrain membranes. We tested CB_1/CB_2 double knockout mice as well ($CB_1^{-/-}/CB_2^{-/-}$) to elucidate the role of the CB_2 receptors. We investigated the direct binding properties of rimonabant to MOR in receptor binding assay experiments using CB_1 knockout forebrain tissues and Chinese hamster ovary cells stably transfected with MOR (CHO-MOR). Next, we carried out docking calculations by docking rimonabant to a homology modeled MOR of its active and inactive states, to gather more information about the interaction between MOR and rimonabant.

Unspecific actions of high concentrations of rimonabant at various non-CB_1 receptors are well known. This study aims to clarify the *in vivo* and *in vitro* effects of rimonabant at MOR and MOR mediated signaling when administered in low doses, highlights the preferred orientations of rimonabant to MOR via *in silico* computational simulation and tests its direct binding ability to MOR.

2. Materials and methods

2.1. Animals

CB_1 receptor knockout ($CB_1^{-/-}$) mice and their controls ($CB_1^{+/+}$) were generated on CD1 background in Dr. Ledent's lab as described in Ledent et al., 1999. $CB_1^{-/-}/CB_2^{-/-}$ double knockout mice were provided by Dr. Zimmer's lab (Járai et al., 1999) and C57BL/6J mice were used as appropriate controls ($CB_1^{+/+}/CB_2^{+/+}$). All the animals were housed at 21–24 °C under a 12:12 light:dark cycle and were provided with water and food *ad libitum*. Different treatment groups were composed of 7–10 animals, each. All housing and experiences were conducted in accordance with the European Communities Council Directives (86/609/ECC) and the Hungarian Act for the Protection of Animals in Research (XXVIII.tv. 32.§).

2.2. Drugs and treatments

2-Arachidonyl glyceryl ether (noladin ether, NE) was purchased from Tocris and injected at the dose of 1 mg/kg in DMSO solution. SR141716 (rimonabant) was provided by SANOFI Research Laboratory (Montpellier, France) and was injected at the dose of 0.1 mg/kg in DMSO solution. Upon acute *in vivo* treatments animals received a single intraperitoneal (i.p.) injection of NE or rimonabant. Control mice were injected with DMSO solution. When used in a combined treatment, rimonabant was delivered 30 minutes prior to the NE treatment as suggested by SANOFI Research Laboratory (Rinaldi-Carmona et al., 1994). Mice were decapitated 24 h after they received the last injection. The enkephalin analog Tyr-D-Ala-Gly-(NMe)Phe-Gly-ol (DAMGO) was obtained from Bachem Holding AG, Bubendorf, Switzerland. [^{3}H]DAMGO (41 Ci/mmol) and [^{3}H]naloxone (31 Ci/mmol) was radiolabeled in the Isotope Laboratory of BRC, Szeged, Hungary.

2.3. Forebrain membrane preparations

Forebrain membrane fractions from $CB_1^{-/-}$ and $CB_1^{-/-}/CB_2^{-/-}$ mice and their controls ($CB_1^{+/+}$ and $CB_1^{+/+}/CB_2^{+/+}$, respectively) were prepared according to the method previously described (Benyhe et al., 1997). Briefly, mice were decapitated and the brain was quickly removed. The forebrain part was collected and homogenized on ice in 50 mM Tris–HCl buffer (pH 7.4) with a Teflon-glass homogenizer. The homogenate was centrifuged at 40,000*g* for 20 min at 4 °C and the pellet was resuspended in fresh buffer and incubated for 30 min at 37 °C. This centrifugation step was repeated, and the final pellet was resuspended in 50 mM Tris–HCl buffer (pH 7.4) containing 0.32 M sucrose and stored at −80 °C until use.

2.4. Cell culture and cell membrane preparations

Chinese hamster ovary cells stably transfected with MORs (MOR-CHO) were kindly provided by Dr. Zvi Vogel (Rehovot, Israel). MOR-CHO cells were grown in Dulbecco's modified Eagle's medium (DMEM, Gibco) and in α-minimum essential medium (αMEM, Gibco), respectively. Both media were supplemented with 10% fetal calf serum, 2 mM glutamine, 100 IU/ml penicillin, 100 mg/ml streptomycin, 25 mg/ml fungizone and 0.5 mg/ml geneticin. Cells were kept in culture at 37 °C in a humidified atmosphere consisting of 5% CO_2 and 95% air.

Membranes were prepared from subconfluent cultures. Cells were rinsed three times with 10 ml PBS and removed with 50 mM Tris–HCl pH 7.4, 1 mM EGTA, 1 mM EDTA and 0.1 mM PMSF buffer and homogenized for 15 s with a polytron homogenizer in an ice-bath. Homogenates were centrifuged two times at 18,000 g for 20 min. The final pellet was resuspended in the above buffer and stored in aliquots at −80 °C until use.

2.5. Functional [^{35}S]GTPγS binding experiments

Membrane preparations of $CB_1^{-/-}$ and $CB_1^{-/-}/CB_2^{-/-}$ forebrains and their proper controls were diluted in 50 mM Tris–HCl buffer

(pH 7.4) to get appropriate protein content for the assays (~10 μg of protein/sample). Membrane fractions were incubated at 30 °C for 60 min in Tris–EGTA buffer (pH 7.4) composed of 50 mM Tris–HCl, 1 mM EGTA, 3 mM $MgCl_2$, 100 mM NaCl, containing 20 MBq/0.05 cm^3 [^{35}S]GTPγS (0.05 nM) and increasing concentrations (10^{-10}–10^{-5} M) of DAMGO in the presence of excess GDP (30 μM) in a final volume of 1 ml, according to Sim et al. (1995) and Traynor and Nahorski (1995), with slight modifications. Total binding (T) was measured in the absence of test compounds, non-specific binding (NS) was determined in the presence of 10 μM unlabeled GTPγS and subtracted from total binding. The difference (T–NS) represents basal activity. Bound and free [^{35}S]GTPγS were separated by vacuum filtration through Whatman GF/B filters with Brandel M24R Cell harvester. Filters were washed three times with 5 ml ice-cold buffer (pH 7.4), and the radioactivity of the dried filters was detected in UltimaGold™ F scintillation cocktail with Packard Tricarb 2300TR liquid scintillation counter. Stimulation is given as percent of the specific [^{35}S]GTPγS binding observed in the absence of receptor ligands (basal activity). [^{35}S]GTPγS binding experiments were performed in triplicates and repeated at least three times. For the *in vitro* experiments, forebrain membranes were incubated with 10^{-10}–10^{-5} M of DAMGO in the presence or absence of 1 μM rimonabant. Log EC_{50} (potency) and E_{max} (efficacy) values were determined by GraphPad Prism 5.0.

2.6. Receptor binding assays

Aliquots of frozen $CB_1^{+/+}$ and $CB_1^{-/-}$ mice forebrain membranes were centrifuged (40,000*g*, 20 min, 4 °C) to remove sucrose and the pellets were suspended in 50 mM Tris–HCl buffer (pH 7.4). Membranes were incubated with gentle shaking at 35 °C for 45 min in a final volume of 1 ml with unlabeled DAMGO or rimonabant (10^{-11}–10^{-5} M) and ~1 nM of [^{3}H]DAMGO. Wild type mice forebrain membrane homogenates were also incubated in the presence or absence of 10, 50 and 100 μM rimonabant together with labeled and unlabeled DAMGO in the same experimental conditions. MOR-CHO cell membrane fractions were incubated in a final volume of 1 ml with 1 nM [^{3}H]naloxone (~1 nM) or ~1 nM of [^{3}H]DAMGO and unlabeled rimonabant (10^{-11}–10^{-5} M) at 35 °C for 60 min. Total binding was measured in the presence of radioligand and the non-specific binding was determined in the presence of 10 μM unlabeled naloxone. The reaction was terminated by rapid filtration under vacuum (Brandel M24R Cell Harvester), and washed three times with 5 ml ice-cold 50 mM Tris–HCl (pH 7.4) buffer through Whatman GF/C ([3H]DAMGO) or Whatman GF/B glass fibers ([^{3}H]naloxone). The radioactivity of the dried filters was detected in UltimaGold™ F scintillation cocktail with Packard Tricarb 2300TR liquid scintillation counter. Radioligand binding assays were performed in duplicate and repeated at least three times. Experimental data were analyzed by GraphPad Prism 5.0 to determine the concentration of the drug that displaced 50% of [^{3}H]DAMGO (IC_{50}).

2.7. Docking experiments

The 3D coordinates of the active and inactive conformations of the MOR prepared by homology modeling were downloaded from the Mosberg group's webpage (see Web references; although the homology model of MOR was prepared for the rat, the part of the sequence modeled was 100% identical to that of mice). The activated receptor model contained the MOR selective agonist, H-Tyr-c(S-Et-S)[D-Cys-Phe-D-Pen]NH_2 (JOM-6; downloaded as: OPRM_RAT_AD_JOM6), and the inactive receptor model contained the κ-opioid antagonist, norbinaltorphimine (nor-BNI; downloaded as: OPRM_RAT_ID_BNI). The 3D coordinates of rimonabant, DAMGO and naloxone were downloaded from the Cactus web site (see Web references) using Avogadro (see Web references), the open source chemical structure editor program. The embedded Openbabel (O'Boyle et al., 2011) program suite was used to energy minimize the structures with the MMFF94s (Halgren, 1999) force field. Ligands were prepared for docking using the AutoDockTools (Morris et al., 2009) program suite and then docked by the program AutoDock4 (Morris et al., 2009). In AutoDock, the maximum number of energy evaluations, the number of individuals in population and the number of Lamarckian Genetic Algorithm runs were 250,00,000, 350 and 20, respectively to achieve an exhaustive search for the docked poses. The size of the grid docking box was 50 Å and centered at the middle of the binding pocket. Each docking started with a random translation, rotation and torsional modification of the ligands. Results were analyzed and visualized by the program Chimera (Pettersen et al., 2004). The receptors were kept rigid in the docking calculations because the limitation in the number of the flexible torsional angles prevented to treat the whole binding pocket and the ligands flexible simultaneously. In addition, the docking calculations were repeated by using the flexible ring method, a specific feature of AutoDock. Calculations by AutoDock4 resulted in estimated docking free energies in kcal/mol.

3. Results

3.1. Effect of rimonabant on noladin ether caused attenuation at MOŔs G protein activation in $CB_1^{+/+}$ and $CB_1^{-/-}$ mice forebrain membrane fractions after a single i.p. administration

As we previously reported 24 h after a single i.p. injection of NE at the dose of 1 mg/kg there was a significant decrease in DAMGO-stimulated [^{35}S]GTPγS binding in both $CB_1^{+/+}$ and $CB_1^{-/-}$ mice forebrain. This effect was reversed partially by the CB_2 antagonist SR144528 (Páldyová et al., 2008). NE is known to be putative endocannabinoid acting mainly at CB_1. Rimonabant is considered to be a selectively acting antagonist/inverse agonist at CB_1 receptors. In this experiment we co-treated $CB_1^{+/+}$ and $CB_1^{-/-}$ mice with NE and rimonabant to see whether rimonabant is able to reverse NE caused inhibition of MOR at the level of G-proteins.

Agonist-mediated G-protein activation of MOR was measured in functional [^{35}S]GTPγS binding experiments, in which the nucleotide exchange process is monitored using a non-hydrolysable radioactive GTP analog, [^{35}S]GTPγS. MOR was stimulated with a highly MOR specific pure agonist peptide, DAMGO. G-protein activation can be characterized by the potency (EC_{50}) and by the efficacy (also known as maximal stimulation, E_{max}).

During NE treatment (1 mg/kg) there was a significant decrease in the potency of DAMGO (0.05 μM → 1.14 μM, $P < 0.001$, $F = 1.47$, df = 9, Fig. 1A, Table 1), and a slight but not significant decrease in the efficacy (165.3% vs. 156.6%, Fig. 1A, Table 1), as shown previously (Páldyová et al., 2008). After injecting rimonabant at the dose of 0.1 mg/kg prior to the NE treatment the efficacy of DAMGO decreased even more (E_{max} 156.6% → 140.2%, $P < 0.05$, $F = 1.82$, df = 7, Fig. 1A, Table 1) whereas the potency remained unaltered (1.14 μM vs. 1.52 μM, Fig. 1A, Table 1), when compared to the single NE treated group.

In CB_1 receptor deficient mice single NE injection resulted a significant reduction in MOR G-protein stimulation (E_{max} 159% → 138.3%, $P < 0.01$, $F = 4.02$, df = 11, Fig. 1B, Table 1) but the affinity of DAMGO remained unaltered (0.45 μM vs. 0.26 μM). As it was seen in $CB_1^{+/+}$ animals, rimonabant pretreatment significantly diminished the efficacy (E_{max} changed 138.3% → 126.3%, $P < 0.01$, $F = 1.68$, df = 10, Fig. 1B; Table 1), but not the potency of DAMGO (0.26 μM vs. 0.1 μM) compared to single NE administration.

Taken together, acute i.p. injection of rimonabant prior to NE treatment caused a prominent decrease in MOR G protein-activation in both $CB_1^{+/+}$ and $CB_1^{-/-}$ mice forebrain when compared to

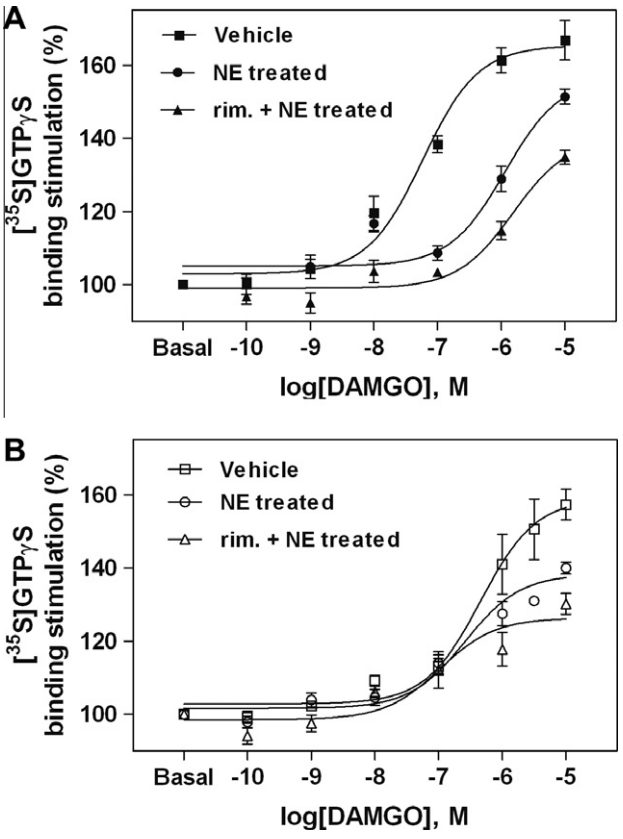

Fig. 1. MOR signaling in $CB_1^{+/+}$ (A) and $CB_1^{-/-}$ (B) mice forebrain membranes after acute *in vivo* treatment with NE and combined treatment of rimonabant + NE as described under Section 2.2. Data are presenting the specifically bound [^{35}S]GTPγS above basal activity in percentage during MOR activation with increasing concentrations of DAMGO. Points represent means ± S.E.M. for at least three experiments performed in triplicate. The E_{max} and logEC_{50} values are shown in Table 1 with statistical analysis.

NE administration alone, suggesting a CB_1 receptor independent antagonizing effect of rimonabant at MOR's activity.

3.2. Acute effect of rimonabant on DAMGO-stimulated [^{35}S]GTPγS binding in $CB_1^{+/+}$ and $CB_1^{-/-}$ mice forebrain membrane fractions after a low dose i.p. administration

To confirm our suggestion, namely that rimonabant has an inhibitory action at MOR signaling, we injected CB_1 deficient mice with rimonabant at the dose of 0.1 mg/kg. This concentration is at least ten times lower than that of usually used especially when observing the unspecific actions of this compound (Verty et al., 2003; Beyer et al., 2010). After 24 h the mice were sacrificed and the forebrain membrane fractions were tested for MOR activity changes in [^{35}S]GTPγS binding assay.

In $CB_1^{+/+}$ mice acute injection of rimonabant caused a significant decrease in maximal stimulation of DAMGO when compared to vehicle injected animals (E_{max} changed 165.3% → 140.5%, $P < 0.001$, $F = 1.83$, df = 13, Fig. 2, Table 2). The potency of DAMGO did not change significantly (0.11 μM vs. 0.17 μM, Fig. 2, Table 2).

Similarly, rimonabant administration attenuated MOR G-protein activation (E_{max} changed 157.2% → 140.7%, $P < 0.05$, $F = 4.72$, df = 13, Fig. 2, Table 2) and had no significant effect on the affinity of DAMGO in $CB_1^{-/-}$ mice forebrain membrane fractions (0.74 μM vs. 2.2 μM, Fig. 2, Table 2).

These results show that an acute, low dose of rimonabant is capable of attenuating DAMGO-stimulated [^{35}S]GTPγS binding in both $CB_1^{+/+}$ and $CB_1^{-/-}$ forebrain indicating a CB_1 independent action.

3.3. In vitro effect of rimonabant on DAMGO-stimulated [^{35}S]GTPγS binding in $CB_1^{+/+}$and $CB_1^{-/-}$ mice forebrain membrane fractions

After the *in vivo* studies we wanted to examine whether the inhibition seen in MOR G-protein stimulation after acute rimonabant treatment can be observed when directly applying the compound to forebrain membranes. For this we performed DAMGO-stimulated [^{35}S]GTPγS binding experiments in the presence and absence of rimonabant using membrane preparations of untreated $CB_1^{+/+}$ and $CB_1^{-/-}$ forebrain tissues (Fig. 3). We applied 1 μM of rimonabant, which is again ten times lower concentration than published previously by others (Cinar and Szücs, 2009).

In accordance with our *in vivo* data, in $CB_1^{+/+}$ mice we observed a significant decrease in the maximal stimulation of DAMGO (E_{max} changed 161.7% → 143.9%, $P < 0.01$, $F = 1.26$, df = 11, Fig. 3, Table 3) and a prominent decrease in the potency when co-applied with rimonabant (EC_{50} values of DAMGO increased 0.13 μM → 1.92 μM, $n = 4$, $P < 0.001$, Fig. 3, Table 3).

In CB_1 knockouts the maximal stimulation of DAMGO at MORs was also significantly diminished by rimonabant (E_{max} changed to 160% → 139.9%, $P < 0.05$, $F = 9.95$, df = 10, Fig. 3, Table 3), whereas the potency of DAMGO remained unaltered (1.65 μM vs. 1.63 μM, Fig. 3, Table 3).

Similarly to our *in vivo* data, *in vitro* administered rimonabant causes an inhibition at MOR G-protein activation in both $CB_1^{+/+}$ and in $CB_1^{-/-}$ mice forebrain membranes.

3.4. In vitro effect of rimonabant on DAMGO-stimulated [^{35}S]GTPγS binding in CB_1/CB_2 double knockout mice forebrain membrane fractions

Increasing amount of publications show the presence of CB_2 cannabinoid receptors – known as the "peripheral cannabinoid receptor" – in neuronal and non-neuronal cells of the central nervous system. In our previous work, we have shown a CB_2 mediated NE effect on MOR signaling in mice forebrain (Páldyová et al., 2008) as well as an inhibitory effect of a CB_2 antagonist at MOR in brainstem (Páldy et al., 2008). In this study we observed an attenuation of rimonabant on MORs activity both *in vivo* and *in vitro* not only in $CB_1^{+/+}$ forebrain but in $CB_1^{-/-}$ as well, suggesting a CB_1 independent action. To exclude the possible involvement of the CB_2 receptors, we used CB_1/CB_2 double knockout mice and performed our experiments under the same conditions as seen in the *in vitro* study of the CB_1 single knockouts. Namely, DAMGO-stimulated [^{35}S]GTPγS binding was measured in the presence or absence of 1 μM rimonabant on untreated CB_1/CB_2 double knockout forebrain membranes and their controls.

As it was expected applying 1 μM rimonabant to $CB_1^{+/+}/CB_2^{+/+}$ mice forebrain homogenates markedly attenuated the efficacy of DAMGO (194.1% → 174.3%, $P < 0.01$, $F = 1.02$, df = 6, Fig. 4, Table 4). Interestingly, the lack of both cannabinoid receptors did not modulate the inhibitory effect of rimonabant on MOR G-protein stimulation (200% → 178.8%, $P < 0.01$, $F = 1.83$, df = 8, Fig. 4, Table 4), therefore we can rule out the role of the CB_2 receptors in the observed effects.

Rimonabant's inhibition at MORs G protein activation is very clear after a single i.p. injection as well as after directly applied to forebrain membranes. This effect is similar in both $CB_1^{-/-}$ single knockout and $CB_1^{-/-}/CB_2^{-/-}$ double knockout mice, which seemingly denotes a cannabinoid receptor independent action of rimonabant to MOR at G-protein level.

Table 1
G-protein activation by the MOR agonist DAMGO in forebrain membranes of $CB_1^{+/+}$ and $CB_1^{-/-}$ mice after acute NE and rimonabant + NE combined treatment.

	$CB_1^{+/+}$ mice acutely treated with			$CB_1^{-/-}$ mice acutely treated with		
	Vehicle (control)	NE	Rim. + NE	Vehicle (control)	NE	Rim. + NE
E_{max} ± S.E.M. (%)	165.3 ± 2.8	156.6 ± 4.7^{NS}	140.2 ± 3.9*	159 ± 3.9	138.3 ± 2.1***	126.3 ± 2.7**
Log EC_{50} ± S.E.M.	−7.23 ± 0.11	−5.94 ± 0.15***	−5.81 ± 0.15^{NS}	−6.34 ± 0.17	−6.58 ± 0.13^{NS}	−6.98 ± 0.23^{NS}
(EC_{50})	(0.05 μM)	(1.14 μM)	(1.52 μM)	(0.45 μM)	(0.26 μM)	(0.1 μM)

Drugs were injected *in vivo* as described under Section 2.2. Forebrain membranes were used in the [^{35}S]GTPγS binding assay with 10^{-10}–10^{-5} M concentrations of DAMGO. The significance level of E_{max} and logEC_{50} values are indicated by asterisks (unpaired *t*-test, two-tailed *P* value) related to the comparison of NE treatment with control, or represents the comparison of the combined treatment (rim. + NE) with NE treatment alone. $^{***}P < 0.001$; $^{**}P < 0.01$; $^{*}P < 0.05$ S.E.M.: standard error of means; NS: not significant; NE: noladine ether; rim.: rimonabant.

3.5. Direct affinity measurements of rimonabant on MOR in competition binding experiments in $CB_1^{+/+}$ and $CB_1^{-/-}$ mice forebrain membrane fractions

Because we can exclude the role of the cannabinoid receptors from the inhibitory actions of rimonabant on MOR signaling, we wanted to compare the direct binding affinity of rimonabant to the MOR binding site with the highly MOR specific peptide, DAMGO. For this, we performed competition binding experiments with [^{3}H]DAMGO (∼1 nM) using membranes prepared from $CB_1^{+/+}$ and $CB_1^{-/-}$ mice forebrain. The competing ligands were unlabeled DAMGO or rimonabant added in increasing concentrations. Our results demonstrate that rimonabant had no specific effect on [^{3}H]DAMGO binding in $CB_1^{+/+}$ and CB_1 knock-out mice. Even the highest concentration of the CB_1 antagonist rimonabant caused only a very small, 20% reduction in [^{3}H]DAMGO specific binding (Fig. 5). The IC_{50} values of rimonabant were in the micromolar range (in $CB_1^{+/+}$ mice: 9.56 μM; in $CB_1^{-/-}$ mice: 2.72 μM) which is much higher compared to DAMGO's ($CB_1^{+/+}$: 4.32 nM; $CB_1^{-/-}$: 6.41 nM). These results show that rimonabant is unable to compete for the binding site of MOR at low concentrations in $CB_1^{+/+}$ and $CB_1^{-/-}$ mice forebrain membranes.

As it was described previously in several studies (Arnone et al., 1997; Beyer et al., 2010; Le Foll and Goldberg, 2005; Verty et al., 2003) rimonabant has numerous non CB_1 receptor related actions in higher concentrations. Therefore, next we wanted to investigate how rimonabant is affecting the specific binding of DAMGO to MOR in higher concentration. We performed homolog binding capacity measurements but this time we added rimonabant in every unlabeled DAMGO concentration point (Fig. 6). Applying 10 μM of rimonabant did not affect the binding of DAMGO, however in 50 and 100 μM concentrations the compound highly decreased the specific binding of [^{3}H]DAMGO, nearly down to 10–20% (Fig. 6), The observed massive reduction of [^{3}H]DAMGO specific binding is due to the much higher applied concentration of rimonabant compared to the administered radioligand (50 and 100 μM vs. ∼1 nM), that might be due to an interaction with the membrane or filter which is a well known phenomenon. Therefore the observed effect of rimonabant in higher concentrations can be claimed as highly unspecific.

Our results from competition binding experiments support the outcome of previous publications that refer to the unspecific actions of rimonabant when used in higher concentrations. Also, when applied in lower concentrations, rimonabant is unable to compete with DAMGO.

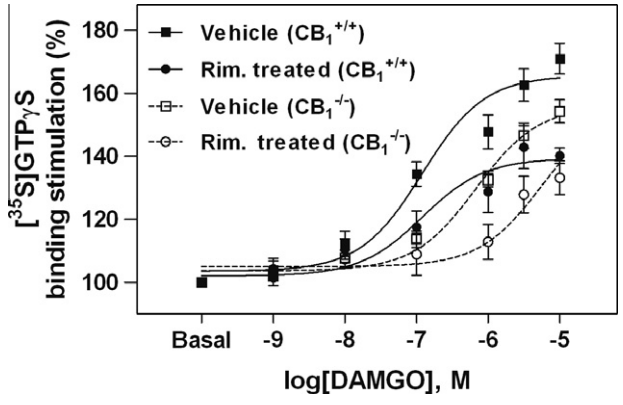

Fig. 2. MOR signaling in $CB_1^{+/+}$ and $CB_1^{-/-}$ mice forebrain membranes after acute *in vivo* treatment with rimonabant as described under Section 2.2. Data are presenting the specifically bound [^{35}S]GTPγS above basal activity in percentage during MOR activation with increasing concentrations of DAMGO. Points represent means ± S.E.M. for at least three experiments performed in triplicate. The E_{max} and logEC_{50} values are shown in Table 2 with statistical analysis.

3.6. Docking experiments with rimonabant to inactive and active MOR homology model

Docking, a particular field of molecular modeling is a widely used tool to simulate the preferred orientations of a ligand in the binding site. Rimonabant was docked to the homology models of the inactive and active state of the MOR. The highly specific μ-agonist DAMGO and the opioid specific antagonist naloxone were also docked to the receptor models. Because DAMGO contains an *N*-MePhe (*N*-methylphenylalanine) in its sequence, there is a possibility that it adopts a *cis* Gly^3-*N*-MePhe^4 peptide bond (Misicka et al., 1998). According to this, DAMGO was docked both in all-*trans* form and with a *cis* Gly^3-*N*-MePhe^4 peptide bond (*cis*-DAMGO). Since the applied active and inactive MOR homology models already contained JOM-6 and nor-BNI, respectively, these ligands were also docked to the receptor models to cross validate our docking experiments. Each ligand was docked to both receptor conformations to compare their preference for the specific state of MOR (Table 5).

Docking of the ligands was performed by two methods (Table 5, Docking experiments 1 and 2) to contract the most reliable bound poses. The lowest docking free energies obtained were used to rank the ability of the ligands to bind to the receptor. Additionally, an apparent energy balance of the receptor activation process was calculated for each ligand, subtracting the docking energy of the ligand-active receptor complex from that of the ligand-inactive receptor complex ("activation energy", Table 5). This value was used to characterize the agonistic-antagonistic nature of rimonabant which has not been well investigated with MOR.

In the first calculation the receptors were rigid and the ligands were flexible except that the aliphatic rings of the ligands were kept in the conformation obtained by the energy minimization (Table 5, Docking experiment 1). As expected during our docking experiments JOM-6 and nor-BNI achieved the same docking poses as published previously (Pogozheva et al., 2005). Even though rimonabant is a highly specific CB_1 receptor antagonist, the ligand bound to the active state of MOR with surprisingly low docking energies. Moreover, rimonabant bound to the inactive state of

Table 2
G-protein activation by the MOR agonist DAMGO in forebrain membranes of $CB_1^{+/+}$ and $CB_1^{-/-}$ mice after acute rimonabant treatment.

	$CB_1^{+/+}$ mice acutely treated with		$CB_1^{-/-}$ mice acutely treated with	
	Vehicle	Rimonabant	Vehicle	Rimonabant
E_{max} ± S.E.M. (%)	165.3 ± 3	140.5 ± 3.1***	157.2 ± 2.9	140.7 ± 9*
Log EC_{50} ± S.E.M. (EC_{50})	−6.95 ± 0.13 (0.11 μM)	−6.76 ± 0.23^{NS} (0.17 μM)	−6.12 ± 0.11 (0.74 μM)	−5.65 ± 0.33^{NS} (2.2 μM)

Drugs were injected *in vivo* as described under Section 2.2. Forebrain membranes were used in the [^{35}S]GTPγS binding assay with 10^{-10}–10^{-5} M concentration of DAMGO. The significance level of E_{max} and logEC_{50} values are indicated by asterisks (unpaired *t*-test, two-tailed *P* value), ***$P < 0.001$; *$P < 0.05$ S.E.M.: standard error of means; NS: not significant.; rim.: rimonabant.

the MOR with a much lower docking energy, resulting in a positive activation energy unlike DAMGO, *cis*-DAMGO and JOM-6 (Table 5). In fact the activation energy of rimonabant was very similar to that of the antagonist naloxone (Table 5). In the second calculation the possibility of applying flexible aliphatic rings during the experiments did not improve the docking energies in general (Table 5, Docking experiment 2).

As an important difference between the binding modes, rimonabant docked to the inactive and active state of the receptor by the opposite ends (Fig. 7A and B). Also a hydrogen bond occurs between T218 and the hydrazide group of rimonabant (Fig. 7C) in the inactive state of the binding pocket, while no hydrogen bonds were observed in the binding pocket of the active receptor.

Summarizing the results of our docking calculations, we observed that rimonabant binds to the active conformation of MOR with a surprisingly low energy similar to the agonist DAMGO. However, the docking energies were even lower in the inactive state of the MOR suggesting that rimonabant has a preference for the inactive state of MOR. These findings raise the possibility that rimonabant acts as an antagonist on MOR. Nevertheless, only the inactive state gives the opportunity to form a hydrogen bond between rimonabant and one of the residues in the binding pocket.

3.7. Effect of rimonabant on MOR in competition binding experiments in MOR-CHO cell membranes

The docking energy levels of rimonabant in the docking calculations (Table 5) pointed out that rimonabant prefers the inactive state of MOR, which conformation is more suitable for antagonists. To underpin the results from docking simulation we carried out radiolabeled competition binding experiments using a tritiated opioid antagonist [^{3}H]naloxone to see how effectively rimonabant is able to bind to the inactive state of MOR. The MOR agonist [^{3}H]DAMGO was utilized for comparison. Both tritiated ligands were added in fixed concentrations (∼1 nM) and incubated together with increasing concentrations of rimonabant (10^{-11}–10^{-5} M). The experiments were performed in MOR-CHO cell membranes to avoid any possible interactions with other receptors and to measure an accurate MOR-ligand binding. We presume that the inactive-active state of MOR will be overturned to the inactive state when naloxone is applied and to the active state when DAMGO is used.

Rimonabant displaced [^{3}H]naloxone with a significantly lower logIC_{50} value (Fig. 8, logIC_{50}: −6.7373 ± 0.13, $P < 0.001$, $F = 2.71$, df = 5, unpaired *t*-test, two-tailed *P* value, IC_{50}: 0.18 μM) compared to [^{3}H]DAMGO (Fig. 8, logIC_{50}: −5.75 ± 0.12, IC_{50}: 1.74 μM), which corresponds with our results described under Section 3.5, and also similar to with previously reported data published by Cinar and Szücs (2009). Moreover, the specific binding of [^{3}H]naloxone can be fitted with the "two-site competition binding curve" thus the CB_1 antagonist can also displace the opioid antagonist from a different binding site with a high affinity (Fig. 8; IC_{50}: 0.08 nM) in very low concentrations, although the amount of these sites are exiguous (about 20% of the total binding site population; see Fig. 8, shaded area).

Taken together our *in silico* and *in vitro* affinity results, rimonabant has a higher affinity to the inactive conformation state of the MOR and has a significantly lower binding capacity to the more agonist favorable conformation of the receptor. Our direct affinity measurements on MOR-CHO cells also pointed out that rimonabant is able to bind to a high affinity binding site of the MOR, in displacing [^{3}H]naloxone, which explains the very low docking energies of rimonabant when it was docked in the inactive MOR.

4. Discussion

Rimonabant is considered to be an inverse cannabinoid agonist acting selectively at CB_1 receptors. In the course of time several

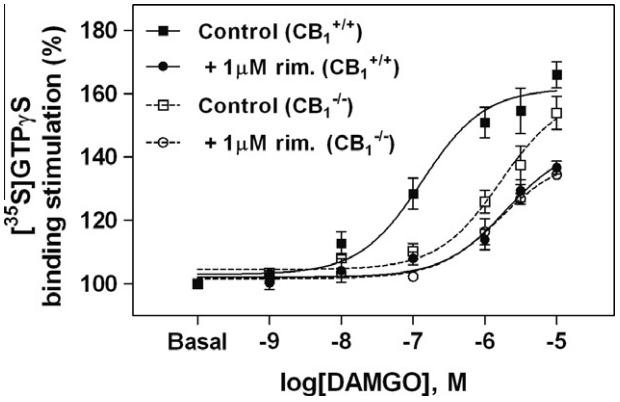

Fig. 3. MOR signaling in $CB_1^{+/+}$ and $CB_1^{-/-}$ mice forebrain membranes after *in vitro* administration of rimonabant as described under Section 2.5. Data are presenting the specifically bound [^{35}S]GTPγS above basal activity in percentage during MOR activation with increasing concentrations of DAMGO in the presence or absence of 1 μM rimonabant. Points represent means ± S.E.M. for at least three experiments performed in triplicate. The E_{max} and logEC_{50} values are shown in Table 3 with statistical analysis.

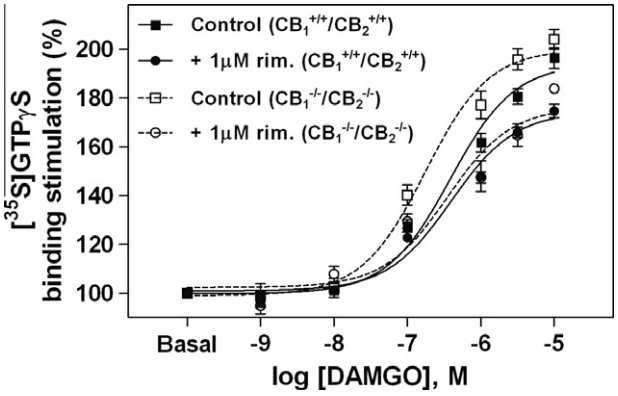

Fig. 4. MOR signaling in $CB_1^{+/+}/CB_2^{+/+}$ and $CB_1^{-/-}/CB_2^{-/-}$ mice forebrain membranes after *in vitro* administration of rimonabant as described under as described under Section 2.5. Data are presenting the specifically bound [^{35}S]GTPγS above basal activity in percentage during MOR activation with increasing concentrations of DAMGO in the presence or absence of 1 μM rimonabant. Points represent means ± S.E.M. for at least three experiments performed in triplicate. The E_{max} and logEC_{50} values are shown in Table 4 with statistical analysis.

Table 3
In vitro effect of rimonabant on DAMGO-stimulated [^{35}S]GTPγS binding in forebrain membranes of $CB_1^{+/+}$ and $CB_1^{-/-}$ mice.

	$CB_1^{+/+}$ mice		$CB_1^{-/-}$ mice	
	Control	+1 μM rim.	Control	+1 μM rim.
E_{max} ± S.E.M. (%)	161.7 ± 2.9	143.9 ± 4.9**	160 ± 5.7	139.9 ± 2.5*
Log EC_{50} ± S.E.M. (EC_{50})	−6.87 ± 0.14 (0.13 μM)	−5.71 ± 0.17*** (1.92 μM)	−5.78 ± 0.13 (1.65 μM)	−5.78 ± 0.1^{NS} (1.63 μM)

Forebrain membranes were used from untreated $CB_1^{+/+}$ and $CB_1^{-/-}$ animals. Rimonabant was *in vitro* administered as described under Section 2.5. The significance level of E_{max} and log EC_{50} values are indicated by asterisks (unpaired *t*-test, two-tailed *P* value), ***$P < 0.001$; **$P < 0.01$; *$P < 0.05$ S.E.M.: standard error of means; NS: not significant; rim.: rimonabant.

Table 4
In vitro effect of rimonabant on DAMGO-stimulated [^{35}S]GTPγS binding in forebrain membranes of wild type and $CB_1^{-/-}/CB_2^{-/-}$ double knockout mice.

	$CB_1^{+/+}/CB_2^{+/+}$ mice		$CB_1^{-/-}/CB_2^{-/-}$ mice	
	Control	+1 μM rim.	Control	+1 μM rim.
E_{max} ± S.E.M. (%)	194.1 ± 3.4	174.3 ± 3.3**	200 ± 3.3	178.7 ± 4.5**
Log EC_{50} ± S.E.M. (EC_{50})	−6.41 ± 0.09 (0.38 μM)	−6.4 ± 0.11^{NS} (0.39 μM)	−6.75 ± 0.09 (0.17 μM)	−6.45 ± 0.14^{NS} (0.35 μM)

Forebrain membranes were extracted from untreated $CB_1^{+/+}/CB_2^{+/+}$ and $CB_1^{-/-}/CB_2^{-/-}$ animals. Rimonabant was *in vitro* administered as described under Section 2.5. The significance level of E_{max} and log EC_{50} values are indicated by asterisks (unpaired *t*-test, two-tailed *P* value), **$P < 0.01$; S.E.M.: standard error of means. NS: not significant; rim.: rimonabant.

studies have been released demonstrating numerous non-cannabinoid related effects of rimonabant, thus its specificity has become questionable (reviewed in Pertwee, 2010). Very recently it was suggested to have a bimodal profile, meaning that in sub-nanomolar range acts as a selective CB_1 antagonist, whereas in high concentrations it is rather acting via CB_1 independent manner involving MORs as well (Raffa and Ward, 2011).

This paper is focusing on studying the effects of rimonabant in the μ-opioid system in forebrain, where CB_1 and MORs are highly co-distributed. First, changes in MOR G-protein coupling were investigated. G-protein activation, which is the primary step in the GPCR signaling process, was monitored in functional [^{35}S]GTPγS binding assays using a highly MOR specific agonist DAMGO to activate the receptor. Previously, we have reported a prominent decrease in DAMGO-stimulated [^{35}S]GTPγS binding in CB_1 knockout forebrain when animals were acutely treated with the putative endocannabinoid NE (Páldyová et al., 2008). Because NE is known to be acting mainly at CB_1 now we clarified whether rimonabant, that is considered to be a specific CB_1 antagonist/inverse agonist, is able to reverse this effect of NE. Surprisingly enough, a combined treatment with rimonabant and NE caused a further decrease on DAMGO-stimulated MOR signaling instead of antagonizing the effect of NE. This observation, which was similar in both CB_1 knockouts and their wild type controls, suggests that rimonabant might have a CB_1 receptor independent antagonistic effect at MOR G-protein level.

Therefore next we tested rimonabant's effect after a single i.p. treatment in a 0.1 mg/kg concentration. This concentration is at least ten times lower than that of usually applied when noting the unspecific actions of this compound (Beyer et al., 2010; Verty et al., 2003). In wild type mice 24 h after rimonabant treatment DAMGO-stimulated [^{35}S]GTPγS binding was decreased when compared to vehicle treated animals. Injection of rimonabant caused a similar impact in CB_1 deficient mice. These findings indicate that an acute, low dose of rimonabant is capable of attenuating DAMGO-stimulated [^{35}S]GTPγS binding in both $CB_1^{+/+}$ and $CB_1^{-/-}$ forebrain pointing out a CB_1 independent action.

After the *in vivo* studies we wanted to know, whether rimonabant caused attenuation at MOR G-protein signaling is present when directly applied to forebrain membrane homogenates. After adding 1 μM rimonabant to wild type and CB_1 knockout forebrain membrane a significant reduction in DAMGO-stimulated G-protein

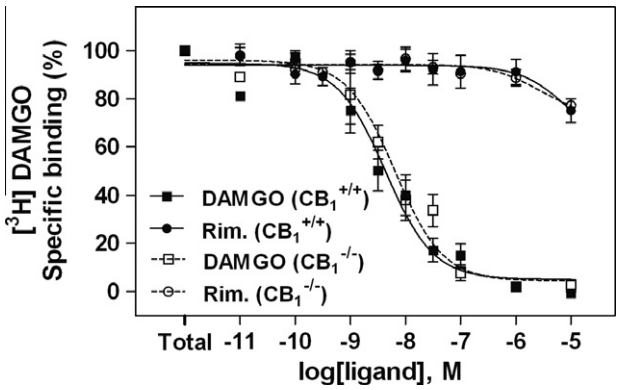

Fig. 5. Competition binding curves of [^{3}H]DAMGO binding in $CB_1^{+/+}$ and $CB_1^{-/-}$ mice forebrain membranes as described under Section 2.6. Data are presented as the percentage of specific [^{3}H]DAMGO binding (~1 nM) observed in the presence of increasing concentrations of unlabeled DAMGO and rimonabant. Points represent means ± S.E.M. for at least three experiments performed in duplicate.

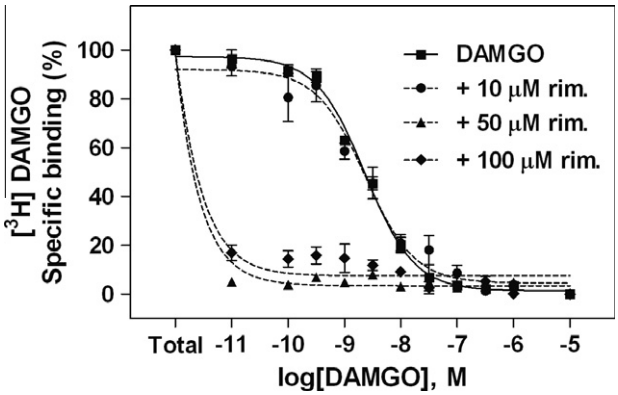

Fig. 6. Competition binding curves of [^{3}H]DAMGO binding in forebrain membranes of wild type mice as described under Section 2.6. Data are presented as the percentage of specific [^{3}H]DAMGO binding (~1 nM) observed in the presence of increasing concentrations of unlabeled DAMGO and in the presence or absence of indicated concentrations of rimonabant. Points represent means ± S.E.M. for at least three experiments (except in the case of 50 μM rimonabant) performed in duplicate.

Table 5
Docking energies and the calculated activation energy of rimonabant compared to naloxone, DAMGO, *cis*-DAMGO, JOM-6 and nor-BNI during the indicated docking experiments in inactive and active MOR.

Docking experiments	Ligands	Docking energy		Activation energy
		MOR inactive	MOR active	
1. Rigid receptor, rigid ring	Rimonabant	−12.70	−10.94	1.76
	Naloxone	−10.44	−8.73	1.71
	DAMGO	−10.40	−11.44	−1.04
	cis-DAMGO	−9.99	−10.61	−0.62
	JOM-6	−10.27	−13.88	−3.61
	Nor-BNI	−18.35	−8.58	9.77
2. Rigid receptor, flexible ring	Rimonabant	−12.56	−10.94	1.62
	Naloxone	−10.46	−8.74	1.72
	DAMGO	−8.70	−9.14	−0.44
	cis-DAMGO	−10.59	−10.81	−0.22
	JOM-6	−11.26	−13.91	−2.65
	Nor-BNI	−18.35	−8.57	9.78

The 3D coordinates of the inactive and active conformations of MOR, and the preparations of the ligands for docking are described under Section 2.7. Activation energy was calculated by subtracting the docking energy of the activated MOR from that of the inactive MOR. The data are represented in kcal/mol.

activity was observed. It is worth to note that the used concentration is again ten times lower than published previously by others (Cinar and Szücs, 2009). These *in vitro* effects are in match with those observed *in vivo*, showing a CB_1 independent inhibitory action of rimonabant at MOR signaling.

The exact mechanisms and interactions involved in the effects of our *in vivo* data are hard to explain. However, these data serve as an admonition indicating that a low dosage of i.p. injected rimonabant has an impact on the functional activity of forebrain MORs. Our *in vitro* results are easier to interpret. One plausible explanation can be a cross regulation via direct interaction between MOR and another G-protein coupled receptor, because dimerization or oligomerization is a common occurrence between GPCRs. According to our results it is unlikely that dimerization between MOR and CB_1 occur. However, CB_2 cannabinoid receptor can be a possible player in the observed effects. Despite of CB_2 is mostly present in non-neuronal peripheral tissues, increasing amount of data are showing its neuronal and non-neuronal presence in the CNS (Ross et al., 2001; Van Sickle et al., 2005). Previously we also showed a CB_2 mediated NE influence on forebrain MOR G-protein activation (Páldyová et al., 2008) as well as an inhibitory role of a CB_2 antagonist at MOR activity in brainstem (Páldy et al., 2008). To examine whether the CB_2 receptor has a role (if any) in the observed changes in MOR G-protein stimulation, in the next step we performed DAMGO-stimulated [^{35}S]GTPγS binding experiments on CB_1/CB_2 double knockout mice forebrain. According to our data, particularly that rimonabant decreased MOR signaling in the same extent in double knockouts and their controls, the role of the CB_2 can be excluded as well. These results were however expected since rimonabant has a very poor affinity for the CB_2 receptor (Rinaldi-Carmona et al., 1994). Our *in vitro* functional [^{35}S]GTPγS binding results clearly indicate that rimonabant has an inhibitory action at MORs when used in low concentrations. This effect is correlative in both $CB_1^{-/-}$ single knockout and $CB_1^{-/-}/CB_2^{-/-}$ double knockout mice highlighting a cannabinoid receptor independent action.

In our functional binding experiments we ruled out the involvement of the cannabinoid receptors in the noted effects of rimonabant. But, the question whether rimonabant is able to bind directly to MOR and therefore mediate its effect via direct coupling to MOR remains open. To clarify this aspect, we did competition binding experiments with tritiated opioid agonist [^{3}H]DAMGO. In these experiments a very high IC_{50} value had arose for rimonabant compared to DAMGO. The affinity values of rimonabant accord with earlier binding studies (Cinar and Szücs, 2009; Kathmann et al., 2006). In these papers, it is concluded that the CB_1 antagonist binds directly, albeit with low affinity to MOR and competitively interacts with [^{3}H]DAMGO in dissociation binding experiments. Our results does not support this hypothesis, because rimonabant could only displace [^{3}H]DAMGO in the highest concentrations, and even at that level it could only cause a minor decrease in the specific binding of the radiolabeled MOR agonist. The lack of CB_1 receptor did not affect the binding characteristics of either ligand, as we got comparable results in CB_1 knockouts as well. Because previously several studies reported non CB_1 receptor related actions of rimonabant in higher concentration (Arnone et al., 1997; Beyer et al., 2010; Le Foll and Goldberg, 2005; Verty et al., 2003), we tested the binding properties of DAMGO in the presence of highly concentrated rimonabant as well. In these experiments 50 and 100 μM of rimonabant decreased the ~1 nM [^{3}H]DAMGO binding approximately to non-specific binding level, at the same time at 10 μM concentrations rimonabant remained effectless. In summary, rimonabant cannot compete for the binding site of MOR at low concentrations and it is unspecific in higher concentrations.

Docking calculations gives the opportunity to gather information about the receptor–ligand complex, such as the estimate of binding energy, the possible intermolecular interactions, orientations or the occurring energy alterations, which are hard to achieve in *in vitro* studies. Rimonabant accommodates to both receptor conformations with a low docking energy (which was unexpectedly low in the case of the active state), but with a high energy expense for the activated receptor compared to the inactive one, suggesting an antagonistic character for the ligand. This is supported by our finding that only the inactive state gives the possibility for a hydrogen bond between rimonabant and a residue in the binding pocket of MOR.

To support the docking results, we carried out radiolabeled competition binding experiments using a tritiated opioid antagonist [^{3}H]naloxone to see how effectively rimonabant is able to bind to the inactive state of MOR. To exclude any possible interactions with other receptors, for the experiments we used CHO-MOR cells. [^{3}H]naloxone was given in a ~1 nM fixed concentration and was incubated together with increasing concentrations of rimonabant. Rimonabant was able to displace [^{3}H]naloxone with a significantly lower $\log IC_{50}$ value compared to [^{3}H]DAMGO. Moreover a higher affinity binding site for rimonabant was measured in the displacement of [^{3}H]naloxone. The high and low affinity binding sites are common in GPCRs (Baker and Hill, 2007), and previously our group had demonstrated it on opioid receptors, including on the MOR (Krizsán et al., 1991). The high binding energies of rimonabant docked to the activated MOR still remains to be understood. A possible explanation is that rimonabant is accepted by MOR in

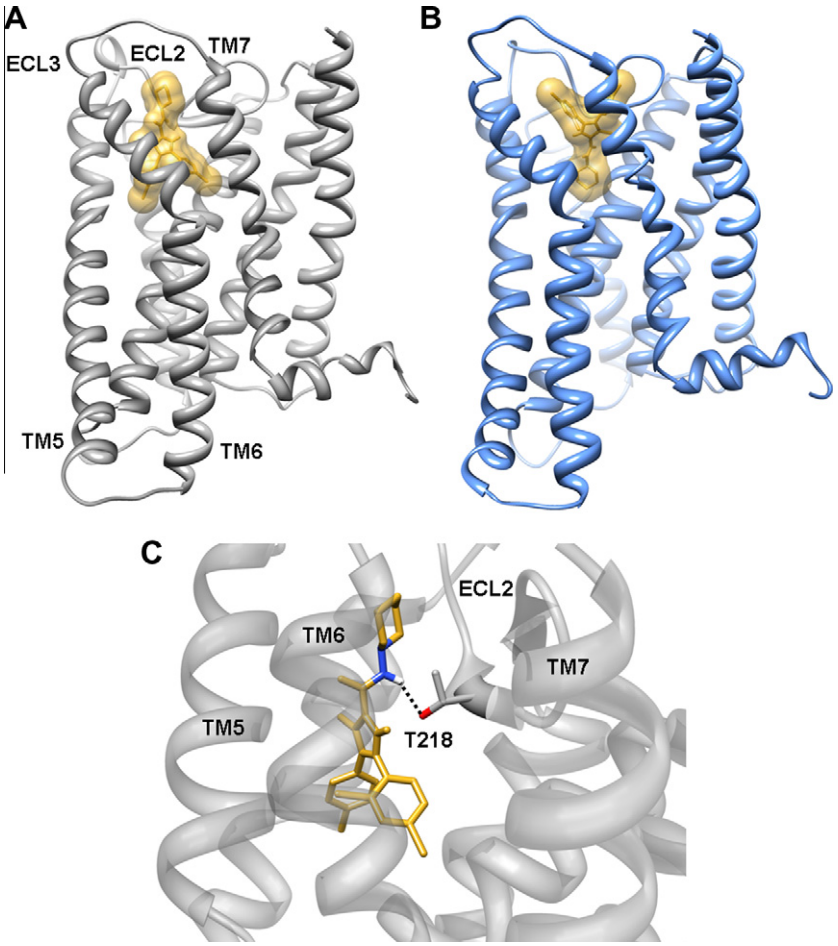

Fig. 7. The docking pose of rimonabant in the inactive (A) and active (B) MOR, and the hydrogen bond between rimonabant and T218 (C). Rimonabant is indicated in yellow (the nitrogen and hydrogen atoms of the hydrazide group are shown in blue and white, respectively). The hydrogen bond is highlighted with a black dotted line; the hydrogen acceptor (oxygen) is shown in red on T218. The essential extracellular loops (ECL) and transmembrane regions (TM) are indicated on the inactive conformation of MOR for clarity.

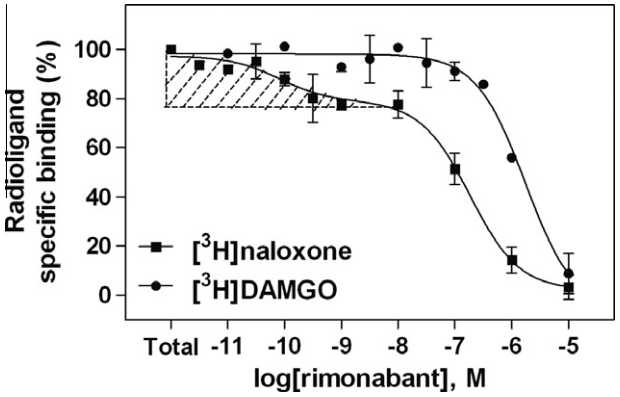

Fig. 8. Competition binding curves of [^{3}H]naloxone and [^{3}H]DAMGO binding in MOR-CHO cell membranes as described under Section 2.6. Data are presented as the percentage of specific radioligand binding (~1 nM) observed in the presence of increasing concentrations of unlabeled rimonabant. The shaded area indicates the high affinity binding site of the curve. Points represent means ± S.E.M. for at least three experiments performed in duplicate.

its resting (inactive) state which is maintained by bound naloxone, including the high affinity state. This is in accordance with its lower docking energies to the inactive receptor compared to that of naloxone. The subsequent receptor activation is prevented by the energy barrier restricting rimonabant as an antagonist. Contrary to these, bound DAMGO maintains the receptor in its active conformation and the high affinity binding site related to the inactive state is not present in the otherwise small ligand free population of MOR which released DAMGO. Nevertheless the inhibitory actions of rimonabant upon MOR G-protein stimulation could be interpreted with its antagonistic behavior on MOR.

Since rimonabant was first described as the potent CB_1 receptor antagonist, it is widely used for blocking cannabimimetic effects *via* blocking CB_1 receptor mediated signaling pathways (for review see Pertwee, 2005), due to its very high affinity towards CB_1 receptor. However growing number of evidences is showing that CB_1 specific compounds conspicuously act in a CB_1 independent manner, including rimonabant. There are several publications supporting that rimonabant can bind with low affinity to other GPCRs, including κ-opioid receptors, GPR55 or can activate several types of ion channels, among others (for review see Pertwee, 2010). In our study we emphasize that rimonabant is able to inhibit the functional activity of forebrain MORs in low concentrations both *in vivo* and *in vitro*. This inhibition is CB receptor independent and comprises MOR's where rimonabant acts as a MOR antagonist on a higher affinity binding site. However, our *in vivo* data underline another, most likely indirect a possible direct mechanisms that are additionally involved in the observed effects. This can be due to a wild range of cross talks that occur in the signaling pathways of GPCRs, which in consequence might activate a ray of entirely new pathways. Because CB_1 receptors are the most widely distributed

GPCRs in the brain, unspecific actions of rimonabant are inevitable. This assumption is underpinned by our study along with others. Despite of being far from the complete understanding of the exact mechanisms behind the impact of rimonabant on the opioid system, our data presented above partially elucidate its actions.

Acknowledgements

This study was supported by funds from the National Development Agency (NFÜ), Budapest, Hungary; Grant No. CK-78566. The authors would like to thank Sanofi Research Laboratory for providing rimonabant, and to Prof. Wenger Tibor and co-workers for providing the CB_1 knock-out mice and finally for the assistance of Zsuzsa Canjavec. We are also grateful to Prof. Mária Wollemann for critical reading of the manuscript.

References

Arnone, M., Maruani, J., Chaperon, F., Thiébot, M.H., Poncelet, M., Soubrié, P., Le Fur, G., 1997. Selective inhibition of sucrose and ethanol intake by SR 141716, an antagonist of central cannabinoid (CB1) receptors. Psychopharmacology 132, 104–106.

Baker, J.G., Hill, S.J., 2007. Multiple GPCR conformations and signalling pathways: implications for antagonist affinity estimates. Trends Pharmacol. Sci. 28, 374–381.

Begg, M., Pacher, P., Bátkai, S., Osei-Hyiaman, D., Offertáler, L., Mo, F.M., Liu, J., Kunos, G., 2005. Evidence for novel cannabinoid receptors. Pharmacol. Ther. 106, 133–145.

Beltramo, M., Bernardini, N., Bertorelli, R., Campanella, M., Nicolussi, E., Fredduzzi, S., Reggiani, A., 2006. CB2 receptor-mediated antihyperalgesia: possible direct involvement of neural mechanisms. Eur. J. Neurosci. 23, 1530–1538.

Benyhe, S., Farkas, J., Tóth, G., Wollemann, M., 1997. Met5-enkephalin-Arg6-Phe7, an endogenous neuropeptide, binds to multiple opioid and nonopioid sites in rat brain. J. Neurosci. Res. 48, 249–258.

Beyer, C.E., Dwyer, J.M., Piesla, M.J., Platt, B.J., Shen, R., Rahman, Z., Chan, K., Manners, M.T., Samad, T.A., Kennedy, J.D., Bingham, B., Whiteside, G.T., 2010. Depression-like phenotype following chronic CB1 receptor antagonism. Neurobiol. Dis. 39, 148–155.

Braida, D., Pozzi, M., Parolaro, D., Sala, M., 2001. Intracerebral self-administration of the cannabinoid receptor agonist CP 55,940 in the rat: interaction with the opioid system. Eur. J. Pharmacol. 413, 227–234.

Breivogel, C.S., Griffin, G., Di Marzo, V., Martin, B.R., 2001. Evidence for a new G protein-coupled cannabinoid receptor in mouse brain. Mol. Pharmacol. 60, 155–163.

Breivogel, C.S., Sim, L.J., Childers, S.R., 1997. Regional differences in cannabinoid receptor/G-protein coupling in rat brain. J. Pharmacol. Exp. Ther. 282, 1632–1642.

Burford, N.T., Wang, D., Sadée, W., 2000. G-protein coupling of mu-opioid receptors (OP3): elevated basal signalling activity. Biochem. J. 348, 531–537.

Canals, M., Milligan, G., 2008. Constitutive activity of the cannabinoid CB1 receptor regulates the function of co-expressed mu opioid receptors. J. Biol. Chem. 283, 11424–11434.

Christensen, R., Kristensen, P.K., Bartels, E.M., Bliddal, H., Astrup, A., 2007. Efficacy and safety of the weight-loss drug rimonabant: a meta-analysis of randomised trials. Lancet 370, 1706–1713.

Cinar, R., Szücs, M., 2009. CB1 receptor-independent actions of SR141716 on G-protein signaling: coapplication with the mu-opioid agonist Tyr-D-Ala-Gly-(NMe)Phe-Gly-ol unmasks novel, pertussis toxin-insensitive opioid signaling in mu-opioid receptor-Chinese hamster ovary cells. J. Pharmacol. Exp. Ther. 330, 567–574.

Demuth, D.G., Molleman, A., 2006. Cannabinoid signaling. Life Sci. 78, 549–563.

Egertová, M., Elphick, M.R., 2000. Localisation of cannabinoid receptors in the rat brain using antibodies to the intracellular C-terminal tail of CB. J. Comp. Neurol. 422, 159–171.

Fattore, L., Spano, S., Cossu, G., Deiana, S., Fadda, P., Fratta, W., 2005. Cannabinoid CB(1) antagonist SR 141716A attenuates reinstatement of heroin self-administration in heroin-abstinent rats. Neuropharmacology 48, 1097–1104.

Gibson, H.E., Edwards, J.G., Page, R.S., Van Hook, M.J., Kauer, J.A., 2008. TRPV1 channels mediate long-term depression at synapses on hippocampal interneurons. Neuron 57, 746–759.

Glass, M., Dragunow, M., Faull, R.L., 1997. Cannabinoid receptors in the human brain: a detailed anatomical and quantitative autoradiographic study in the fetal, neonatal and adult human brain. Neuroscience 77, 299–318.

Hanus, L., Abu-Lafi, S., Fride, E., Breuer, A., Vogel, Z., Shalev, D.E., Kustanovich, I., Mechoulam, R., 2001. 2-Arachidonyl glyceryl ether, an endogenous agonist of the cannabinoid CB1 receptor. Proc. Natl. Acad. Sci. U S A 98, 3662-365.

Halgren, T.A., 1999. MMFF VI. MMFF94s option for energy minimization studies. J. Comput. Chem. 20, 720–729.

Herkenham, M., Lynn, A.B., Johnson, M.R., Melvin, L.S., de Costa, B.R., Rice, K.C., 1991. Characterization and localization of cannabinoid receptors in rat brain: a quantitative in vitro autoradiographic study. J. Neurosci. 11, 563–583.

Hough, L.B., Svokos, K., Nalwalk, J.W., 2009. Non-opioid antinociception produced by brain stem injections of improgan: significance of local, but not cross-regional, cannabinoid mechanisms. Brain Res. 1247, 62–70.

Howlett, A.C., 1998. The CB1 cannabinoid receptor in the brain. Neurobiol. Dis. 5, 405–416.

Hur, E.M., Kim, K.T., 2002. G protein-coupled receptor signalling and cross-talk: achieving rapidity and specificity. Cell. Signal. 14, 397–405.

Jansen, E.M., Haycock, D.A., Ward, S.J., Seybold, V.S., 1992. Distribution of cannabinoid receptors in rat brain determined with aminoalkylindoles. Brain Res. 575, 93–102.

Járai, Z., Wagner, J.A., Varga, K., Lake, K.D., Compton, D.R., Martin, B.R., Zimmer, A.M., Bonner, T.I., Buckley, N.E., Mezey, E., Razdan, R.K., Zimmer, A., Kunos, G., 1999. Cannabinoid-induced mesenteric vasodilation through an endothelial site distinct from CB1 or CB2 receptors. Proc. Natl. Acad. Sci. U S A 96, 14136–14141.

Julian, M.D., Martin, A.B., Cuellar, B., Rodriguez De Fonseca, F., Navarro, M., Moratalla, R., Garcia-Segura, L.M., 2003. Neuroanatomical relationship between type 1 cannabinoid receptors and dopaminergic systems in the rat basal ganglia. Neuroscience 119, 309–318.

Kathmann, M., Flau, K., Redmer, A., Tränkle, C., Schlicker, E., 2006. Cannabidiol is an allosteric modulator at mu- and delta-opioid receptors. Naunyn Schmiedebergs Arch. Pharmacol. 372, 354–361.

Krizsán, D., Varga, E., Hosztafi, S., Benyhe, S., Szücs, M., Borsodi, A., 1991. Irreversible blockade of the high and low affinity (^{3}H) naloxone binding sites by C-6 derivatives of morphinane-6-ones. Life Sci. 48, 439–451.

Le Foll, B., Goldberg, S.R., 2005. Cannabinoid CB1 receptor antagonists as promising new medications for drug dependence. J. Pharmacol. Exp. Ther. 312, 875–883.

Ledent, C., Valverde, O., Cossu, G., Petitet, F., Aubert, J.F., Beslot, F., Böhme, G.A., Imperato, A., Pedrazzini, T., Roques, B.P., Vassart, G., Fratta, W., Parmentier, M., 1999. Unresponsiveness to cannabinoids and reduced addictive effects of opiates in C_{B1} receptor knockout mice. Science 283, 401–404.

Matsuda, L.A., Lolait, S.J., Brownstein, M.J., Young, A.C., Bonner, T.I., 1990. Structure of a cannabinoid receptor and functional expression of the cloned cDNA. Nature 346, 561–564.

Misicka, A., Verheyden, P.M., Van Bist, G., 1998. Equilibrium of the *cis–trans* isomerisation of the peptide bond with N-alkyl amino acids measured by 2D NMR. Lett. Pept. Sci. 5, 375–377.

Mitchell, P.B., Morris, M.J., 2007. Depression and anxiety with rimonabant. Lancet 370, 1671–1672.

Morris, G.M., Huey, R., Lindstrom, W., Sanner, M.F., Belew, R.K., Goodsell, D.S., Olson, A.J., 2009. AutoDock4 and AutoDockTools4: automated docking with selective receptor flexibility. J. Comput. Chem. 16, 2785–2791.

Navarro, M., Carrera, M.R., Fratta, W., Valverde, O., Cossu, G., Fattore, L., Chowen, J.A., Gomez, R., del Arco, I., Villanua, M.A., Maldonado, R., Koob, G.F., Rodriguez de Fonseca, F., 2001. Functional interaction between opioid and cannabinoid receptors in drug self-administration. J. Neurosci. 21, 5344–5350.

O'Boyle, N.M., Banck, M., James, C.A., Morley, C., Vandermeersch, T., Hutchison, G.R., 2011. Open Babel: an open chemical toolbox. J. Cheminf. 3.

Padwal, R.S., Majumdar, S.R., 2007. Drug treatments for obesity: orlistat, sibutramine, and rimonabant. Lancet 369, 71–77.

Páldy, E., Bereczki, E., Sántha, M., Wenger, T., Borsodi, A., Zimmer, A., Benyhe, S., 2008. CB2 cannabinoid receptor antagonist SR144528 decreases mu-opioid receptor expression and activation in mouse brainstem: Role of CB2 receptor in pain. Neurochem. Int. 52, 309–316.

Páldyová, E., Bereczki, E., Sántha, M., Wenger, T., Borsodi, A., Benyhe, S., 2008. Noladin ether, a putative endocannabinoid, inhibits mu-opioid receptor activation via CB2 cannabinoid receptors. Neurochem. Int. 52, 321–328.

Pertwee, R.G., Howlett, A.C., Abood, M.E., Alexander, S.P., Di Marzo, V., Elphick, M.R., Greasley, P.J., Hansen, H.S., Kunos, G., Mackie, K., Mechoulam, R., Ross, R.A., 2010. International Union of Basic and Clinical Pharmacology. LXXIX. Cannabinoid receptors and their ligands: beyond CB_1 and CB_2. Pharmacol. Rev. 62, 588–631.

Pertwee, R.G., 2005. Inverse agonism and neutral antagonism at cannabinoid CB1 receptors. Life Sci. 76, 1307–1324.

Pertwee, R.G., 2010. Receptors and channels targeted by synthetic cannabinoid receptor agonists and antagonists. Curr. Med. Chem. 17, 1360–1381.

Pettersen, E.F., Goddard, T.D., Huang, C.C., Couch, G.S., Greenblatt, D.M., Meng, E.C., Ferrin, T.E., 2004. UCSF Chimera – a visualization system for exploratory research and analysis. J. Comput. Chem. 13, 1605–1612.

Pickel, V.M., Chan, J., Kash, T.L., Rodríguez, J.J., MacKie, K., 2004. Compartment-specific localization of cannabinoid 1 (CB1) and mu-opioid receptors in rat nucleus accumbens. Neuroscience 127, 101–112.

Pogozheva, I.D., Przydzial, M.J., Mosberg, H.I., 2005. Homology modeling of opioid receptor–ligand complexes using experimental constraints. AAPS J. 7, 434–448.

Raffa, R.B., Ward, S.J., 2011. CB(1)-independent mechanisms of Δ(9)-THCV, AM251 and SR141716 (rimonabant). J. Clin. Pharm. Ther. [Epub. ahead of print].

Rinaldi-Carmona, M., Barth, F., Congy, C., Martinez, S., Oustric, D., Pério, A., Poncelet, M., Maruani, J., Arnone, M., Finance, O., Soubrié, P., Le Fur, G., 1994. SR147778 [5-(4-bromophenyl)-1-(2,4-dichlorophenyl)-4-ethyl-*N*-(1-piperidinyl)-1H-pyrazole-3-carboxamide], a new potent and selective antagonist of the CB1 cannabinoid receptor: biochemical and pharmacological characterization. J. Pharmacol. Exp. Ther. 310, 905–914.

Rios, C., Gomes, I., Devi, L.A., 2006. Mu opioid and CB1 cannabinoid receptor interactions: reciprocal inhibition of receptor signaling and neuritogenesis. Br. J. Pharmacol. 148, 387–395.

Robbe, D., Alonso, G., Duchamp, F., Bockaert, J., Manzoni, O.J., 2001. Localization and mechanisms of action of cannabinoid receptors at the glutamatergic synapses of the mouse nucleus accumbens. J. Neurosci. 21, 109–116.

Rodriguez, J.J., Mackie, K., Pickel, V.M., 2001. Ultrastructural localization of the CB1 cannabinoid receptor in mu-opioid receptor patches of the rat Caudate putamen nucleus. J. Neurosci. 21, 823–833.

Ross, R.A., Coutts, A.A., McFarlane, S.M., Anavi-Goffer, S., Irving, A.J., Pertwee, R.G., MacEwan, D.J., Scott, R.H., 2001. Actions of cannabinoid receptor ligands on rat cultured sensory neurones: implications for antinociception. Neuropharmacology 40, 221–232.

Salio, C., Fischer, J., Franzoni, M.F., Mackie, K., Kaneko, T., Conrath, M., 2001. CB1-cannabinoid and mu-opioid receptor co-localization on postsynaptic target in the rat dorsal horn. NeuroReport 12, 3689–3692.

Savinainen, J.R., Saario, S.M., Niemi, R., Järvinen, T., Laitinen, J.T., 2003. An optimized approach to study endocannabinoid signaling: evidence against constitutive activity of rat brain adenosine A1 and cannabinoid CB1 receptors. Br. J. Pharmacol. 140, 1451–1459.

Schoffelmeer, A.N., Hogenboom, F., Wardeh, G., De Vries, T.J., 2006. Interactions between CB1 cannabinoid and mu opioid receptors mediating inhibition of neurotransmitter release in rat nucleus accumbens core. Neuropharmacology 51, 773–781.

Sim, L.J., Selley, D.E., Childers, S.R., 1995. *In vitro* autoradiography of receptor-activated G proteins in rat brain by agonist-stimulated guanylyl 5′-[gamma-[^{35}S]thio]-triphosphate binding. Proc. Natl. Acad. Sci. U S A 92, 7242–7246.

Skaper, S.D., Buriani, A., Dal Toso, R., Petrelli, L., Romanello, S., Facci, L., Leon, A., 1996. The ALIAmide palmitoylethanolamide and cannabinoids, but not anandamide, are protective in a delayed postglutamate paradigm of excitotoxic death in cerebellar granule neurons. Proc. Natl. Acad. Sci. U S A 93, 3984–3989.

Traynor, J.R., Nahorski, S.R., 1995. Modulation by mu-opioid agonists of guanosine-5′-*O*-(3-[^{35}S](thio)triphosphate binding to membranes from human neuroblastoma SH-SY5Y cells. Mol. Pharmacol. 47, 848–854.

Van Sickle, M.D., Duncan, M., Kingsley, P.J., Mouihate, A., Urbani, P., Mackie, K., Stella, N., Makriyannis, A., Piomelli, D., Davison, J.S., Marnett, L.J., Di Marzo, V., Pittman, Q.J., Patel, K.D., Sharkey, K.A., 2005. Identification and functional characterization of brainstem cannabinoid CB2 receptors. Science 310, 329–332.

Verty, A.N., Singh, M.E., McGregor, I.S., Mallet, P.E., 2003. The cannabinoid receptor antagonist SR 141716 attenuates overfeeding induced by systemic or intracranial morphine. Psychopharmacology 168, 314–323.

Web references

MOR homology model: http://www.mosberglab.phar.umich.edu (last accessed: 2009).

Cactus: http://cactus.nci.nih.gov/chemical/structure (last accessed: 2011).

Avogadro: http://avogadro.openmolecules.net/wiki/Main_Page (last accessed: 2011).

II.

Zádor, F., Kocsis, D., Borsodi, A., Benyhe, S. **Micromolar concentrations of rimonabant directly inhibits delta opioid receptor specific ligand binding and agonist-induced G-protein activity.** *Neurochem Int* 67, 14-22 (2014).

(2.66 impact factor)

Neurochemistry International 67 (2014) 14–22

Contents lists available at ScienceDirect

Neurochemistry International

journal homepage: www.elsevier.com/locate/nci

Micromolar concentrations of rimonabant directly inhibits delta opioid receptor specific ligand binding and agonist-induced G-protein activity

Ferenc Zádor *, Dóra Kocsis, Anna Borsodi, Sándor Benyhe

Institute of Biochemistry, Biological Research Centre, Hungarian Academy of Sciences, Temesvári krt. 62, H-6726 Szeged, Hungary

ARTICLE INFO

Article history:
Received 24 June 2013
Received in revised form 26 November 2013
Accepted 17 December 2013
Available online 4 February 2014

Keywords:
Rimonabant
Delta opioid receptor
Cannabinoid receptor
G-protein
[^{35}S]GTPγS binding
Radioligand binding

ABSTRACT

What is known: There is a growing number of evidence showing, that the cannabinoid receptor 1 (CB_1) antagonist rimonabant has many non-cannabimimetic actions, such as affecting the opioid system. The direct effect of rimonabant on opioid receptors has been studied so far mainly on μ-opioid receptors. However recently the δ-opioid receptor (DOR) receives much more attention as before, due to its potential therapeutic applications, such as nociception or treatment for psychiatric disorders.
Objectives: To investigate the direct effect of rimonabant on DOR specific ligand binding and on the DOR mediated G-protein activation.
Results: Micromolar concentrations of rimonabant directly inhibited the DOR specific agonist binding in radioligand competition binding experiments using Chinese hamster ovary cells stably transfected with mouse DOR (CHO-mDOR). However the inhibition occurred also in the subnanomolar range during DOR specific antagonist binding in similar experimental conditions. In functional [^{35}S]GTPγS binding assays rimonabant significantly decreased the basal receptor activity in CHO-mDOR but also in parental CHO cell membranes. During DOR agonist stimulation, micromolar concentration of rimonabant attenuated the DOR G-protein activation and the potency of the activator ligand in [^{35}S]GTPγS binding assays performed in CHO-mDOR, in wild type and also in CB_1/CB_2 double knock-out mouse forebrain membranes. Yet again this inhibitory action was DOR specific, since it did not occur during other specific GPCR agonist mediated G-protein activation.
Conclusion: Rimonabant directly inhibited DOR function in the micromolar concentrations. The inhibitory actions indicate an antagonistic behavior towards DOR which was established by the followings: (i) rimonabant inhibited DOR antagonist binding more effectively than agonist binding, (ii) the inverse agonistic, agonistic effect of the compound can be excluded, and (iii) additionally according to previous findings the allosteric mechanism can also be foreclosed.

1. Introduction

Among the opioid receptors, μ, δ and κ (MOR, DOR and KOR, respectively), the DOR is relatively studied in a less extent compared to its two other companions, especially to MOR (Pradhan et al., 2012). However recently there is an increasing number of studies showing DOR as a potential therapeutic target (for review see Pradhan et al., 2011), more interestingly the activation of DOR represents less of the known adverse effects of MOR stimulation such as addiction, respiratory depression, or constipation (Codd et al., 2009). Additionally certain DOR agonists have anxiolytic and anti-depressant effects too (Broom et al., 2002; Perrine et al., 2006; Saitoh et al., 2004).

Both cannabinoid receptor types – type 1 (CB_1) and type 2 (CB_2) – share many features with the opioid receptors: they all belong to the G-protein coupled receptor (GPCR) superfamily, and couple

Abbreviations: [^{35}S]GTPγS, guanosine-5′-*O*-(3-[^{35}S]thio)triphosphate; BBB, blood–brain-barrier; CB_1, type 1 cannabinoid receptor; CB_1/CB_2 K.O., CB_1/CB_2 double knock-out; CB_2, type 2 cannabinoid receptor; CHO, Chinese hamster ovary cell line; CHO-mDOR, Chinese hamster ovary cell line overexpressed with mouse δ-opioid receptor; CHO-MOR, Chinese hamster ovary cell line overexpressed with μ-opioid receptor; DMSO, dimethyl sulphoxide; DOR, δ-opioid receptor; DPDPE, [D-Pen^{2,5}]-enkephalin hydrate; EGTA, ethyleneglycol-tetraacetate; GDP, guanosine 5′-diphosphate; GPCR, G-protein coupled receptor; GTP, guanosin 5′-triphosphate; GTPγS, guanosine-5′-*O*-[γ-thio] triphosphate; KOR, κ-opioid receptor; MOR, μ-opioid receptor; NTI, naltrindole; pCHO, parental CHO cell line; rim., rimonabant; S.E.M., standard error of means; TEM, Tris–HCl, EGTA, $MgCl_2$; Tris–HCl, tris-(hydroxymethyl)-aminomethane hydrochloride; w.t., wild type.

* Corresponding author. Address: Institute of Biochemistry, Biological Research Center, Hungarian Academy of Sciences, PO Box 521, H-6701 Szeged, Hungary. Tel.: +36 62 599 636; fax: +36 62 433 506.
E-mail address: zador.ferenc@gmail.com (F. Zádor).

http://dx.doi.org/10.1016/j.neuint.2013.12.005
0197-0186/

mainly to the $G_{i/o}$ type G-proteins (Burford et al., 2000; Demuth and Molleman, 2006), therefore they inhibit the release of different types of neurotransmitters such as GABA, glutamate, noradrenaline, acetylcholine or dopamine (Howlett et al., 2002; Katona et al., 1999; Mansour et al., 1995; Shen et al., 1996). Furthermore their distribution overlaps in certain brain regions such as cerebral cortex or amygdala (Gong et al., 2006; Howlett et al., 2002; Mansour et al., 1995; Sim and Childers, 1997). The CB_1 receptor and DOR have not only similar functions, like nociception (Bie and Pan, 2007; Bushlin et al., 2012; Maldonado and Valverde, 2003; Pertwee, 2001) and mood regulation (Bambico et al., 2007; Filliol et al., 2000), but they can allosterically alter each other's activity (Berrendero et al., 2003; Bushlin et al., 2012; Rozenfeld et al., 2012; Urigüen et al., 2005) and form heteromers as well (Bushlin et al., 2012).

The CB_1 receptor is known for having a well-established role in appetite control (for review see Pagotto et al., 2006), thus both CB_1 agonists and antagonist are developed for therapeutic control of food intake (for review see Lee et al., 2009; Pagotto et al., 2006). The chief among the CB_1 receptor antagonists, rimonabant was firstly developed (Rinaldi-Carmona et al., 1994) and marketed as an appetite suppressant under the trade name Acomplia® (Padwal and Majumdar, 2007). However 2 years after its introduction it was withdrawn from the market because serious psychiatric side effects such as severe depression, anxiety and suicidal thoughts occurred during chronic administration of the drug (see web reference). Before and also after the withdrawal, preclinical rodent studies showed both anxiolytic/antidepressant and anxiogenic effects and depression-like behavior during acute rimonabant administration (Arévalo et al., 2001; Lockie et al., 2011; McGregor et al., 1996; Rodgers et al., 2003; Tzavara et al., 2003), while chronic treatment of rimonabant clearly induced depression-like behavior in the animals (Beyer et al., 2010). Although rimonabant is believed to behave as an antagonist on CB_1 receptor, there are increasing numbers of studies reporting that it can inhibit CB_1 receptor mediated G-protein basal activity (Breivogel et al., 2001; MacLennan et al., 1998; Sim-Selley et al., 2001), thus it can behave as an inverse agonist. This character of rimonabant results in opposite cannabimimetic effects to that of a CB_1 agonist, such as enhanced neurotransmitter release, increased memory activity or even reduced food consumption (for review see Pertwee, 2005). However later on the inverse agonistic actions of rimonabant has been proven to be CB_1 receptor independent, probably occurring via non-receptor mediated manner or allosterically on CB_1 receptor or through other GPCRs different from CB_1 receptor (Breivogel et al., 2001; Cinar and Szücs, 2009; Seely et al., 2012; Sim-Selley et al., 2001).

Rimonabant can interact with other members of the GPCR family, such as opioid receptors (for review see Pertwee, 2010). It has been shown that it can affect the function of MOR through the CB_1 receptor (for review see Foll and Goldberg, 2005 and Robledo et al., 2008), moreover there is an increasing number of studies reporting a direct effect of rimonabant on opioid receptors, mainly focusing on MORs (Cinar and Szücs, 2009; Fong et al., 2009; Kathmann et al., 2006; Seely et al., 2012; Zádor et al., 2012). Recently our group also demonstrated an antagonistic character of rimonabant on MOR (Zádor et al., 2012) which was later affirmed by Seely and coworkers (Seely et al., 2012).

The aim of this study was to examine the direct effect of rimonabant on DOR function, since this opioid receptor type is not well studied in this aspect yet. Herein we investigated the effect of rimonabant on DOR specific ligand binding and for the first time on DOR G-protein basal activity and on DOR G-protein activity during agonist-stimulation. Furthermore we clarified the role of both cannabinoid receptors in the forebrain region regarding to the effect of rimonabant on DOR functionality.

2. Materials and methods

2.1. Chemicals

Tris–HCl, EGTA, NaCl, $MgCl_2 \times 6H_2O$, GDP, the GTP analog GTPγS, the adrenerg receptor agonist L-epinephrine, the DOR specific agonist peptide DPDPE, the DOR antagonist naltrindole and the KOR specific agonist U50488 were purchased from Sigma–Aldrich (St. Louis, MO, USA). The MOR agonist morphine was obtained from the Alkaloid Chemic Factory (Tiszavasvár, Hungary). The radiolabelled GTP analog, [^{35}S]GTPγS (specific activity: >1000 Ci/mmol) was purchased from the Isotope Institute Ltd. (Budapest, Hungary). SR141716 (rimonabant) was acquired from Santa Cruz (Dallas, Texas, USA). The modified DOR specific deltorphin II derivative, Ile^{5,6}deltorphin II was synthesized and tritiated ([^{3}H]Ile^{5,6}deltorphin II; specific activity: 28 Ci/mmol; Nevin et al., 1994) in the Isotope Laboratory of Biological Research Center (Szeged, Hungary). The opioid antagonist naloxone was kindly provided by the company Endo Laboratories DuPont de Nemours (Wilmington, DE, USA). [^{3}H]naltrindole ([^{3}H]NTI; specific activity: 24 Ci/mmol) was purchased from PerkinElmer (Boston, USA). Rimonabant was dissolved in DMSO and similar to the other applied receptor ligands, was stored in 1 mM stock solution at −20 °C.

2.2. Animals

The CB_1/CB_2 receptor double knockout mice were provided by Dr. Andreas Zimmer's laboratory (University of Bonn, Germany), the lack of both cannabinoid receptors was confirmed in previous studies (Járai et al., 1999). The wild type mice were bought from the local animal house of the Biological Research Center (Szeged, Hungary). Both mice genotypes were derived from the C57BL/6J strain and 8 wild type and 8 double knock-out animals were used for membrane preparations. All the animals were housed at 21–24 °C under a 12:12 light: dark cycle and were provided with water and food *ad libitum*. All housing and experiences were conducted in accordance with the European Communities Council Directives (86/609/ECC) and the Hungarian Act for the Protection of Animals in Research (XXVIII.tv. 32.§).

2.3. Cell culture and cell membrane preparations

CHO-mDOR cells overexpressing mouse DORs were provided by Dr. Zvi Vogel (Rehovot, Israel). The maximal DOR binding capacity in the cell lines was 2730 ± 90 fmol/mg according to our group's previous reports (Ioja et al., 2007, 2005).

The growing of the cells was performed as we previously described (Zádor et al., 2012). Briefly the cells were grown in Dulbecco's modified Eagle's medium and in α-minimum essential medium, respectively. Both media were supplemented with 10% fetal calf serum, 2 mM glutamine, 100 IU/ml penicillin, 100 mg/ml streptomycin, 25 mg/ml fungizone and 0.5 mg/ml geneticin. Parental CHO cells (pCHO) were cultured in F-12 medium with L-glutamine which contained 10% fetal bovine serum. Both CHO cell lines were kept in culture at 37 °C in a humidified atmosphere consisting of 5% CO_2 and 95% air.

Cell membranes were prepared for competition binding experiments as we previously described (Zádor et al., 2012). For the [^{35}S]GTPγS binding assays the membrane homogenate was prepared similarly except the cells were diluted in TEM buffer (50 mM Tris–HCl, 1 mM EGTA, and 5 mM $MgCl_2$; pH 7.4).

2.4. Forebrain membrane preparations

Forebrain membrane fractions from CB_1/CB_2 K.O. mice and their wild type controls were prepared according to the method

previously described (Benyhe et al., 1997) until the point where the membrane homogenate was prepared for the [^{35}S]GTPγS binding assay. In this procedure the sucrose was removed by centrifugation (40,000*g*, 20 min, 4 °C) and the pellet was suspended with ice-cold TEM buffer to obtain the appropriate protein content for the assay (~10 μg/ml).

2.5. Radioligand competition binding assays

The direct binding affinity of rimonabant towards DOR was investigated in radioligand competition binding experiments, where we measure the inhibition of fix concentrations of specific radioligand binding in the presence of increasing concentrations of unlabeled competitor ligands.

Aliquots of frozen pCHO and CHO-mDOR membranes were first centrifuged (40,000*g*, 20 min, 4 °C) to remove sucrose and the pellets were suspended in 50 mM Tris–HCl buffer (pH 7.4). Membranes were incubated with gentle shaking at 35 °C for 35 min ([^{3}H]Ile^{5,6}deltorphin II) or 25 °C for 60 min ([^{3}H]NTI) in a final volume of 1 ml with 10^{-10} to 10^{-5} M concentration interval of unlabeled rimonabant together with ~1 nM of [^{3}H]Ile^{5,6}deltorphin II or [^{3}H]NTI. Total binding was measured in the presence of radioligand, in the absence of the competitor ligands. The non-specific binding was determined in the presence of 10 μM unlabeled naloxone. The reaction was terminated by rapid filtration under vacuum (Brandel M24R Cell Harvester), and washed three times with 5 ml ice-cold 50 mM Tris–HCl (pH 7.4) buffer through Whatman GF/C ([^{3}H]Ile^{5,6}deltorphin II) or GF/B ([^{3}H]NTI; washed in 3% polyethylenimine for 60 min) glass fiber filters. The radioactivity of the filters was detected in UltimaGold™ MV aqueous scintillation cocktail with Packard Tricarb 2300TR liquid scintillation counter. The competition binding assays were performed in duplicate and repeated at least three times.

2.6. Functional [^{35}S]GTPγS binding assays

The G-protein activation of DOR was measured in functional [^{35}S]GTPγS binding experiments, which monitors the nucleotide exchange process of the G_α-protein using a non-hydrolysable radiolabeled GTP analog, [^{35}S]GTPγS in the presence of increasing concentrations of the observed ligand.

The assays were performed according to previous studies (Sim et al., 1995; Traynor et al., 1995), with slight modifications. Membrane fractions of pCHO, CHO-mDOR and CB_1/CB_2 K.O. and wild type mouse forebrains were incubated in a final volume of 1 ml at 30 °C for 60 min in Tris-EGTA buffer (pH 7.4) composed of 50 mM Tris–HCl, 1 mM EGTA, 3 mM $MgCl_2$, 100 mM NaCl, containing 0.05 nM [^{35}S]GTPγS (20 MBq/0.05 cm^3) and 30 μM GDP together with the indicated concentrations of DPDPE, rimonabant, NTI, U50488, morphine or L-epinephrine. Total binding (*T*) was measured in the absence of the ligands, non-specific binding (NS) was determined in the presence of 10 μM unlabeled GTPγS and subtracted from total binding. The difference (TNS) represents basal activity. Bound and free [^{35}S]GTPγS were separated by vacuum filtration through Whatman GF/B filters with Brandel M24R Cell harvester. Filters were washed three times with 5 ml ice-cold buffer (pH 7.4), and the radioactivity of the dried filters was detected in UltimaGold™ MV scintillation cocktail with Packard Tricarb 2300TR liquid scintillation counter. The [^{35}S]GTPγS binding experiments were performed in triplicates and repeated at least three times.

2.7. Data analysis

Experimental data were presented as means ± S.E.M. and were fitted with the professional curve fitting program, GraphPad Prism 5.0 (GraphPad Prism Software Inc., San Diego, CA), using non-linear regression. During the competition binding assays the 'One site competition' or in the case of [^{3}H]NTI displacement studies the 'Two sites-Fit logIC50' fitting equation was applied to determine the concentration of the competitor ligands that displaced 50% of the radioligand (IC_{50}). The inhibition of specifically bound [^{3}H]Ile^{5,6}deltorphin II and [^{3}H]NTI was given in percentage, the total specific binding and the minimum level of non-specific binding was defined as 100% and 0% respectively. Additionally competition binding experiments applied in pCHO cell membranes the bound [^{3}H]Ile^{5,6}deltorphin II was represented in cpm (counts per minute) since there was no specific binding observed in this experiments (see Fig. 1A). In the [^{35}S]GTPγS binding assays the 'Sigmoid dose-response' fitting was used to establish the maximal stimulation or efficacy (E_{max}) of the receptors G-protein, and the potency (EC_{50}) of the stimulator ligand. Stimulation was given as percent of the specific [^{35}S]GTPγS binding observed over or under the basal activity, which was settled as 100%. In case of two data sets unpaired *t*-test with two-tailed P value statistical analysis was used, while in case of three or more data sets One-way ANOVA with Bonferroni's Multiple Comparison post hoc test was performed to determine the significance level, using GraphPad Prism 5.0. Since both the competitor and stimulator ligands were presented in the logarithm form, the curve fitting program could only calculate S.E.M. for the logarithm form of IC_{50} ($logIC_{50}$) and EC_{50} ($logEC50$) values. At the same time their antilogarithm form has also been indicated on the figures for better understanding. Significance was accepted at the $P < 0.05$ level.

3. Results

3.1. Direct binding affinity measurements of rimonabant towards DOR in competition binding experiments in CHO-mDOR membrane fractions

Our first objective was to measure the binding affinity of rimonabant directly towards DOR. Equilibrium competition binding experiments were carried out with the DOR specific tritiated agonist Ile^{5,6}deltorphin II ([^{3}H]Ile^{5,6}deltorphin II) using membrane fractions of CHO cells overexpressing mouse DOR (CHO-mDOR) to insure a better receptor-ligand interaction. Additionally we also applied the DOR specific tritiated antagonist naltrindole ([^{3}H]NTI) to see whether rimonabant can alter agonist or antagonist specific binding differently on DOR. Initially we determined the presence of DOR binding in parental CHO (pCHO) cell lines, which were not overexpressed with DORs. According to our results no significant displacement was observed between [^{3}H]Ile^{5,6}deltorphin II and unlabeled Ile^{5,6}deltorphin II (Fig. 1A), therefore the points could not be fitted with non-linear regression. Additionally similar [^{3}H]Ile^{5,6}deltorphin II binding values were detected in the presence of unlabeled Ile^{5,6}deltorphin II and 10 μM naloxone (Fig. 1A), which is applied for the calculation of non-specific binding (see Section 2.5). Thus the detected bound [^{3}H]Ile^{5,6}deltorphin II was due to non-specific binding. Accordingly we can conclude that in pCHO cell lines DOR are not expressed physiologically.

Rimonabant reduced the total specific binding (=100%) of the agonist [^{3}H]Ile^{5,6}deltorphin II only in micromolar concentrations (Fig 1B). In 10 μM concentrations the specific binding of the radioligand was inhibited approximately 50% (Fig. 1B) resulting a 2.8 μM IC_{50} value for rimonabant (Fig 1C). During the displacement of the antagonist [^{3}H]NTI – similar to [^{3}H]Ile^{5,6}deltorphin II – rimonabant at the highest applied concentrations reduced the total specific binding of the radioligand approximately 50% (Fig. 1B). However interestingly rimonabant also inhibited the total specific [^{3}H]NTI binding in the nanomolar range (10^{-10} to 10^{-9} M), which was followed by a short plateau phase (10^{-9} to 10^{-7} M) and in

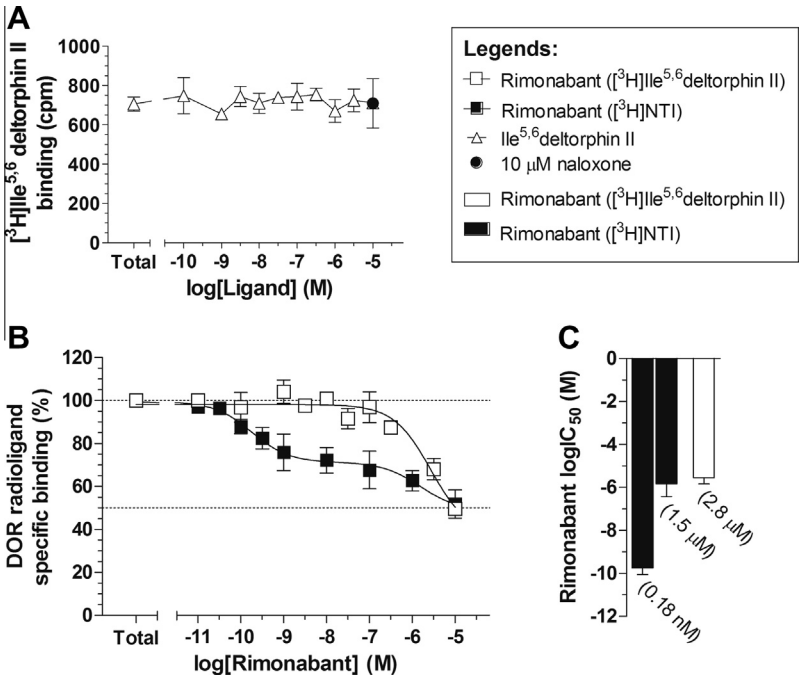

Fig. 1. Direct binding affinity measurements of rimonabant towards DOR in competition binding experiments in CHO-mDOR membrane fractions and DOR specific ligand binding in pCHO cell membranes. (A) Bound [^{3}H]Ile^{5,6}deltorphin II in counts per minute (cpm) in fixed concentrations in the presence of increasing (10^{-10} to 10^{-5} M) concentrations of unlabeled DPDPE and 10 μM naloxone in pCHO cell membranes. (B) Specifically bound fixed concentrations of [^{3}H]Ile^{5,6}deltorphin II or [^{3}H]naltrindole in percentage in the presence of increasing (10^{-10} to 10^{-5} M) concentrations of unlabeled rimonabant in CHO-mDOR membrane fractions. (C) The calculated logIC$_{50}$ (binding capacity) of unlabeled rimonabant. Points and columns represent means ± S.E.M. for at least three experiments performed in duplicate. "Total" on the *X* axis refers to the points which did not contain competitor ligands and also represents the total specific binding (=100%, indicated by the dotted line) in the presence of either radioligand. Additionally the level of 50% DOR specific radioligand binding is represented with a dotted line. The two black columns indicate the logIC$_{50}$ values of rimonabant on the high and low affinity binding sites. The antilogarithm form of logIC$_{50}$ (IC$_{50}$) values are presented in brackets.

the micromolar range the specific binding was again decreased (Fig 1B). The "two phase" inhibition suggests a higher and a lower affinity binding site on the DOR, which can be both occupied by rimonabant with a subnanomolar (high affinity) and micromolar (low affinity) IC$_{50}$ value (Fig. 1C).

Thus in the micromolar range rimonabant can affect the ligand binding of DOR directly, moreover rimonabant can also inhibit specific antagonist binding in the nanomolar range with very high affinity. Accordingly rimonabant might behave as an antagonist towards DOR, since it can inhibit DOR antagonist binding more effectively.

3.2. The effect of rimonabant on DOR G-protein basal activity in [^{35}S]GTPγS binding assays, in CHO-mDOR and pCHO cell membranes

In the next step we examined whether rimonabant alters the basal activity of the DOR mediated G-protein stimulation in functional [^{35}S]GTPγS binding experiments, with a non-hydrolysable radiolabeled GTP analog, [^{35}S]GTPγS. The experiments were accomplished in CHO-mDOR and pCHO cell membranes, to avoid interaction of DORs with other opioid and cannabinoid receptors, and also to see clearly the direct actions of rimonabant on DOR G-protein coupling.

According to our results rimonabant significantly decreased the DORs basal activity (=100%, dotted line; Fig. 2A), with an efficacy (E_{max}) of 48.1% and with a potency (EC$_{50}$) of 1.3 μM (Fig. 2A, inset figure). Thus rimonabant may behave as an inverse agonist at DOR.

To investigate whether the inverse agonistic effect of rimonabant on DOR is indeed DOR related, we measured the specifically bound [^{35}S]GTPγS when 10 μM rimonabant was incubated together with 1 μM of the DOR specific antagonist naltrindole again in CHO-mDOR cell membranes. Our results pointed out that NTI failed to reverse the inverse agonistic effect of rimonabant (Fig. 2B), therefore DOR is not involved in this action. For comparison, NTI significantly inhibited DPDPE-stimulated [^{35}S]GTPγS binding (Fig. 2B). Also the MOR agonist morphine and the KOR agonist U50488, together with NTI failed to alter the G-protein basal activity of DOR significantly (Fig. 2B). This confirms the lack of both MOR and KOR in the CHO-mDOR cell membranes, and the pure antagonistic character of naltrindole. Additionally rimonabant also significantly decreased G-protein basal activity in pCHO cell membranes (Fig 2C, inset figure), which did not contain DORs (DPDPE did not alter basal activity, see Fig. 2C), which underpins the non-DOR related inverse agonistic effect of rimonabant.

3.3. The effect of rimonabant on DOR G-protein activation in DPDPE-stimulated [^{35}S]GTPγS binding, in CHO-mDOR cell membranes

Since rimonabant directly inhibited DORs ligand binding in the micromolar range, we further examined whether rimonabant at the same concentration range has any effect on DORs G-protein activation during receptor stimulation. The experiments were again accomplished in functional [^{35}S]GTPγS binding experiments using CHO-mDOR cell membranes. The receptor was stimulated with the enkephalin analog DOR specific agonist DPDPE, which activated the DOR the most effectively compared to our other DOR activator ligand candidates (data not shown).

DPDPE stimulated the DOR with a potency (EC$_{50}$) of 12.4 nM and the receptors G-protein had a maximal stimulation or efficacy (E_{max}) of 285.6% during DPDPE stimulated receptor activation (Fig. 3A–C). Rimonabant in 1 and 10 μM concentrations significantly decreased the DORs G-protein efficacy (Fig. 3B) and also the potency of DPDPE but only in 10 μM concentrations (Fig. 3C).

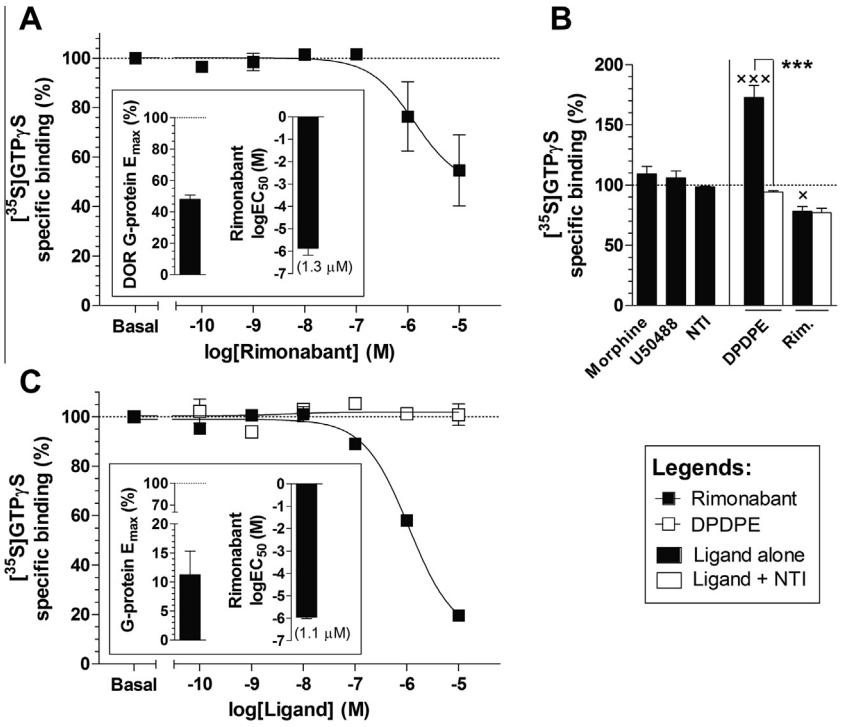

Fig. 2. The effect of rimonabant on DOR G-protein basal activity in ligand-modulated [^{35}S]GTPγS binding assays, in CHO-mDOR and in pCHO cell membranes. (A) Specifically bound [^{35}S]GTPγS in percentage in the presence of increasing concentrations (10^{-10} to 10^{-5} M) of rimonabant in CHO-mDOR cell membranes. E_{max} and $logEC_{50}$ values are presented in the inset figure. *Denotes the significant alterations of DOR G-protein E_{max} value (unpaired *t*-test, two-tailed *P* value) compared to basal activity (=100%) in the presence of rimonabant. (B) Specifically bound [^{35}S]GTPγS in percentage in the presence of 10 μM of the indicated ligands alone or together with 1 μM naltrindole in CHO-mDOR cell membranes. ×Indicates the significant alterations in specifically bound [^{35}S]GTPγS (One-way ANOVA, Bonferroni's Multiple Comparison post hoc test), compared to basal activity (=100%) in the presence of rimonabant or DPDPE. *Indicates the significant reduction in the specifically bound [^{35}S]GTPγS during DPDPE stimulation in the presence of NTI compared to DPDPE alone. (C) Specifically bound [^{35}S]GTPγS in percentage in the presence of increasing concentrations (10^{-10} to 10^{-5} M) of rimonabant or DPDPE in pCHO cell membranes. In case of rimonabant error bars are shorter than the points itself. The $logEC_{50}$ value of rimonabant and the G-protein E_{max} value after rimonabant activation are presented in the inset figure. *denotes the significant alterations of G-protein E_{max} value (unpaired *t*-test, two-tailed *P* value) compared to basal activity (=100%) in the presence of rimonabant. Points and columns represent means ± S.E.M. for at least three experiments performed in triplicate. "Basal" on the *X* axis refers to the points which did not contain ligands. The dotted line represents the receptors basal activity level, which was defined as 100%. ×××, ***: $P < 0.001$; ×: $P < 0.05$.

Thus rimonabant inhibited the DPDPE-induced maximal G-protein stimulation of the DOR and also the potency of the stimulator ligand in the micromolar range when no cannabinoid or other opioid receptors were present in the experimental system.

3.4. The effect of rimonabant on DOR G-protein activation in DPDPE-stimulated [^{35}S]GTPγS binding, in wild type and CB_1/CB_2 receptor double knock-out mouse forebrain membranes

Our next objective was to examine whether the inhibitory action of rimonabant upon DOR G-protein activation and stimulatory ligand potency occurs when the receptor is expressed in physiological conditions, when cannabinoid and other opioid receptors are present, thus interactions may occur between them. Membrane fractions of mice forebrain were used, since both opioid and cannabinoid receptors are expressed in eligible amount in this brain region (Lever, 2007; Sim and Childers, 1997; Svízenská et al., 2008). Since the inhibitory actions of rimonabant occurred from 1 μM in CHO-mDOR cell membranes, we carried out our further experiments with this concentration.

In the wild type (w.t.) mouse forebrain DPDPE stimulated the DOR to a maximal stimulation level of 138.1% with an EC_{50} value of 13.8 nM (Fig. 4A–C). The presence of rimonabant produced a significant attenuation in the maximal efficacy of DORs G-protein activity (Fig. 4A and B) and in the potency of the stimulatory ligand as well (Fig. 4C).

Previously our group demonstrated an interaction between the CB_2 receptor and MOR in mice forebrain (Páldyová et al., 2008) therefore we studied the possible role of the CB_1 receptor in the inhibitory actions of rimonabant, and also the role of the CB_2 receptor. To achieve this, we carried out our DPDPE-induced [^{35}S]GTPγS binding assays in CB_1/CB_2 K.O. mouse forebrain membranes. Accordingly the reduced maximal efficacy of the receptor and the potency of the activating ligand (Fig. 4A–C, respectively) were also established in the CB_1/CB_2 K.O. mouse forebrain when rimonabant was added. Interestingly in the absence of rimonabant, the lack of both cannabinoid receptors did not affect significantly the maximal stimulation of the G-protein activity or the stimulatory potency of DPDPE (Fig. 4A–C).

Further on we wanted to verify that the inhibitory actions of rimonabant are not due to the unspecific inverse agonistic effect discussed previously under Section 3.2. To exclude this possibility we applied L-epinephrine, which is a non-selective endogenous adrenergic receptor agonist, in [^{35}S]GTPγS binding assays in CB_1/CB_2 K.O. mouse forebrain membranes. Adrenergic receptors are highly expressed in the forebrain structures and can coupled to $G_{i/o}$ type G-proteins such as the α_2 type receptors (Cottingham and Wang, 2012), therefore they can be monitored by L-epinephrine-stimulated [^{35}S]GTPγS binding assays. L-epinephrine activated its specific receptor with a 31.6 nM potency (Fig. 5C) and the coupled G-protein had a 166.8% maximal efficacy during the activation (Fig. 5A and B). In the presence of 10 μM rimonabant neither of the parameters changed significantly (E_{max}: 162%; EC_{50}: 26.7 nM; Fig. 5A–C), thus the inhibitory actions of rimonabant are indeed DOR specific.

To summarize the DPDPE-activated [^{35}S]GTPγS binding experiments accomplished in the forebrain, we can conclude that rimonabant inhibits agonist-stimulated DOR G-protein efficacy

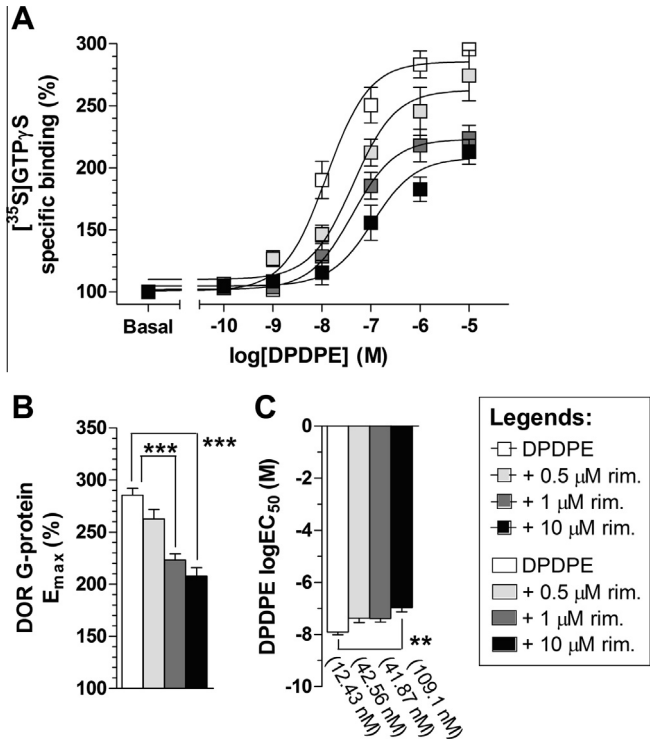

Fig. 3. The effect of rimonabant on DOR G-protein activation in DPDPE-stimulated [^{35}S]GTPγS binding, in CHO-mDOR cell membranes. (A) Specifically bound [^{35}S]GTPγS in percentage in the presence of increasing concentrations (10^{-10} to 10^{-5} M) of DPDPE in the absence or presence of the indicated rimonabant concentrations. (B) The calculated E_{max} (maximal efficacy) value of DOR G-protein. (C) The calculated $logEC_{50}$ (ligand potency) value of DPDPE. Points and columns represent means ± S.E.M. for at least three experiments performed in triplicate. *Indicates the significant reduction in E_{max} and $logEC_{50}$ values in the presence of rimonabant compared to DPDPE alone (One-way ANOVA, Bonferroni's Multiple Comparison post hoc test). "Basal" on the *X* axis refers to the points which did not contain DPDPE. The antilogarithm form of $logEC_{50}$ (EC_{50}) values are presented in brackets. ***: $P < 0.001$; **: $P < 0.01$.

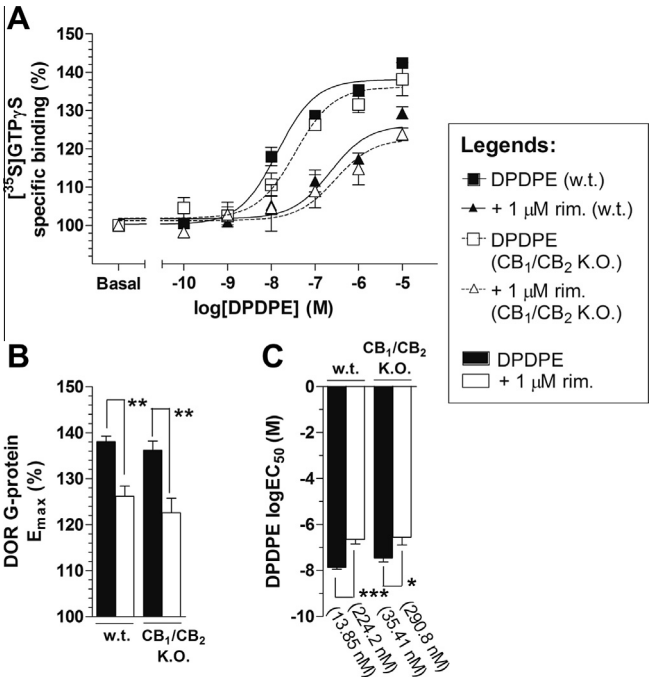

Fig. 4. The effect of rimonabant on DOR G-protein activation in DPDPE-stimulated [^{35}S]GTPγS binding in wild type and CB_1/CB_2 receptor double knock-out mouse forebrain membranes. (A) Specifically bound [^{35}S]GTPγS in percentage in the presence of increasing concentrations (10^{-10} to 10^{-5} M) of DPDPE in the absence or presence of rimonabant. (B) The calculated E_{max} (maximal efficacy) value of DOR G-protein. (C) The calculated $logEC_{50}$ (ligand potency) value of DPDPE. Points and columns represent means ± S.E.M. for at least three experiments performed in triplicate. *Indicates the significant reduction in E_{max} and $logEC_{50}$ values in the presence of rimonabant compared to DPDPE alone in wild type or in CB_1/CB_2 receptor double knock-out mouse (unpaired *t*-test, two-tailed *P* value). "Basal" on the *X* axis refers to the points which did not contain activator ligands. The antilogarithm form of $logEC_{50}$ (EC_{50}) values are presented in brackets. ***: $P < 0.001$; **: $P < 0.01$; *: $P < 0.05$.

and activator ligand potency in the micromolar range, when the receptor is expressed in physiological conditions. Further on this inhibitory action is independent from both cannabinoid receptors and it is DOR specific.

4. Discussion

Rimonabant was the first CB_1 receptor antagonist/inverse agonist to be developed, and it is still a perfect tool for antagonizing CB_1 related effects (for review see Pertwee, 2005). Later it turned out that rimonabant had several non-cannabinoid related effects such as decreasing alcohol intake, opiate self-administration and increasing smoking cessation (for review see Foll and Goldberg, 2005). There is also evidence that rimonabant can interact with several GPCRs and ion channels (for review see Pertwee, 2010).

This study focuses on the interaction between rimonabant and DOR. The interaction was studied at ligand-receptor level in competition binding experiments, and at the receptor-G-protein level in functional [^{35}S]GTPγS binding assays. These assays gather information about the receptors ligand binding capacity (Schütz, 1991) and functionality (Strange, 2010).

To our knowledge there has been only one paper so far studying the direct effect of rimonabant on DOR (Kathmann et al., 2006) in competition binding experiments and in saturation and kinetic binding assays in cerebral cortical membranes with the DOR specific tritiated antagonist [^{3}H]NTI. In competition binding experiments they found that rimonabant inhibited [^{3}H]NTI binding by only 20%, while in our binding studies rimonabant decreased 50% of [^{3}H]Ile^{5,6}deltorphin II and [^{3}H]NTI total specific binding (Fig. 1B). The diverse results in case of [^{3}H]NTI can be partly explained by the different experimental conditions applied during the assay (incubation time and temperature, final volume etc.) and by the applied CHO cell lines, which contained a homogeneous population of overexpressed mouse DORs. CHO-mDOR cell membranes insure near optimal conditions for a rimonabant–DOR interaction since no other opioid or even cannabinoid receptors were present in the membrane preparation. Additionally in case of both radioligands rimonabant reached an IC_{50} value in the micromolar range (Fig. 1C), similar to our previously reported data on CHO-MOR cell membranes (Zádor et al., 2012) and to other studies (Cinar and Szücs, 2009; Fong et al., 2009; Kathmann et al., 2006). Interestingly rimonabant also bound with an IC_{50} in the micromolar range to other members of the GPCR family, such as adrenergic or 5-HT_6 receptors or to ion channels, like calcium, sodium and potassium channels (for review see Pertwee, 2010). However rimonabant also displaced the antagonist [^{3}H]NTI in the subnanomolar range (Fig. 1B) with a very high affinity (Fig. 1C), which did not occur during the displacement of the agonist [^{3}H]Ile^{5,6}deltorphin II (Fig. 1B and C). It is known that antagonists stabilize the receptors in the inactive state, thus they prefer the inactive receptor form, while agonists prefer the active receptor state, since they stabilize the active form (Rosenbaum et al., 2009; Strange, 2002). Accordingly in our competition binding experiments rimonabant may behave as an antagonist since it displaced [^{3}H]NTI (which probably stabilized the DOR to the inactive state) from the higher affinity

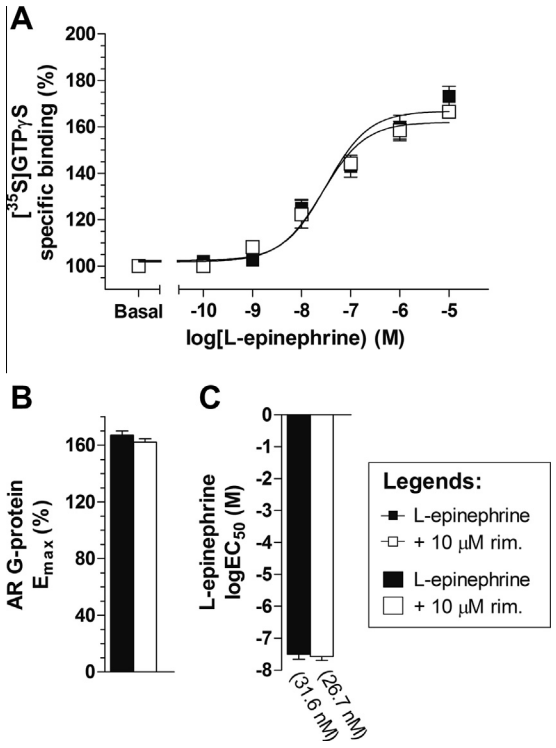

Fig. 5. The effect of rimonabant on AR G-protein activation in L-epinephrine-stimulated [^{35}S]GTPγS binding in CB_1/CB_2 receptor double knock-out mouse forebrain membranes. (A) Specifically bound [^{35}S]GTPγS in percentage in the presence of increasing concentrations (10^{-10} to 10^{-5} M) of L-epinephrine in the absence or presence of rimonabant. (B) The calculated E_{max} (maximal efficacy) value of AR G-protein. (C) The calculated $logEC_{50}$ (ligand potency) value of L-epinephrine. Points and columns represent means ± S.E.M. for at least three experiments performed in triplicate. "Basal" on the *X* axis refers to the points which did not contain L-epinephrine. The antilogarithm form of $logEC_{50}$ (EC_{50}) values are presented in brackets. AR: adrenergic receptor.

binding site, which did not occur during the displacement of the agonist [^{3}H]Ile^{5,6}deltorphin II (which probably stabilized the DOR in the active state). In our previous paper similar results were observed when rimonabant displaced the opioid antagonist [^{3}H]naloxone from the high affinity binding site in CHO-MOR cell membranes (Zádor et al., 2012). The high and low affinity binding sites were previously described in the GPCR superfamily among the MORs as well (Baker and Hill, 2007; Krizsan et al., 1991).

It is well known that G-proteins have a constitutive activity (for review see Seifert and Wenzel-Seifert, 2002) which can be further modified upon ligand binding. In turn the altered basal activity initiates different types of signaling cascades (Hamm, 1998). For further investigations we examined the impact of rimonabant on the basal activity of the DORs G-protein, which can give us valuable information about the binding character of rimonabant on DOR. In our [^{35}S]GTPγS binding assays rimonabant significantly inhibited receptor basal activity in CHO-mDOR membranes (Fig. 2A), however we proved that this was not DOR related, since the effect was not reversed by the DOR specific antagonist NTI (Fig. 2B) and it also occurred in pCHO cell membranes (Fig. 2C) which did not express DORs (Figs. 1A and 2C). These findings also confirms previous reports in similar experimental conditions (Cinar and Szücs, 2009; Seely et al., 2012). Therefore the agonistic (since rimonabant did not enhance DOR G-protein basal activity) and inverse agonistic character of rimonabant at DOR can be excluded. As regard to the non-CB_1 related inverse agonistic effect of rimonabant it has been proven to be pertussis toxin sensitive and it has been demonstrated in different types of brain tissues in several other publications (Breivogel et al., 2001; Cinar and Szücs, 2009; MacLennan et al., 1998; Sim-Selley et al., 2001).

Since rimonabant affected the DORs ligand binding, it raises the possibility that it can also interfere with the receptors G-protein activation during DOR specific agonist stimulation. Indeed, when G-protein signaling was initiated with the cyclic enkephalin analog DPDPE, rimonabant inhibited the maximal stimulation of the DORs G-protein and also the potency of the stimulator ligand significantly (Fig. 3A–C). Moreover the inhibition occurred in the micromolar concentration range, similarly as in direct affinity measurements in CHO-mDOR cell membranes. For comparison, in CHO-MOR cell membrane preparations rimonabant (10 μM) did not alter the DAMGO-stimulated (10 μM) G-protein activation significantly (Cinar and Szücs, 2009), in contrast in morphine-induced [^{35}S]GTPγS assays accomplished in CHO-MOR cell membranes rimonabant reduced the potency of morphine (Seely et al., 2012). Thus so far the inhibitory action of rimonabant on the maximal stimulation of the DOR G-protein and on the potency of the stimulator ligand in agonist-induced [^{35}S]GTPγS experiments indicates that rimonabant may behave as an antagonist on DOR.

The CHO cell line with homogeneous population of overexpressed DOR is a useful tool to investigate the direct interaction between rimonabant and DOR, since there is no cannabinoid or other opioid receptors in the system which can interact with DOR, thus the direct effect of rimonabant can be measured more accurately. However, it is well known that in physiological conditions GPCR receptors often communicate with each other via overlapping signaling pathways or more even via heterodimerization (González-Maeso, 2011; Hur and Kim, 2002; Jordan and Devi, 1999; Rozenfeld and Devi, 2011), which in addition alters there functionality (Birdsall, 2010; Jordan and Devi, 1999). Taking this into consideration we investigated the impact of rimonabant on DOR G-protein activation in mouse forebrain, where the cannabinoid and opioid receptors are expressed in adequate quantity (Gong et al., 2006; Howlett et al., 2002; Mansour et al., 1995; Sim and Childers, 1997). According to our results, in micromolar concentrations the inhibitory action of rimonabant also occurred when the DOR and its G-protein were expressed in physiological conditions (Fig. 4A–C). More importantly the inhibition was also observed when neither cannabinoid receptors were expressed in the forebrain (Fig. 4A–C); therefore it was a cannabinoid receptor independent action, at least in the forebrain region. Previously our group demonstrated a cannabinoid independent G-protein inhibitory action of rimonabant on MOR, in the forebrain region as well (Zádor et al., 2012). In another study, micromolar concentrations of rimonabant decreased the potency of the MOR stimulator ligand CB_1 receptor independently (Cinar and Szücs, 2009). However the inhibitory action of rimonabant on DPDPE-stimulated DOR G-protein activation might be due to the non-CB_1 related inverse agonistic effect. To investigate this possibility we examined L-epinephrine-induced G-protein activity in the presence of rimonabant in CB_1/CB_2 receptor double knock-out mouse forebrain membranes. According to our results micromolar concentrations of rimonabant did not have any effect on adrenergic receptor G-protein maximal activity or L-epinephrine potency during L-epinephrine stimulation (Fig. 5A–C). Therefore we can conclude that the decreased agonist mediated DOR G-protein activation by rimonabant are truly DOR specific.

Thus rimonabant can directly inhibit DOR specific binding and agonist-stimulated DOR G-protein efficacy and potency. The mechanism behind these actions can be due to the antagonistic character of rimonabant towards the DOR, which possibility is confirmed by our results in many levels: (1) the reduced specific binding of the antagonist [^{3}H]NTI in the subnanomolar concentration range, (2) rimonabant did not enhanced the basal activity of

DOR, therefore it did not behave as an agonist towards DOR, (3) the inverse agonistic character can also be excluded since it was not a DOR specific action, (4) the reduced potency of the stimulator ligand and (5) the reduced E_{max} value of the DOR G-protein during agonist stimulation, which were in addition DOR specific actions. Further on the allosteric effect can also be excluded since Kathmann and co-workers demonstrated previously that rimonabant did not show any allosteric properties on DOR in dissociation kinetic studies (Kathmann et al., 2006). According to our previous and Seely and co-workers study rimonabant is also believed to have antagonistic properties towards the MOR (Seely et al., 2012; Zádor et al., 2012), which was analyzed in receptor binding assays together with *in vivo* (Seely et al., 2012) and *in silico* (Zádor et al., 2012) experiments.

After chronic rimonabant treatment the plasma protein level of the compound in humans is reported to be in the mid nanomolar range (Cinar and Szücs, 2009; Henness et al., 2006; Kathmann et al., 2006), which is ten times lower than the inhibitory concentration range of rimonabant observed in DOR agonist binding and DOR agonist stimulated G-protein activation. However there is no data referring to the bioavailability of rimonabant or the tissue distribution during chronic treatment. Additionally rimonabant is a highly hydrophobic molecule, thus it can deposit in the fat tissue and easily penetrate through the BBB (Rinaldi-Carmona et al., 1995), also it has a long half-life (6–9 days with normal BMI and 16 days with higher than 30 kg/m^2, see web reference), because of its high plasma protein binding, which is almost 100% (see web reference). Therefore it can be possible that rimonabant may reach micromolar concentrations in peripheral tissues or even in the brain during chronic treatment. Being aware of these informations the inhibitory actions of rimonabant on DOR function observed in the micromolar range might have pharmacological relevance. If so the antagonistic behavior of rimonabant on DOR could partially explain the psychiatric side effects of the compound during chronic treatments, since DOR antagonists are proved to cause anxiogenic and depressive-like behavior (Perrine et al., 2006; Saitoh et al., 2004). It is worth to note that the mediatory role of KOR in the mood related side effects of rimonabant has been demonstrated previously (Lockie et al., 2011).

In this study we demonstrated in *in vitro* experiments that rimonabant can directly inhibit DOR function in the micromolar range and that this inhibitory action is possibly due to its antagonist property towards DOR. Despite the high effective concentration, considering the pharmacological and chemical properties of rimonabant this concentration range may have pharmacological relevance.

Acknowledgements

This study was supported by funds from the National Development Agency (NFÜ), Budapest, Hungary (grant number: TÁMOP-4.2.2A-11/1KONV-2012-0024); OTKA 108518 and finally the Dr. Rollin D. Hotchkiss Foundation. The authors would like to thank Dr. Zvi Vogel for providing us the CHO-mDOR cell lines, and also Erzsébet Kusz for growing the cell cultures for us. We would also want to thank Dr. Andreas Zimmer's laboratory for providing us the CB_1/CB_2 double knock-out mice and the Isotope Laboratory of BRC for synthetizing and radiolabeling the Ile^{5,6}deltorphin II ligand. The authors would also like to thank Gergő Kovács for the growing of the parental CHO cell lines and Dr. Melinda Pirity for providing them for us. Finally we are also grateful for the assistance of Zsuzsa Canjavec and Ildikó Némethné, and to Prof. Mária Wollemann and Dr. Reza Samavati for critical reading of the manuscript.

References

Arévalo, C., de Miguel, R., Hernández-Tristán, R., 2001. Cannabinoid effects on anxiety-related behaviours and hypothalamic neurotransmitters. Pharmacol. Biochem. Behav. 70, 123–131.
Baker, J.G., Hill, S.J., 2007. Multiple GPCR conformations and signalling pathways: implications for antagonist affinity estimates. Trends Pharmacol. Sci. 28, 374–381.
Bambico, F.R., Katz, N., Debonnel, G., Gobbi, G., 2007. Cannabinoids elicit antidepressant-like behavior and activate serotonergic neurons through the medial prefrontal cortex. J. Neurosci. 27, 11700–11711.
Benyhe, S., Farkas, J., Tóth, G., Wollemann, M., 1997. Met5-enkephalin-Arg6-Phe7, an endogenous neuropeptide, binds to multiple opioid and nonopioid sites in rat brain. J. Neurosci. Res. 48, 249–258.
Berrendero, F., Mendizabal, V., Murtra, P., Kieffer, B.L., Maldonado, R., 2003. Cannabinoid receptor and WIN 55 212-2-stimulated [^{35}S]-GTPgammaS binding in the brain of mu-, delta- and kappa-opioid receptor knockout mice. Eur. J. Neurosci. 18, 2197–2202.
Beyer, C.E., Dwyer, J.M., Piesla, M.J., Platt, B.J., Shen, R., Rahman, Z., Chan, K., Manners, M.T., Samad, T.a., Kennedy, J.D., Bingham, B., Whiteside, G.T., 2010. Depression-like phenotype following chronic CB1 receptor antagonism. Neurobiol. Dis. 39, 148–155.
Bie, B., Pan, Z.Z., 2007. Trafficking of central opioid receptors and descending pain inhibition. Mol. Pain. 3, 37.
Birdsall, N.J.M., 2010. Class A GPCR heterodimers: evidence from binding studies. Trends Pharmacol. Sci. 31, 499–508.
Breivogel, C.S., Griffin, G., Di Marzo, V., Martin, B.R., 2001. Evidence for a new G protein-coupled cannabinoid receptor in mouse brain. Mol. Pharmacol. 60, 155–163.
Broom, D.C., Jutkiewicz, E.M., Folk, J.E., Traynor, J.R., Rice, K.C., Woods, J.H., 2002. Convulsant activity of a non-peptidic delta-opioid receptor agonist is not required for its antidepressant-like effects in Sprague-Dawley rats. Psychopharmacology 164, 42–48.
Burford, N., Wang, D., Sadee, W., 2000. G-protein coupling of mu-opioid receptors (OP3): elevated basal signalling activity. Biochem. J. 348, 531–537.
Bushlin, I., Gupta, A., Stockton, S.D., Miller, L.K., Devi, L.A., 2012. Dimerization with cannabinoid receptors allosterically modulates delta opioid receptor activity during neuropathic pain. PLoS One 7, e49789.
Cinar, R., Szücs, M., 2009. CB_1 receptor-independent actions of SR141716 on G-protein signaling: coapplication with the mu-opioid agonist Tyr-D-Ala-Gly-(NMe)Phe-Gly-ol unmasks novel, pertussis toxin-insensitive opioid signaling in mu-opioid receptor-Chinese hamster ovary cells. J. Pharmacol. Exp. Ther. 330, 567–574.
Codd, E.E., Carson, J.R., Colburn, R.W., Stone, D.J., Besien, C.R.Van., Zhang, S., Wade, P.R., Gallantine, E.L., Meert, T.F., Molino, L., Pullan, S., Razler, C.M., Dax, S.L., Flores, C.M., 2009. JNJ-20788560 [9-(8-azabicyclo[3.2.1]oct-3-ylidene)-9H-xanthene-3-carboxylic acid diethylamide], a selective delta opioid receptor agonist, is a potent and efficacious antihyperalgesic agent that does not produce respiratory depression, pharmacologic tolerance, or physical dependence. J. Pharmacol. Exp. Ther. 329, 241–251.
Cottingham, C., Wang, Q., 2012. α2 adrenergic receptor dysregulation in depressive disorders: implications for the neurobiology of depression and antidepressant therapy. Neurosci. Biobehav. Rev. 36, 2214–2225.
Demuth, D., Molleman, A., 2006. Cannabinoid signalling. Life Sci. 78, 549–563.
Filliol, D., Ghozland, S., Chluba, J., Martin, M., Matthes, H.W., Simonin, F., Befort, K., Gavériaux-Ruff, C., Dierich, A., LeMeur, M., Valverde, O., Maldonado, R., Kieffer, B.L., 2000. Mice deficient for delta- and mu-opioid receptors exhibit opposing alterations of emotional responses. Nat. Genet. 25, 195–200.
Foll, B.Le., Goldberg, S.R., 2005. Cannabinoid CB_1 receptor antagonists as promising new medications for drug dependence. J. Pharmacol. Exp. Ther. 312, 875–883.
Fong, T.M., Shearman, L.P., Stribling, D.S., Shu, J., Lao, J., Huang, C.R.-R., Xiao, J.C., Shen, C.-P., Tyszkiewicz, J., Strack, A.M., DeMaula, C., Hubert, M.-F., Galijatovic-Idrizbegovic, A., Owen, R., Huber, A.C., Lanning, C.L., 2009. Pharmacological efficacy and safety profile of taranabant in preclinical species. Drug Dev. Res. 70, 349–362.
Gong, J.P., Onaivi, E.S., Ishiguro, H., Liu, Q.R., Tagliaferro, P.A., Brusco, A., Uhl, G.R., 2006. Cannabinoid CB2 receptors: immunohistochemical localization in rat brain. Brain Res. 1071, 10–23.
González-Maeso, J., 2011. GPCR oligomers in pharmacology and signaling. Mol. Brain. 4, 20.
Hamm, H., 1998. The many faces of G protein signaling. J. Biol. Chem. 273, 669–772.
Henness, S., Robinson, D.M., Lyseng-Williamson, K.A., 2006. Rimonabant. Drugs 66, 2109–2119 (discussion 2120–2121).
Howlett, A.C., Barth, F., Bonner, T.I., Cabral, G., Casellas, P., Devane, W.a., Felder, C.C., Herkenham, M., Mackie, K., Martin, B.R., Mechoulam, R., Pertwee, R.G., 2002. International Union of Pharmacology. XXVII. Classification of cannabinoid receptors. Pharmacol. Rev. 54, 161–202.
Hur, E.M., Kim, K.T., 2002. G protein-coupled receptor signalling and cross-talk: achieving rapidity and specificity. Cell. Signal. 14, 397–405.
Ioja, E., Tóth, G., Benyhe, S., Tourwe, D., Péter, A., Tömböly, C., Borsodi, A., 2005. Opioid receptor binding characteristics and structure-activity studies of novel tetrapeptides in the TIPP (Tyr-Tic-Phe-Phe) series. Neurosignals 14, 317–328.
Ioja, E., Tourwé, D., Kertész, I., Tóth, G., Borsodi, A., Benyhe, S., 2007. Novel diastereomeric opioid tetrapeptides exhibit differing pharmacological activity profiles. Brain Res. Bull. 74, 119–129.

Járai, Z., Wagner, J.A., Varga, K., Lake, K.D., Compton, D.R., Martin, B.R., Zimmer, A.M., Bonner, T.I., Buckley, N.E., Mezey, E., Razdan, R.K., Zimmer, A., Kunos, G., 1999. Cannabinoid-induced mesenteric vasodilation through an endothelial site distinct from CB1 or CB2 receptors. Proc. Natl. Acad. Sci. USA 96, 14136–14141.
Jordan, B., Devi, L., 1999. G-protein-coupled receptor heterodimerization modulates receptor function. Nature 399, 697–700.
Kathmann, M., Flau, K., Redmer, A., Tränkle, C., Schlicker, E., 2006. Cannabidiol is an allosteric modulator at mu- and delta-opioid receptors. Naunyn. Schmiedebergs. Arch. Pharmacol. 372, 354–361.
Katona, I., Sperlágh, B., Sík, A., Käfalvi, A., Vizi, E.S., Mackie, K., Freund, T.F., 1999. Presynaptically located CB1 cannabinoid receptors regulate GABA release from axon terminals of specific hippocampal interneurons. J. Neurosci. 19, 4544–4558.
Krizsan, D., Varga, E., Hosztafi, S., Benyhe, S., Szucs, M., Borsodi, A., 1991. Irreversible blockade of the high and low affinity (^{3}H) naloxone binding sites by C-6 derivatives of morphinane-6-ones. Life Sci. 48, 439–451.
Lee, H.K., Choi, E.B., Pak, C.S., 2009. The current status and future perspectives of studies of cannabinoid receptor 1 antagonists as anti-obesity agents. Curr. Top. Med. Chem. 9, 482–503.
Lever, J.R., 2007. PET and SPECT imaging of the opioid system : receptors, radioligands and avenues for drug discovery and development. Curr. Pharm. Des. 13, 33–49.
Lockie, S.H., Czyzyk, T.A., Chaudhary, N., Perez-Tilve, D., Woods, S.C., Oldfield, B.J., Statnick, M.A., Tschöp, M.H., 2011. CNS opioid signaling separates cannabinoid receptor 1-mediated effects on body weight and mood-related behavior in mice. Endocrinology 152, 3661–3667.
MacLennan, S.J., Reynen, P.H., Kwan, J., Bonhaus, D.W., 1998. Evidence for inverse agonism of SR141716A at human recombinant cannabinoid CB1 and CB2 receptors. Br. J. Pharmacol. 124, 619–622.
Maldonado, R., Valverde, O., 2003. Participation of the opioid system in cannabinoid-induced antinociception and emotional-like responses. Eur. Neuropsychopharmacol. 13, 401–410.
Mansour, A., Fox, C.A., Akil, H., Watson, S.J., 1995. Opioid-receptor mRNA expression in the rat CNS: anatomical and functional implications. Trends Neurosci. 18, 22–29.
McGregor, I.S., Dastur, F.N., McLellan, R.A., Brown, R.E., 1996. Cannabinoid modulation of rat pup ultrasonic vocalizations. Eur. J. Pharmacol. 313, 43–49.
Nevin, S.T., Kabasakal, L., Otvös, F., Töth, G., Borsodi, A., 1994. Binding characteristics of the novel highly selective delta agonist, [^{3}H]IIe5,6deltorphin II. Neuropeptides 26, 261–265.
Padwal, R.S., Majumdar, S.R., 2007. Drug treatments for obesity: orlistat, sibutramine, and rimonabant. Lancet 369, 71–77.
Pagotto, U., Marsicano, G., Cota, D., Lutz, B., Pasquali, R., 2006. The emerging role of the endocannabinoid system in endocrine regulation and energy balance. Endocr. Rev. 27, 73–100.
Páldyová, E., Bereczki, E., Sántha, M., Wenger, T., Borsodi, A., Benyhe, S., 2008. Noladin ether, a putative endocannabinoid, inhibits mu-opioid receptor activation via CB2 cannabinoid receptors. Neurochem. Int. 52, 321–328.
Perrine, S.A., Hoshaw, B.A., Unterwald, E.M., 2006. Delta opioid receptor ligands modulate anxiety-like behaviors in the rat. Br. J. Pharmacol. 147, 864–872.
Pertwee, R.G., 2001. Cannabinoid receptors and pain. Prog. Neurobiol. 63, 569–611.
Pertwee, R.G., 2005. Inverse agonism and neutral antagonism at cannabinoid CB1 receptors. Life Sci. 76, 1307–1324.
Pertwee, R.G., 2010. Receptors and channels targeted by synthetic cannabinoid receptor agonists and antagonists. Curr. Med. Chem. 17, 1360–1381.
Pradhan, A., Befort, K., Nozaki, C., Gavériaux-Ruff, C., Kieffer, B.L., 2011. The delta opioid receptor: an evolving target for the treatment of brain disorders. Trends Pharmacol. Sci. 32, 581–590.
Pradhan, A.A., Smith, M.M.L., Kieffer, B.L., Evans, C.J., 2012. Ligand-directed signalling within the opioid receptor family. Br. J. Pharmacol. 167, 960–969.
Rinaldi-Carmona, M., Barth, F., Héaulme, M., Shire, D., Calandra, B., Congy, C., Martinez, S., Maruani, J., Néliat, G., Caput, D., 1994. SR141716A, a potent and selective antagonist of the brain cannabinoid receptor. FEBS Lett. 350, 240–244.
Rinaldi-Carmona, M., Barth, F., Héaulme, M., 1995. Biochemical and pharmacological characterisation of SR141716A, the first potent and selective brain cannabinoid receptor antagonist. Life Sci. 56, 1941–1947.
Robledo, P., Berrendero, F., Ozaita, A., Maldonado, R., 2008. Advances in the field of cannabinoid–opioid cross-talk. Addict. Biol. 13, 213–224.
Rodgers, R.J., Haller, J., Halasz, J., Mikics, E., 2003. "One-trial sensitization" to the anxiolytic-like effects of cannabinoid receptor antagonist SR141716A in the mouse elevated plus-maze. Eur. J. Neurosci. 17, 1279–1286.
Rosenbaum, D.M., Rasmussen, S.G.F., Kobilka, B.K., 2009. The structure and function of G-protein-coupled receptors. Nature 459, 356–363.
Rozenfeld, R., Devi, L.A., 2011. Exploring a role for heteromerization in GPCR signalling specificity. Biochem. J. 433, 11–18.
Rozenfeld, R., Bushlin, I., Gomes, I., Tzavaras, N., Gupta, A., Neves, S., Battini, L., Gusella, G.L., Lachmann, A., Ma'ayan, A., Blitzer, R.D., Devi, L.A., 2012. Receptor heteromerization expands the repertoire of cannabinoid signaling in rodent neurons. PLoS One 7, e29239.
Saitoh, A., Kimura, Y., Suzuki, T., Kawai, K., Nagase, H., Kamei, J., 2004. Potential anxiolytic and antidepressant-like activities of SNC80, a selective delta-opioid agonist, in behavioral models in rodents. J. Pharmacol. Sci. 95, 374–380.
Schütz, W., 1991. The pharmacological basis of receptor binding. Wien. Klin. Wochenschr. 103, 438–442.
Seely, K.A., Brents, L.K., Franks, L.N., Rajasekaran, M., Zimmerman, S.M., Fantegrossi, W.E., Prather, P.L., 2012. AM-251 and rimonabant act as direct antagonists at mu-opioid receptors: implications for opioid/cannabinoid interaction studies. Neuropharmacology 63, 905–915.
Seifert, R., Wenzel-Seifert, K., 2002. Constitutive activity of G-protein-coupled receptors: cause of disease and common property of wild-type receptors. Naunyn. Schmiedebergs. Arch. Pharmacol. 366, 381–416.
Shen, M., Piser, T.M., Seybold, V.S., Thayer, S.A., 1996. Cannabinoid receptor agonists inhibit glutamatergic synaptic transmission in rat hippocampal cultures. J. Neurosci. 16, 4322–4334.
Sim, L.J., Childers, S.R., 1997. Anatomical distribution of mu, delta, and kappa opioid- and nociceptin/orphanin FQ-stimulated [^{35}S]guanylyl-5′-O-(gamma-thio)-triphosphate binding in guinea pig brain. J. Comp. Neurol. 386, 562–572.
Sim, L.J., Selley, D.E., Childers, S.R., 1995. In vitro autoradiography of receptor-activated G proteins in rat brain by agonist-stimulated guanylyl 5′-[gamma-[^{35}S]thio]-triphosphate binding. Proc. Natl. Acad. Sci. U. S. A. 92, 7242–7246.
Sim-Selley, L.J., Brunk, L.K., Selley, D.E., 2001. Inhibitory effects of SR141716A on G-protein activation in rat brain. Eur. J. Pharmacol. 414, 135–143.
Strange, P.G., 2002. Mechanisms of inverse agonism at G-protein-coupled receptors. Trends Pharmacol. Sci. 23, 89–95.
Strange, P.G., 2010. Use of the GTPγS ([^{35}S]GTPγS and Eu-GTPγS) binding assay for analysis of ligand potency and efficacy at G protein-coupled receptors. Br. J. Pharmacol. 161, 1238–1249.
Svízenská, I., Dubový, P., Sulcová, A., 2008. Cannabinoid receptors 1 and 2 (CB1 and CB2), their distribution, ligands and functional involvement in nervous system structures – a short review. Pharmacol. Biochem. Behav. 90, 501–511.
Traynor, R., Nahorski, R., Traynor, J.R., Nahorski, S.R., 1995. Modulation by mu-opioid agonists of guanosine-5′-O-(3-[^{35}S]thio)triphosphate binding to membranes from human neuroblastoma SH-SY5Y cells. Mol. Pharmacol. 47, 848–854.
Tzavara, E.T., Davis, R.J., Perry, K.W., Li, X., Salhoff, C., Bymaster, F.P., Witkin, J.M., Nomikos, G.G., 2003. The CB1 receptor antagonist SR141716A selectively increases monoaminergic neurotransmission in the medial prefrontal cortex: implications for therapeutic actions. Br. J. Pharmacol. 138, 544–553.
Urigüen, L., Berrendero, F., Ledent, C., Maldonado, R., Manzanares, J., 2005. Kappa- and delta-opioid receptor functional activities are increased in the caudate putamen of cannabinoid CB1 receptor knockout mice. Eur. J. Neurosci. 22, 2106–2110.
Zádor, F., Otvös, F., Benyhe, S., Zimmer, A., Páldy, E., 2012. Inhibition of forebrain μ-opioid receptor signaling by low concentrations of rimonabant does not require cannabinoid receptors and directly involves μ-opioid receptors. Neurochem. Int. 61, 378–388.

Further reading

http://en.sanofi.com/press/press_releases/2008/news_list_2008.aspx (last accessed: 2013).
http://www.drugbank.ca/drugs/DB06155 (last accessed: 2013).